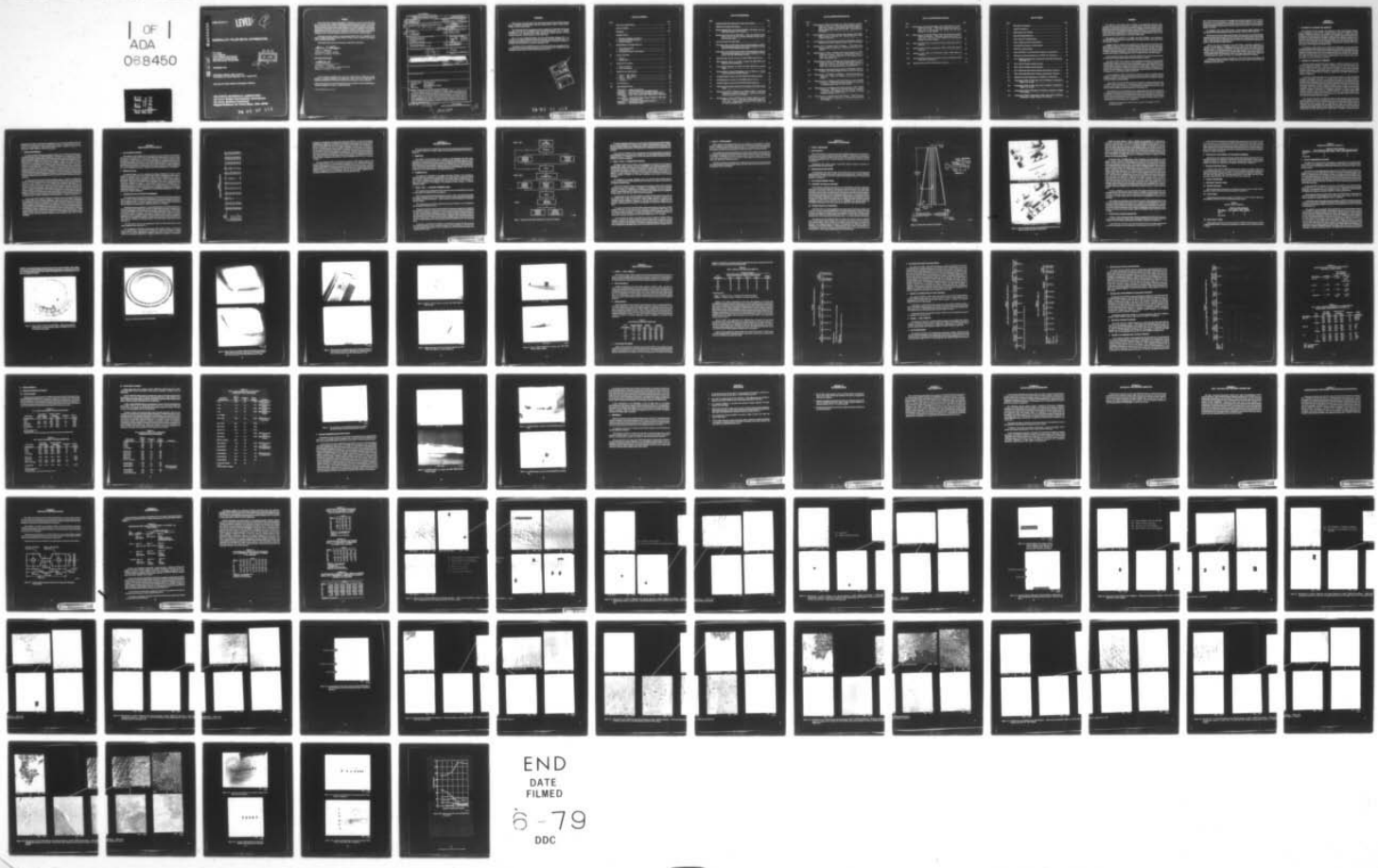
AD-A068 450 PRATT AND WHITNEY AIRCRAFT GROUP WEST PALM BEACH FL G--ETC F/G 11/6
SUPERALLOY FILLER METAL OPTIMIZATION.(U)
DEC 78 W H KING, D W ANDERSON F33615-77-C-5157
UNCLASSIFIED PWA-FR-10621 AFML-TR-78-177 NL

| OF |
ADA
088450



END
DATE
FILMED
6-79
DDC

AD A068450

DDC FILE COPY

AFML-TR-78-177

LEVEL II

SUPERALLOY FILLER METAL OPTIMIZATION

W. H. King
D. W. Anderson
Pratt & Whitney Aircraft Group
Government Products Division
West Palm Beach, Florida 33402

DDC
RECEIVED
MAY 8 1979
C

DECEMBER 1978

TECHNICAL REPORT AFML-TR-78-177
Final Report for Period September 1977 - August 1978

Approved for Public Release; Distribution Unlimited

AIR FORCE MATERIALS LABORATORY
Air Force Wright Aeronautical Laboratories
Air Force Systems Command
Wright-Patterson Air Force Base, Ohio 45433

79 05 07 111

NOTICE

When Government drawings, specifications, or other data are used for any purpose other than in connection with a definitely related Government procurement operation, the United States Government thereby incurs no responsibility nor any obligation whatsoever; and the fact that the Government may have formulated, furnished, or in any way supplied the said drawings, specifications, or other data, is not to be regarded by implication or otherwise as in any manner licensing the holder or any other person or corporation, or conveying any rights or permission to manufacture, use, or sell any patented invention that may in any way be related thereto.

This report has been reviewed by the Information Office (OI) and is releasable to the National Technical Information Service (NTIS). At NTIS, it will be available to the general public, including foreign nations.

This technical report has been reviewed and is approved for publication.

Guinn E. Metzger

GUINN E. METZGER
Structural Metals Branch
Metals & Ceramics Division

FOR THE COMMANDER

L R Bidwell

LAWRENCE R. BIDWELL
Act Chief, Structural Metals Branch
Metals & Ceramics Division

"If your address has changed, if you wish to be removed from our mailing list, or if the addressee is no longer employed by your organization, please notify the Air Force Materials Laboratory (AFML/LLS), W-PAFB, OH 45433 to help us maintain a current mailing list."

Copies of this report should not be returned unless return is required by security considerations, contractual obligations, or notice on a specific document.

AIR FORCE/56780/11 April 1979 — 200

UNCLASSIFIED

SECURITY CLASSIFICATION OF THIS PAGE (When Data Entered)

REPORT DOCUMENTATION PAGE

READ INSTRUCTIONS BEFORE COMPLETING FORM

1. REPORT NUMBER: AFML-TR-78-177	2. GOVT ACCESSION NO.
3. RECIPIENT'S CATALOG NUMBER: Final rept.	
4. TITLE (and Subtitle): SUPERALLOY FILLER METAL OPTIMIZATION	5. TYPE OF REPORT & PERIOD COVERED: 15 Sept [illegible] 1977 — 15 August [illegible] 1978
6. PERFORMING ORG. REPORT NUMBER: PWA-FR-10621	
7. AUTHOR(s): W. H. King, D. W. Anderson	8. CONTRACT OR GRANT NUMBER(s): F33615-77-C-5157
9. PERFORMING ORGANIZATION NAME AND ADDRESS: Pratt & Whitney Aircraft Group, Government Products Division, P. O. Box 2691, West Palm Beach, Florida 33402	10. PROGRAM ELEMENT, PROJECT, TASK AREA & WORK UNIT NUMBERS: Project 24180
11. CONTROLLING OFFICE NAME AND ADDRESS: Air Force Materials Laboratory, Wright-Patterson Air Force Base, Ohio 45433	12. REPORT DATE: 31 December 1978
	13. NUMBER OF PAGES: 87 p.
14. MONITORING AGENCY NAME & ADDRESS (if different from Controlling Office)	15. SECURITY CLASS. (of this report): Unclassified
	15a. DECLASSIFICATION/DOWNGRADING SCHEDULE

16. DISTRIBUTION STATEMENT (of this Report)

[redacted] This document has been approved for public release and sale; its distribution is unlimited.

17. DISTRIBUTION STATEMENT (of the abstract entered in Block 20, if different from Report)

18. SUPPLEMENTARY NOTES

19. KEY WORDS (Continue on reverse side if necessary and identify by block number)

Nickel-base Alloy	Filler Metal Alloys
Superalloy	Fusion Welding
Weld	Heat-Affected Zone Cracking
Filler Metals	Hot Cracking

20. ABSTRACT (Continue on reverse side if necessary and identify by block number)

Pratt & Whitney Aircraft has conducted a two-phase program to optimize an age-hardenable nickel-base filler metal composition for hot-cracking-limited superalloy applications. The approach used was to characterize critical filler metal properties (e.g., melting behavior) and weldability behavior and to use these results to iteratively optimize a filler metal composition. Starting compositions were based on the best filler metals developed previously under AF Contract ~~F33615-75-C-5114~~. In Phase I, an optimum filler metal composition was determined. In Phase II, the optimum composition was evaluated by welding actual hardware and by conducting mechanical property tests.

DD FORM 1 JAN 73 1473 EDITION OF 1 NOV 65 IS OBSOLETE S/N 0102-LF-014-6601

UNCLASSIFIED

SECURITY CLASSIFICATION OF THIS PAGE (When Data Entered)

392 887

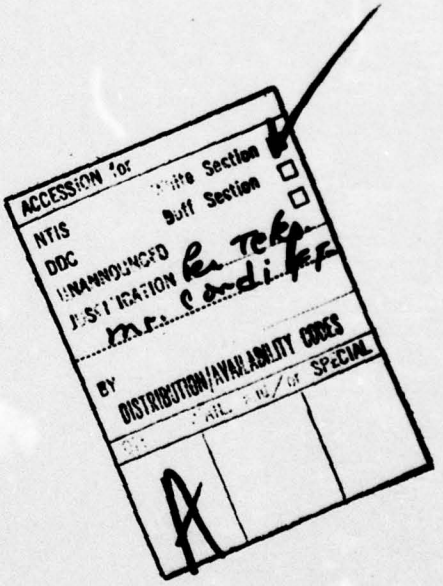
FOREWORD

This document is the final report of the work conducted by the Pratt & Whitney Aircraft Group, Government Products Division, West Palm Beach, Florida, under Air Force Contract F33615-77-C-5157, Project 241804.

The work reported herein was performed during the period from 15 September 1977 through 15 August 1978 and was accomplished under the technical direction of Dr. G. Metzger (AFML/LLS) of the Structural Metals Branch, Metals and Ceramics Division, Air Force Materials Laboratory, Wright-Patterson Air Force Base, Ohio.

Mr. W. H. King, P&WA/Connecticut, was the overall Program Manager. Mr. C. A. Voehringer was Program Manager for P&WA/Florida efforts and he was assisted by Mr. D. W. Anderson, Responsible Engineer. This report was prepared under the Contractor's reference No. FR-10621 and was released by the authors in September 1978.

The purpose of the work described herein was to optimize a filler metal composition for hot-cracking-limited superalloy welding applications. The compositions were modified from alloys developed previously under Air Force Contract F33615-75-C-5114.



79 05 07 111

TABLE OF CONTENTS

Section		Page
	LIST OF ILLUSTRATIONS	vii
	LIST OF TABLES	xi
	SUMMARY	xiii
I	INTRODUCTION	1
	1. Statement of Problem and Objective	1
	2. Superalloy Weldability Problems	1
	3. Previous Experience	2
II	DESCRIPTION OF FILLER METALS	3
	1. Alloy Design Approach	3
	2. Previous Alloys	3
	3. Formulation of Alloys for this Program	3
III	Program Description	7
	1. Objective	7
	2. Program Plan	7
IV	Experimental Procedures	11
	1. Phase I Procedures	11
	2. Phase II Procedures	15
V	RESULTS AND DISCUSSION	23
	1. Phase I — Task 1 Results	23
	2. Phase I — Task 2 Results	26
	3. Phase II — Results	31
	4. Discussion	37
VI	CONCLUSIONS	39
VII	RECOMMENDATIONS	41
	APPENDIX A — WIRE FABRICATION	43
	APPENDIX B — MELTING BEHAVIOR DETERMINATION	45
	APPENDIX C — WELDABILITY TEST SPECIMEN FABRICATION	47
	APPENDIX D — TASK 1 POST-WELD HEAT-TREATMENT CRACKING TEST	49
	APPENDIX E — MICROSTRUCTURE, PHASE STABILITY AND COMPOSITION INVESTIGATION	51
	APPENDIX F — MECHANICAL PROPERTIES TESTING	53
	APPENDIX G — MICROSTRUCTURE	55

LIST OF ILLUSTRATIONS

Figure		Page
1	Superalloy Filler Metal Optimization Program Flow Diagram	8
2	Tapered Hot Cracking Test Specimen	12
3	Massive Stainless Steel Hot Cracking Weldability Test Fixture and Cast Nickel-Base Superalloy Test Specimen	13
4	Forward View of Inconel 713c F100 TOBI — Three areas selected for weld repair are: (A) vane-locating lug radius, (B) edge of air vent, and (C) forward exterior flange	17
5	Aft View of Inconel 713c F100 TOBI	18
6	White-Light (top) and Black-Light (bottom) Photomacrographs of Typical Defects Detected by Fluorescent Dye Penetrant Inspection of As-Cast Inconel 713c F100 TOBI Aft Interior Flange	19
7	White-Light (top) and Black-Light (bottom) Photomacrographs of Typical Defects Detected by Fluorescent Dye Penetrant Inspection of As-Cast Inconel 713c F100 TOBI Forward Air Vent	20
8	Weld Preparation (Arrow) on Inconel 713c F100 TOBI Forward Air Vent	21
9	Weld Preparation (Arrow) in the Body of Inconel 713c F100 TOBI at the Radius of a Vane-Locating Lug	21
10	Views of Weld Preparation on Inconel 713c F100 TOBI Forward Exterior Flange	22
11	Fracture Surface of Inconel 625 Specimen (No. 14) Illustrating Lamellar Failure Along Primary Dendrite Direction	34
12	As-Welded Repair on Inconel 713c F100 TOBI Forward Exterior Flange	35
13	As-Welded Repair on Inconel 713c F100 TOBI Forward Air Vent	36
14	As-Welded Repair on Inconel 713c F100 TOBI Vane-Locating Lug	36
F-1	Tensile and Stress-Rupture Mechanical Test Specimen (Weld Bead Ground Flush)	53
G-1	Microstructure of AFC-4-6 Weldment in As-Welded Condition — Weld metal microstructure consists of γ matrix, fine γ', acicular and blocky CbC carbides and script (Ta, Cb)C carbides	59
G-2	Microstructure of AFC-4-6 Weldment after Thermal Exposure at 843°C (1550°F) for 48 Hours — Weld metal microstructure consists of γ matrix, fine γ', and predominantly script (Ta, Cb)C carbides. Note hot crack in heat-affected zone	61

LIST OF ILLUSTRATIONS (Continued)

Figure		Page
G-3	Microstructure of AFC-4-6 Weldment after Thermal Exposure at 843°C (1550°F) for 200 hours — Weld metal microstructure consists of γ matrix, fine γ', matrix (Ta, Cb)C carbides, heavy grain boundary (Cr, Mo)$_{23}$C$_6$ carbides and evidence of Ni$_3$ (Ta, Cb) — δ and Ni$_3$ (Ta, Cb) Laves phase	63
G-4	Photomicrograph of (Cr, Mo)$_{23}$C$_6$ Carbide in Grain Boundary Within Weld Metal of AFC-4-6 Weldment after Thermal Exposure at 843°C (1550°F) for 200 Hours	64
G-5	Scanning Electron Microscope Photomicrograph of Weld Metal in AFC-4-6 Weldment after Thermal Exposure at 843°C (1550°F) for 200 Hours	64
G-6	Microstructure of As-Welded AFC-6-7 Weldment — Weld metal microstructure consists of γ matrix, fine γ', and small, blocky (Cb, Ti, Ta)C carbides	65
G-7	Microstructure of AFC-6-7 Weldment after Thermal Exposure at 843°C (1550°F) for 48 Hours — Weld metal microstructure consists of γ matrix, fine γ' and small, blocky (Cb, Ta, Ti)C carbides. Note hot crack in heat-affected zone	67
G-8	Microstructure of AFC-6-7 Weldment after Thermal Exposure at 843°C (1550°F) for 200 Hours — Weld metal microstructure consists of γ matrix, fine γ', (Cb, Ta, Ti)C and (Cb, Ta)C carbides and traces of Ni$_3$(Cb, Ta)-δ. Note shrinkage porosity in heat-affected zone	69
G-9	Scanning Electron Microscope Photomicrograph of Weld Metal in AFC-6-7 Weldment after Thermal Exposure at 843°C (1550°F) for 200 Hours	70
G-10	Microstructure of As-Welded C-4 Weldment — Weld metal consists of γ matrix, fine γ', blocky CbC carbides, and some script (Ta, Cb)C carbides	71
G-11	Microstructure of C-4 Weldment after Thermal Exposure at 843°C (1550°F) for 48 Hours — Weld metal microstructure consists of γ matrix, fine γ', and predominantly script (Ta, Cb)C carbides	73
G-12	Microstructure of C-4 Weldment after Thermal Exposure at 843°C (1550°F) for 200 Hours — Weld metal microstructure consists of γ matrix, fine γ', blocky (Ta, Cb)C carbides, heavy grain boundary (Cr, Mo)$_{23}$C$_6$ carbides and needles of Ni$_3$(Cb, Ta)-δ	75
G-13	Microstructure of As-Welded Inconel 625 Weldment — Weld metal microstructure consists of γ matrix, fine γ', CbC carbides, and script (Cb, Ta)C carbides	77

LIST OF ILLUSTRATIONS (Continued)

Figure		*Page*
G-14	Microstructure of Inconel 625 Weldment after Thermal Exposure at 843°C (1550°F) for 48 Hours — Weld metal microstructure consists of γ matrix, fine γ', CbC and (Ta, Cb)C carbides, and heavy grain boundary $(Cr, Mo)_{23}C_6$ carbides	79
G-15	Microstructure of Inconel 625 Weldment after Thermal Exposure at 843°C (1550°F) for 200 Hours — Weld metal microstructure consists of γ matrix, fine γ', CbC and (Cb, Ta)C carbides, and very heavy grain boundary $(Cr, Mo)_{23}C_6$ carbides	81
G-16	Location of Data Points for Concentration Profile in Filler Metal AFC-4-6 Weldment	82
G-17	Location of Data Points for Concentration Profile in Filler Metal AFC-6-7 Weldment	82
G-18	Location of Data Points for Concentration Profile in Filler Metal C-4 Weldment	83
G-19	Location of Data Points for Concentration Profile in Weld Metal of Filler Metal AFC-4-6 Weldment	83
G-20	Elemental Trends in AFC-4-6 Weld Metal Composition	84

LIST OF TABLES

Table		Page
1	Filler Metal Compositions	4
2	Tensile Test Schedule	15
3	Stress Rupture Test Schedule	16
4	Filler Metal Melting Behavior	23
5	Task 1 Initial Hot Cracking Results	24
6	Task 1 Supplemental Hot Cracking Results	25
7	Post-Weld Heat-Treatment Cracking Results	27
8	Task 2 Hot Cracking Results	27
9	Task 2 INCONEL 713c Post-Weld Heat-Treatment Cracking Results	29
10	Microstructure Phase Identification in INCONEL 713c Weld Metal	30
11	871°C (1600°F) Tensile Properties of Experimental Filler Metal Weldments in INCONEL 713c	30
12	871°C (1600°F) Weldment Tensile Properties	31
13	760°C (1400°F) Weldment Tensile Properties	31
14	871°C (1600°F)/317 MPa (46 ksi) Weldment Stress-Rupture Properties	32
15	760°C (1400°F)/552 MPa (80 ksi) Weldment Stress-Rupture Properties	33
G-1	Microstructure Phase Identification in INCONEL 713c Weld Metal	55
G-2	Concentration Profile for Filler Metal AFC-4-6 Weldment; Composition in Weight % by Location	56
G-3	Concentration Profile for Filler Metal AFC-6-7 Weldment; Composition in Weight % by Location	57
G-4	Concentration Profile for Filler Metal C-4 Weldment; Composition in Weight % by Location	57
G-5	Concentration Profile in Weld Metal of Filler Metal AFC-4-6 Weldment; Composition in Weight % (Atomic %) by Location	57

SUMMARY

The objective of this program was to optimize an age-hardenable weld filler metal composition for heat-affected zone (HAZ), hot-cracking-limited, nickel-base superalloy welding applications. Compositions of the alloys examined were based on the best filler metals previously developed under Air Force Materials Laboratory Contract F33615-75-C-5114. These alloys reduce HAZ cracking and are age-hardenable to high strength levels. Emphasis was placed on obtaining a filler metal which reduced HAZ hot cracking, because that accomplishment offers the best opportunity for early implementation of the improved filler metal.

This program was conducted in two phases. The object of Phase I was to identify an optimized filler metal composition; the applicability of the optimized alloy to superalloy welding was evaluated in Phase II.

In Phase I, Task 1, a screening study examined seven alloys. The two primary filler metal characteristics of interest in Task 1 were solidus temperature and HAZ hot cracking resistance. Prior experience has shown a strong correlation between HAZ hot cracking and solidus temperature, with alloys having lower melting temperatures being associated with less cracking. To obtain preliminary information on the weld metal microstructure and thermal stability, specimens were examined metallographically both as-welded and after a thermal exposure.

At the conclusion of Phase I, Task 1, the results obtained on the seven alloys were reviewed to identify the two most promising alloys for further evaluation in Task 2.

The object of Task 2 was to conduct a more comprehensive evaluation of the two selected candidate filler metals to provide a basis for identification of an optimized composition for characterization in Phase II. The ability of the selected filler metals to alleviate HAZ hot cracking and post-weld heat-treatment cracking was re-examined in greater depth, together with a more comprehensive investigation of weldment microstructure, thermal stability, and composition. In addition, a limited comparison was made by determing elevated-temperature tensile properties of weldments in the nickel-base superalloy Inconel 713c.

At the conclusion of Task 2, the results were reviewed to select an optimum alloy for evaluation in Phase II. The primary criterion for selection was the ability to reduce hot cracking; weldment strength and the metallurgical character of the weld also were considered as was post-weld heat-treatment cracking behavior.

During Phase II, the optimized filler metal was evaluated by conducting weld-repair trials on current engine hardware and by determining weldment mechanical properties. These properties were compared with those of C-4, a promising alloy identified in the prior contract, and with Inconel 625 weldment properties generated in simultaneous tests.

The application of the optimized filler metal to current engine hardware was demonstrated by welding an F100 Tangential On-Board Injector (TOBI) which is an Inconel 713c casting that is considered very difficult to weld. Mechanical properties were determined on welds made in Inconel 713c with the optimized filler metal, with C-4, and with Inconel 625. Tensile and stress-rupture testing was conducted at two service temperatures. Based on the Phase I results, AFC-6-7 was selected as the optimum alloy; the composition is:

Ni-balance, Cr-19.4, Fe-11.9, Ta-5.3, Cb-3.2, Ti-0.91, Al-0.78, Mn-2.7, C-0.02, B-0.016, and Zr-0.07.

PRECEDING PAGE BLANK-NOT FILMED

AFC-6-7 showed the best resistance to hot cracking, and the solidus temperature was in the lower group which, as in prior experience, correlated with improved resistance to hot cracking. Attempts to evaluate resistance to post-weld heat-treatment cracking did not produce definitive results, but the tests did indicate that the new filler metal will be equivalent to the existing filler metals, if not better.

No significant weld metal microstructure or phase thermal stability problems were encountered after elevated-temperature exposure with any of the filler metals examined.

Welds made with AFC-6-7 filler metal in Inconel 713c were found to have better elevated-temperature tensile and stress-rupture properties than welds made with the state-of-the-art filler metal, Inconel 625; AFC-6-7 filler metal weld properties were comparable with those of filler metal C-4. The mechanical properties advantage of AFC-6-7 over Inconel 625 is expected to be larger in welds with less base metal dilution.

AFC-6-7 was used in trial repairs of the F100 TOBI to demonstrate applicability to hardware. The alloy offered a weldability advantage in repairs of the more highly restrained forward air vent; no difference in weldability was observed in repairs of less restrained areas. Because AFC-6-7 is an age-hardenable alloy, the higher strength of the weld is expected to provide a more durable repair than can be achieved with the state-of-the-art filler metals. It is recommended that AFC-6-7 filler metal be used to weld repair engine components for engine test to better evaluate the viability of the alloy in an application under service conditions.

Additional testing of mechanical properties on welds with less base-metal dilution and testing to determine oxidation and hot-corrosion behavior would be useful in substantiating the applicability of the filler metal.

SECTION I
INTRODUCTION

1. STATEMENT OF PROBLEM AND OBJECTIVE

The application of fusion welding to the fabrication or repair of high-strength superalloy turbine components has been severely restricted because of the poor weldability of these materials. Weldability problems have increased with development of higher performance superalloys to the point that fusion welding is only used reluctantly, and in some situations, these superalloys are simply regarded as unweldable. Specifically, the weldability problems exist as heat-affected zone (HAZ) cracking in the base metal adjacent to the weld; the cracking can occur either at the time of welding or during subsequent thermal cycles. One traditional approach to avoid these problems has been the use of dissimilar, nonhardenable, nickel-base filler metals which result in low-strength, poor-durability welds.

The objective of this program was to optimize the composition of a new class of age-hardenable, nickel-base filler metals developed previously under Air Force Materials Laboratory Contract F33615-75-C-5114. The new class of alloys alleviated HAZ cracking while being age-hardenable to higher strength levels. The emphasis was placed on obtaining a filler metal that will reduce heat-affected zone hot cracking in nickel-base superalloys, because that accomplishment offers the best opportunity for early implementation of the improved filler metal, particularly in the repair of turbine components.

2. SUPERALLOY WELDABILITY PROBLEMS

Two types of HAZ cracking restrict fusion welding in nickel-base superalloys. At the time of welding, intergranular cracking — termed hot cracking — may occur just after passage of the arc or on cooling. A second form of cracking, also intergranular in mode, may occur during subsequent stress-relief or aging thermal cycles and is denoted as post-weld heat-treatment cracking. The metallurgical causes of these forms of cracking have been studied extensively. The studies, in essence, conclude that the causes are inherent and unavoidable characteristics of nickel-base superalloys.

In practice, cracking tendencies may be somewhat alleviated by design and welding procedures. Nonetheless, these forms of cracking severely restrict the fusion welding of superalloys. For example, the repair of casting defects encountered in the initial fabrication of superalloy turbine components is commonly impeded or prevented by hot cracking and post-weld heat-treatment cracking. This problem is a serious consideration in attempts to cast large turbine components, particularly in higher strength superalloys. Also, the repair of cast turbine components, such as vane airfoils, is susceptible to and limited by hot cracking. Post-weld heat-treatment cracking is encountered in the fabrication and repair of both cast and wrought superalloy components, and it has been a significant deterrent to the design of large welded components made from high-strength wrought alloys. One of the most difficult aspects of post-weld heat-treatment cracking is that once cracking occurs, attempts to repair weld the initial crack frequently generate additional cracking.

One important approach to avoiding the problems of hot cracking and post-weld heat-treatment cracking in superalloy welding has been to use dissimilar filler metals that tend to resist cracking. However, in most cases, the filler metals are not age-hardenable and thus are relatively weak when compared with the superalloy base metal. The resultant weld has significantly poorer properties than the base metal, and the component's structural integrity is compromised accordingly. Repair of turbine components cracked in service with a weld of lower strength than the base metal results in a shorter time to cracking in subsequent service.

Recognizing the problems and limitations associated with use of lower strength filler metals, the development of improved filler metals, combining both reduced cracking tendencies with the ability to be age-hardenable to high strength levels, represents a significant advance in the application of fusion welding to nickel-base superalloys.

3. PREVIOUS EXPERIENCE

As a result of extensive research on superalloy welding, the Pratt & Whitney Aircraft Group, Commercial Products Division (P&WA/Connecticut) developed a novel approach for reducing superalloy weldment cracking problems. Weld filler metals with uniquely tailored properties were added during fusion welding to favorably alter the stress/strain dynamics responsible for heat-affected zone hot cracking and post-weld heat-treatment cracking. The studies of various commercial and experimental filler metals for superalloy welding demonstrated that HAZ cracking can be strongly affected by weld filler metal characteristics, but not in a manner as would be commonly predicted. A positive correlation was found between filler metal solidus temperature and HAZ hot cracking problems. A series of experimental filler metals containing manganese additions to lower the solidus temperature were shown to produce the least amount of HAZ hot cracking in cast Inconel 713c as compared to a variety of widely used commercial filler metals and other experimental compositions. In addition to reducing cracking, the filler metals containing manganese are age-hardenable and thus are capable of superior weldment mechanical properties.

To further develop and characterize these weld filler metals, a program was conducted by the Pratt & Whitney Aircraft Group, Commercial Products Division, under Air Force Materials Laboratory Contract F33615-75-C-5114. The program further developed age-hardenable filler metals that reduce weld HAZ hot cracking in nickel-base superalloys under laboratory test conditions. The limited evaluation of the improved filler metals to determine their potential value for engineering applications demonstrated good weldment mechanical properties and oxidation behavior. Fabrication of wire in these compositions by conventional means appears feasible. Investigations of weldment microstructural stability and base metal dilution effects on weldability were not conclusive. Based on the results obtained, the improved filler metals were considered suitable for further optimization and implementation in engineering applications.

For the range of filler metals investigated, the property that had the greatest influence on hot cracking again was the solidus temperature. Alloys having lower solidus temperatures reduced HAZ hot cracking. The relationship between filler metal properties and post-weld heat-treatment cracking is not fully understood, but it appears to depend on whether or not the alloy is age-hardenable. Nonhardenable alloys, such as Hastelloy W, reduce post-weld heat-treatment cracking because the lower strength weld preferentially strains to accommodate stress relaxation as anticipated. Contrary to expectations, the resistance to post-weld heat-treatment cracking of the age-hardenable filler metals did not correlate with strength, stress-relaxation rate, or aging behavior; however, this may have been influenced by test conditions. The resistance to hot cracking and post-weld heat-treatment cracking of the age-hardenable alloys shows a general correlation.

SECTION II
DESCRIPTION OF FILLER METALS

1. ALLOY DESIGN APPROACH

The approach to alloy design which was successful in the prior work was to develop alloys which had a lower solidus temperature and potentially slower aging kinetics. It was found that the addition of manganese as a melting point depressant was uniquely beneficial. Alloys strengthened by gamma double prime (γ'') plus gamma prime (γ') precipitates were considered potentially advantageous alloys for the control of post-weld heat-treatment cracking because of the relatively slow precipitation kinetics of the body centered tetragonal γ'' phase. Although the effects of aging kinetics were not demonstrated in the previous contract, the alloys strengthened by γ'' plus γ' precipitates were better, in general, than those strengthened by γ' precipitates.

2. PREVIOUS ALLOYS

As described earlier, two very promising filler metals, designated C-4 and C-6, were developed in the previous contract, and they provide the basis for composition modifications to achieve an optimized alloy in this program. Both alloys are strengthened by γ'' plus γ' precipitates. They are of similar compositions, as shown in Table 1, where they are the first two alloys listed. These alloys are modifications of a promising earlier γ'' plus γ' experimental alloy which was a derivative of Inconel 718. The modifications to the earlier composition include substituting tantalum for aluminum, titanium and/or columbium; and increasing iron and molybdenum contents. Tantalum was expected to (1) partially partition to γ'', (2) slow the γ' phase precipitation kinetics, and (3) have less tendency to segregate on solidification. Iron should increase the tendency to form γ''. Molybdenum is a solid solution strengthener of the γ matrix particularly at higher temperatures.

3. FORMULATION OF ALLOYS FOR THIS PROGRAM

The compositions of the seven filler metals which were evaluated in the current contract are shown in Table 1. These compositions are modifications of the two most promising filler metals from the previous contract (C-4 and C-6) which were just discussed. The primary objectives of these modifications were to optimize manganese level and to enhance alloy microstructure thermal stability while maintaining or improving resistance to hot cracking.

Manganese had been recognized as a critical alloying element in the initial development of this class of filler metals. Further effort was made to better define the optimum manganese level. The role of manganese in the filler metals is not completely understood; however, it was found to be beneficial in P&WA work prior to the previous contract where better results were achieved when small amounts of manganese were added to otherwise identical alloys. For example, additions of 0.5 to 2% manganese to Inconel 718 and Waspaloy favorably influenced resistance to HAZ cracking. Manganese is recognized as a melting point depressant in nickel-base alloys, and prior work has correlated hot cracking resistance with filler metals having lower solidus temperatures.

New alloys AFC-6-1 and -6-2 are modifications of alloy C-6; they contain both lower and higher manganese levels than alloy C-6.

The investigation of weldment microstructure phase thermal stability in the previous contract detected sigma phase formation. Although the conditions surrounding the sigma formation did not permit unambiguous conclusions, this aspect of these alloys was studied further and composition modifications to enhance stability were expected to be beneficial.

TABLE 1
FILLER METAL COMPOSITIONS

Filler Metal	*Ni*	*Cr*	*Mo*	*Fe*	*Ta*	*Cb*	*Ti*	*Al*	*Mn*	*C*	*B*	*Zr*
C-4	Bal	19.0	3.5	12.5	7.2	4.8	—	0.98	0.5	0.01	0.018	0.01
C-6	Bal	19.7	3.6	15.3	5.3	3.3	1.0	0.7	1.2	0.02	0.016	0.01
AFC-6-1	Bal	19.6	3.7	15.2	5.2	3.2	0.8	0.69	0.67	0.03	0.016	0.09
AFC-6-2	Bal	19.7	3.7	15.1	5.2	3.2	1.0	0.75	2.5	0.02	0.017	0.07
AFC-6-3	Bal	19.7	—	12.0	5.3	3.1	0.8	0.69	1.2	0.03	0.013	0.09
AFC-4-4	Bal	19.0	—	12.4	7.2	3.0	—	0.96	1.2	0.04	0.018	0.09
AFC-4/11-5	Bal	19.2	—	11.9	3.1	3.0	—	0.94	1.2	0.03	0.018	0.09
AFC-4-6	Bal	18.8	—	12.5	7.4	2.8	—	1.01	2.8	0.01	0.015	0.06
AFC-6-7	Bal	19.4	—	11.9	5.3	3.2	0.91	0.78	2.7	0.02	0.016	0.07

Consequently, molybdenum was omitted from three alloys, AFC-6-3, -4-4, and -4/11-5, because molybdenum is recognized as contributing to the formation of sigma phase; also, results from the previous contract suggest that it may favor the formation of Laves phase in this class of alloys. (Laves was observed in the alloy with highest molybdenum content.) Iron was reduced in AFC-6-3 in a general attempt to improve stability; specifically, iron contributes to the formation of Laves phase (while favoring the beneficial γ' precipitate). The tantalum level was lowered in alloy AFC-4/11-5; previous work suggests that tantalum may contribute to sigma phase formation and a leaner alloy would be generally more desirable. Based on results of preliminary weldability trials conducted during the initial phases of the current program, two additional filler metals were formulated. Compositions of these alloys, which are designated AFC-4-6 and -6-7, are shown in Table 1.

The alloy designated AFC-4-6 was derived from AFC-4-4 which showed promise in hot cracking resistance and very little intergranular precipitation in the weldment after thermal exposure. The manganese level in AFC-4-6 was increased to 2.5% from 1.2% in AFC-4-4 because of the beneficial effects of manganese discussed earlier. The second additional filler metal was designated AFC-6-7, and it was derived from alloys AFC-6-2 and -6-3 which showed promise. AFC-6-7 was designed to have no molybdenum, less iron (12.0%) and higher manganese (2.5%); the effects of these alloying elements also have been discussed previously.

SECTION III
PROGRAM DESCRIPTION

This section describes the program plan and notes the experimental approaches used to achieve specific objectives in the plan. Details of the experimental techniques are discussed in Section IV.

1. OBJECTIVE

The objective of this program was to optimize an age-hardenable weld filler metal composition for heat-affected zone (HAZ), hot-cracking-limited, nickel-base superalloy welding applications. Compositions of the alloys examined were based on the best filler metals previously developed under Air Force Materials Laboratory Contract F33615-75-C-5114. These alloys reduce HAZ cracking and are age-hardenable to high strength levels. Emphasis was placed on obtaining a filler metal which reduced HAZ hot cracking, because that accomplishment offers the best opportunity for early implementation of the improved filler metal.

2. PROGRAM PLAN

The program was conducted in two phases. The object of Phase I was to identify an optimized filler metal composition; the applicability of the optimized alloy to superalloy welding was evaluated in Phase II. A promising alloy from the previous contract (designated alloy C-4) and a typical nonhardenable commercial filler metal (Inconel 625) also were evaluated in Phase II for comparison. A flow diagram of the program is shown in Figure 1; a detailed description follows.

a. Phase I, Task 1 — Composition Modification Study

This screening study examined seven alloys. Five alloys were examined initially; then based on these results, two additional alloys were selected.

The two primary filler-metal characteristics of interest in Task 1 were solidus temperature and HAZ hot cracking resistance. Prior experience has shown a strong correlation between HAZ hot cracking and solidus temperature — alloys with lower melting temperature are associated with less cracking.

The melting behavior of the filler metals was determined through the use of a differential thermal analyzer (see Section IV.1b).

The ability of the filler metals to alleviate HAZ hot cracking was evaluated in a weldability test described in Section IV.1c. Initially, four tests were made with each filler metal and Inconel 713c base metal weldability test specimens. As in prior work, the number of HAZ cracks observed was used to judge the relative hot cracking resistance. During this initial investigation, difficulty was encountered with this test which did not produce results that clearly discriminated between the alloys. Consequently, a newly acquired automatic welding machine which provided better control of welding parameters was used to perform additional testing of the five most promising alloys.

In addition to determining the resistance to hot cracking, an attempt was made to use the hot cracking specimens to gain a preliminary indication of the resistance to post-weld heat-treatment cracking. This approach was not successful; post-weld heat treatment cracking was evaluated again in Task 2.

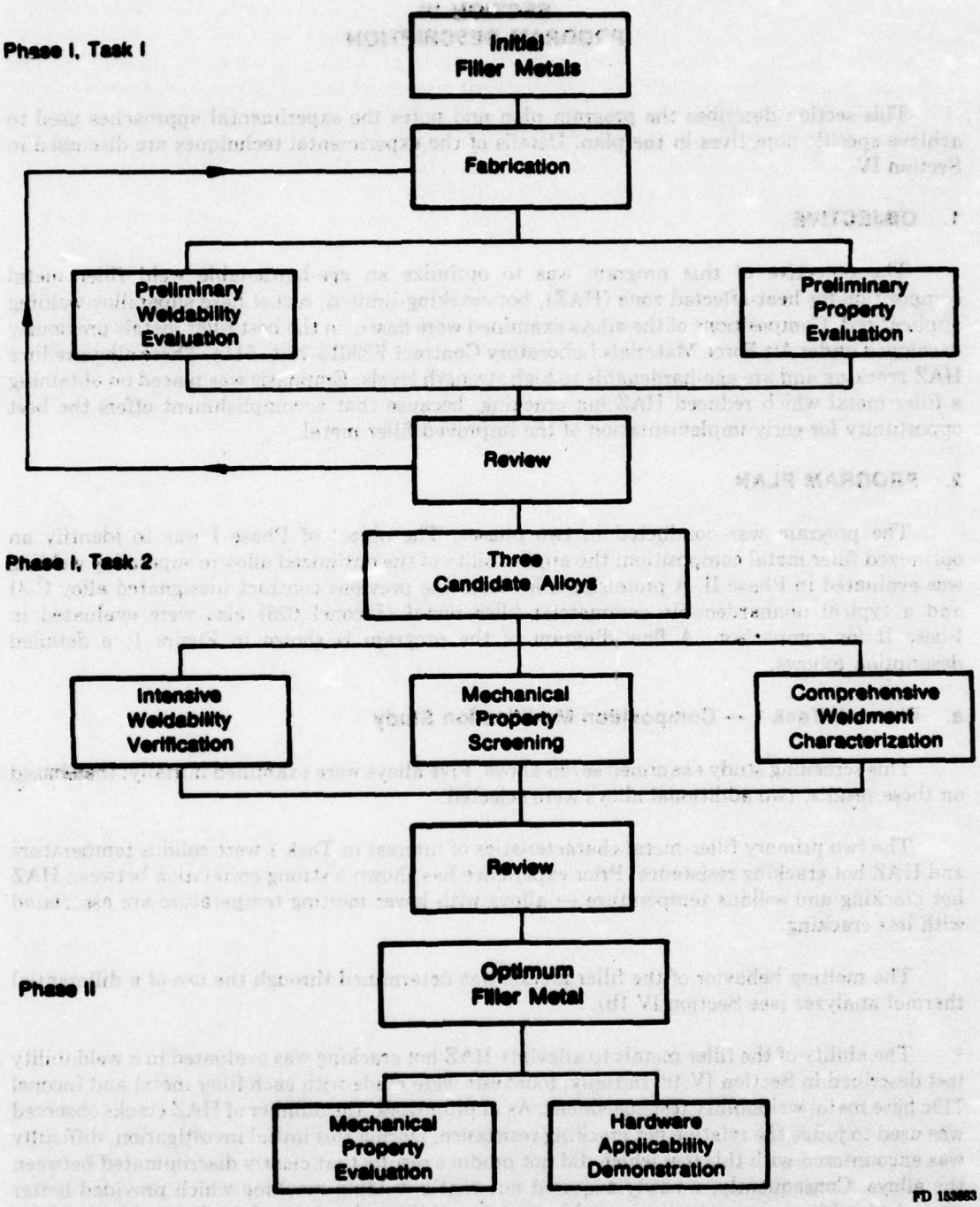


Figure 1. Superalloy Filler Metal Optimization Program Flow Diagram

To obtain preliminary information on the weld metal microstructure and thermal stability, the hot cracking weldability test specimens were examined metallographically both as-welded and after a thermal exposure at a representative turbine component service temperature. The weld metal microstructure, stability, and composition were characterized more comprehensively in Task 2.

At the conclusion of Phase I, Task 1, the contractor and the Program Monitor reviewed the results obained on the seven alloys and identified the two most promising alloys for further evaluation in Task 2. In addition, alloy C-4 from the previous contract and Inconel 625 were included in Task 2 for comparison.

b. Phase I, Task 2 — Candidate Alloy Evaluation

The object of Task 2 was to conduct a more comprehensive evaluation of the two selected candidate filler metals to provide a basis for identification of an optimized composition for characterization in Phase II. The ability of the selected filler metals to alleviate HAZ hot cracking and post-weld heat-treatment cracking was reexamined in greater depth, together with a more comprehensive investigation of weldment microstructure, thermal stability, and composition. In addition, a limited comparison was made by determining the mechanical properties of the resulting weldment in Inconel 713c. This work is described in more detail in the following paragraphs.

Five additional hot cracking weldability tests were conducted with each filler metal to provide a broader data base. These specimens also were used for the weldment characterization investigation described below.

Since the compositions of improved filler metals are somewhat unique among commercial nickel-base alloys, it was important to investigate the metallurgical nature of the resulting weldments. In addition to identifying the microstructural constituents and weld composition profile, the thermal stability of the weldment microstructure was studied, because the possibility of sigma phase in weld metal was noted in the previous program.

The propensity for post-weld heat-treatment cracking of welds in Inconel 713c made with the candidate filler metals was investigated using techniques described in Section IV.1.d. Although the primary program objective was to obtain a filler metal for hot-cracking-limited superalloy welding applications, resistance to post-weld heat-treatment cracking also was important. Welds were made on Inconel 713c and exposed to a 4-hour, 843°C (1550°F) thermal cycle.

An important advantage of this class of filler metals is their capacity to age-harden to higher strength levels than can be achieved with commercial nonhardenable filler metals. This advantage increases in significance at elevated temperatures where the hardening precipitates more strongly influence properties. To compare the strengths, 871°C (1600°F) tensile tests were conducted on specimens machined from butt welds between Inconel 713c cast plates.

At the conclusion of Task 2, the results were reviewed to select an optimum alloy for evaluation in Phase II. The primary criterion for selection was the ability to reduce hot cracking; weldment strength and the metallurgical character of the weld also were considered as was post-weld heat-treatment cracking behavior. The results and basis for selection of the alloy for Phase II were discussed with and agreed upon by the Air Force Materials Laboratory Program Monitor.

c. Phase II — Alloy Evaluation

During Phase II the optimized filler metal was evaluated by weld repairing a limited amount of selected current engine hardware and by determining weldment mechanical properties. These properties were compared with those of C-4, a promising alloy identified in the prior contract, and with Inconel 625 weldment properties generated in simultaneous tests.

The application of the optimized filler metal to current engine hardware was demonstrated by welding an F100 Tangential On-Board Injector (TOBI) which is an Inconel 713c casting that is considered very difficult to weld due to the high restraint conditions present and to the base metal. Serious casting difficulties have resulted in a high rejection rate and attempts to weld repair these defects have had little success.

Mechanical properties were determined on welds made in Inconel 713c with the optimized filler metal and with C-4 and Inconel 625. Tensile and stress-rupture testing was conducted at two representative service temperatures.

SECTION IV
EXPERIMENTAL PROCEDURES

1. PHASE I PROCEDURES

a. Wire Fabrication

Wire, 2.5 mm (0.100 in.) in diameter for Phase I weldability testing and 0.76 mm (0.030 in.) in diameter for the Phase II hardware welding demonstration, was fabricated by swaging from 12.7-mm (0.5-in.) diameter arc-melted, drop-cast bars. The bars had been made from a 500-gm (one-lb) arc-melted master billet. A detailed description of the fabrication procedure is provided in Appendix A.

Compositions were verified through conventional analytical chemistry procedures on samples taken from the drop castings.

b. Melting Behavior Determination

A small sample of each alloy was taken from the filler metal wires and used to determine melting behavior: incipient melting, solidus and liquidus temperatures. A Dupont Model 900 Differential Thermal Analyzer was used to determine the melting behavior with the procedure described in Appendix B.

c. Hot Cracking Weldability Testing

(1) Weldability Test Specimen Fabrication

The hot cracking weldability specimens were cast and machined to the same configuration used in the previous contract (Figure 2). The specimens were cast in Inconel 713c, an alloy highly susceptible to hot cracking. The majority of specimens used in the program were cast from the same heat of material, and all casting was done on the same day in order to maximize uniformity. A second group of specimens was used for additional testing in Task 1. The same precautions as used for the first group were used in the preparation of this second group of specimens; however, they were made from a different heat of Inconel 713c. Details of the casting procedure are found in Appendix C. Preparation of the specimen edges for welding (as shown in Figure 2) and other machining required to ensure good fit-up in the weldability test restraint fixture was accomplished by grinding in the manner commonly employed for nickel-base superalloys.

(2) Welding Procedure and Examination

The initial Task 1 hot cracking weldability tests were conducted in the same manner used in the prior contract with minor modifications to the welding parameters to improve weld bead geometry by reducing drop-through. Later in the program, testing utilized a recently acquired automatic gas tungsten arc welding system, since it provided superior control of parameters as discussed below. The test specimens and restraint fixture were the same throughout the program.

Hot-cracking tests were conducted with the tapered, cast-to-shape specimens described above. The specimens were held mechanically in a massive fixture (Figure 3) which provided the high restraint needed to obtain cracking. As mentioned, the specimen edges were prepared by grinding to the configuration shown in Figure 2. The specimens were cleaned in acetone and assembled in the test fixture (Figure 3). A single length of 2.5-mm (0.100-in.) diameter filler wire (corresponding to about 8.5 to 9.0 grams) was tack-welded in place at the ends. This amount of wire resulted in a weld nugget of approximately 30 to 40% filler metal.

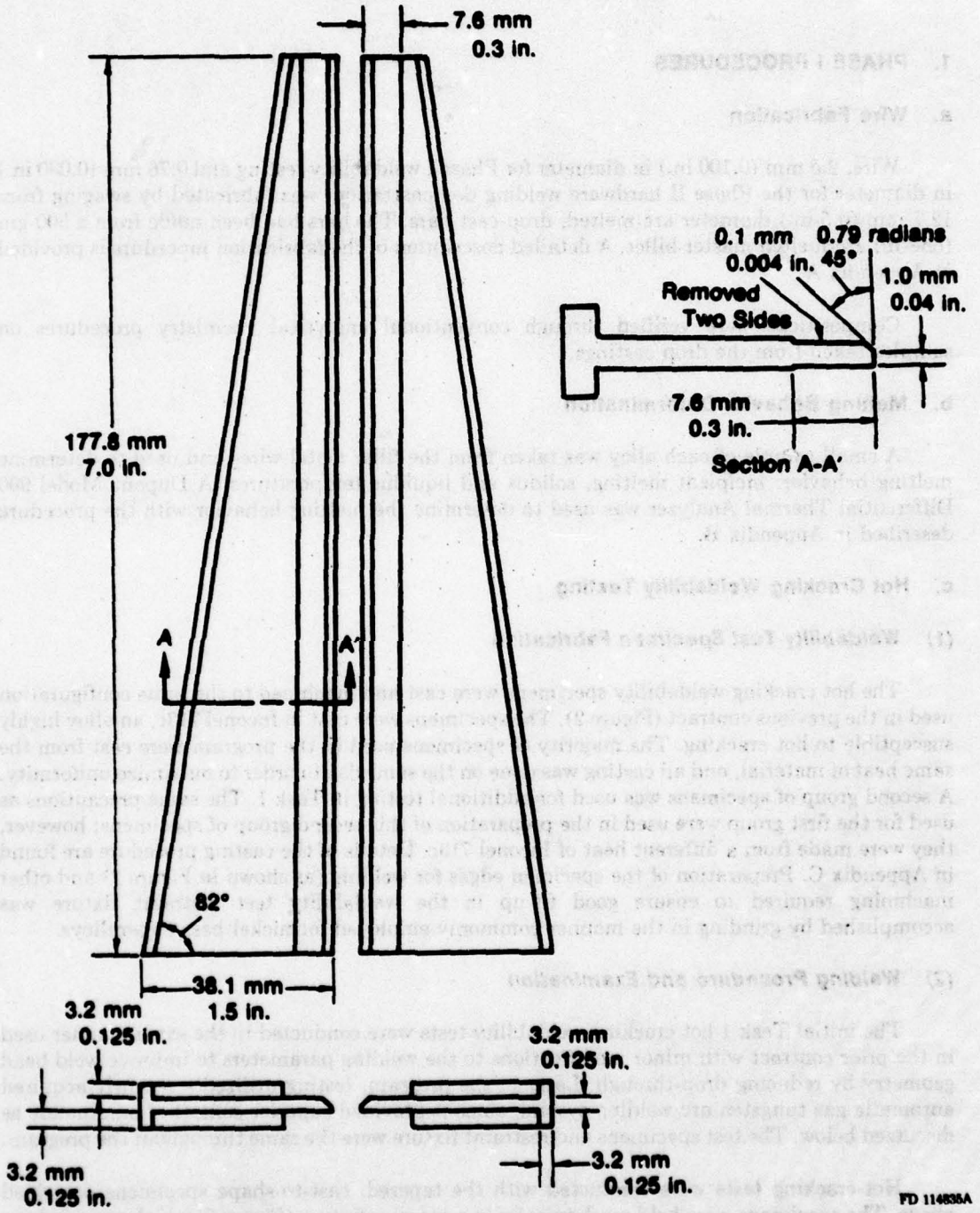
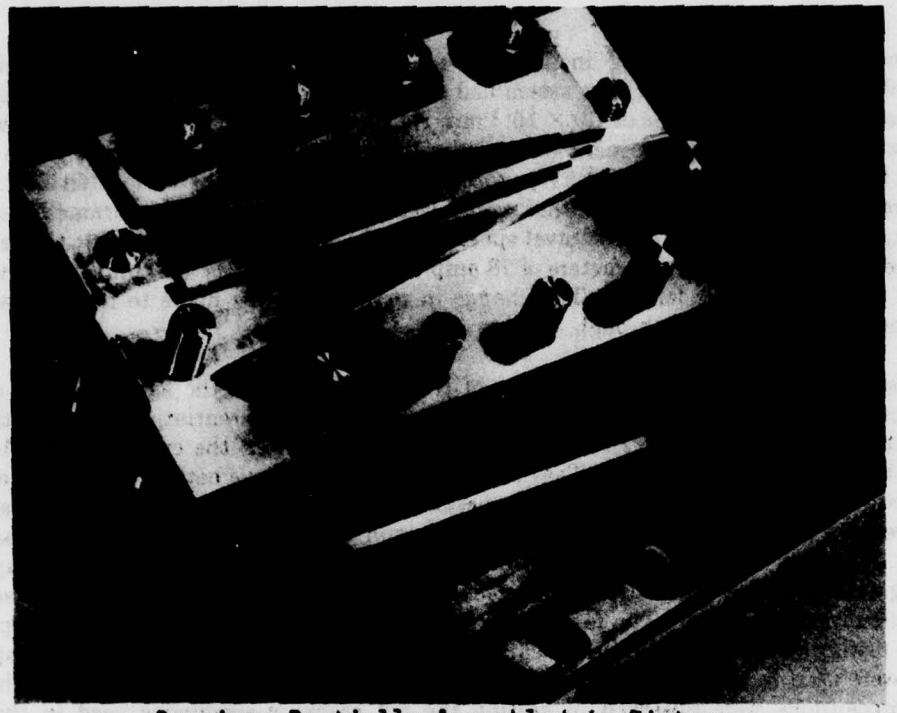
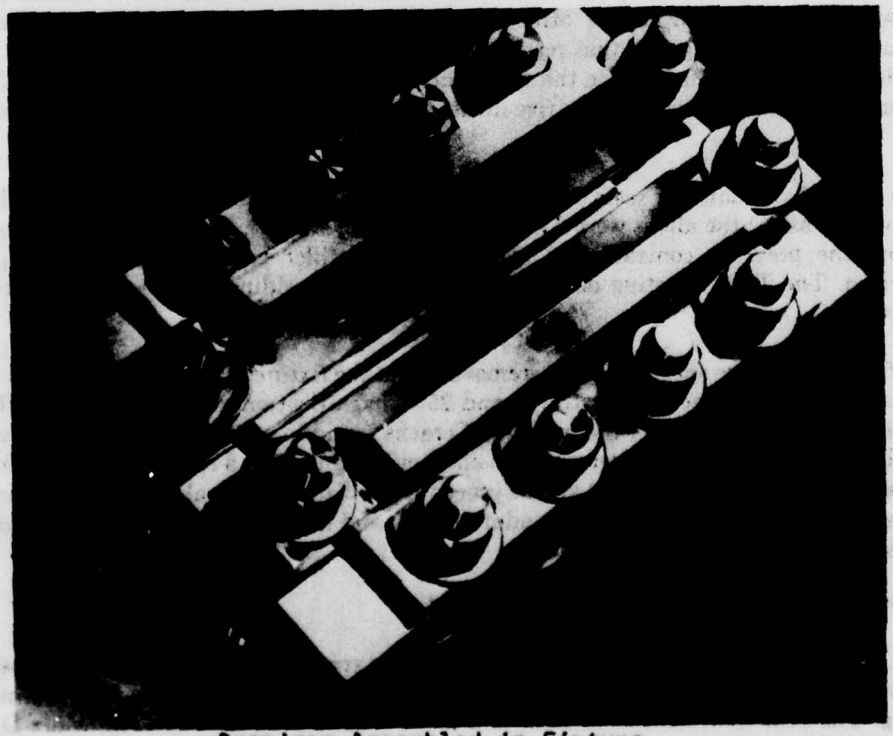


Figure 2. Tapered Hot Cracking Test Specimen



Specimen Partially Assembled in Fixture



Specimen Assembled in Fixture

FD 148832

Figure 3. Massive Stainless Steel Hot Cracking Weldability Test Fixture and Cast Nickel-Base Superalloy Test Specimen

During the initial testing in Task 1, welding was accomplished in a vacuum/inert-atmosphere welding chamber. The assembled specimen and restraint fixture was placed in the chamber, a vacuum in excess of 1.0×10^{-4} mm Hg was established and the chamber was back-filled with high-purity argon inert gas to atmospheric pressure. The specimen was machine welded by the gas tungsten arc (GTAW) process utilizing a straight, bare tungsten electrode. The first two tests (of the four tests per filler metal) were conducted with weld parameters of 75 amp current, 1.1 mm/sec (2.6 in./min) travel speed, and 15 volts (set by arc length); the second two tests were performed with parameters of 78 amp current, 1.3 mm/sec (3.0 in./min) travel speed, and 15 volts (set by arc length). The change in parameters was made to improve weld bead geometry by reducing drop-through.

As discussed later, the initial series of tests, conducted in the same manner as in the previous contract, produced cracking results which made differentiation between the alloys difficult. This was due in part to the similarity of the alloys in the current work. Additional testing was conducted as a part of Task 1 in an attempt to achieve better results with a recently acquired welding system which provided superior control of welding parameters. The parameters used were 75 amp current, 0.85 mm/sec (2.0 in./min) travel speed, and 8.7 volts (set by arc length). Welding was done in an argon-flooded enclosure of the type commonly employed in welding small turbine components. A conventional GTAW torch was employed instead of the straight tungsten electrode. The Inconel 713c hot cracking specimens used in the supplemental Task 1 testing were from a different heat code and cast at a different time than the specimens which were used in the initial Task 1 testing and the subsequent Task 2 testing. Although the same precautions were observed in casting the hot cracking specimens used in the Task 1 supplemental testing, prior experience has shown that direct comparison of results cannot be made with those taken from the other group of specimens used in the initial Task 1 and subsequent Task 2 testing. For that reason these results can only be compared within the group. Five filler metals were compared in the supplemental testing; they include AFC-6-2, -6-3 and 4-4, considered the most promising of the five initial alloys, and AFC-4-6 and -6-7, the two additional alloys.

In Task 2, weldability tests were performed with the more promising alloys which were identified in Task 1; the alloys were AFC-4-6 and -6-7. In addition, tests were conducted on alloy C-4 from the previous contract and the commercial filler metal Inconel 625 to provide a comparison. The Task 2 testing used the newly acquired welding system and the latter set of parameters.

After welding, the specimens were removed from the fixture and examined for heat-affected zone cracks using fluorescent penetrants and 25× magnification visual inspection. This visual inspection involves counting of the number of cracks found in a given specimen, with variations in number of cracks from one filler metal to another being used as a relative index of weldability. The examiner must be experienced at this procedure to distinguish real cracks from other surface features in the HAZ, such as grain boundary offsets and deformation bands, which look similar to cracks.

d. Post-Weld Heat Treatment Cracking Test

In Task 1, two hot cracking specimens of the four specimens for each filler metal were given a post-weld heat-treatment in order to gain a preliminary indication of the extent of additional cracking. The heat-treatment conditions and test details are described in Appendix D.

As discussed later, the Task 1 post-weld heat treatment of the hot cracking specimens did not produce meaningful results. Consequently, another approach was utilized in Task 2.

Task 2 post-weld heat-treatment cracking tests were conducted on 3.2-mm (0.125-in.) thick by 31.7-mm (1.25-in.) by 101.6-mm (4.0-in.) slabs of Inconel 713c using bead-on-plate and edge welds. The filler metal was preplaced 2.5-mm (0.10-in.) diameter wire, and welds were made using the parameters from the hot cracking tests. Welding was followed by a thermal exposure at 843°C (1550°F) for 4 hr in argon [14°C/min (25°F/min) heating rate] in a resistance-heated box furnace. The numbers of cracks were determined as-welded and after heat treament by visual and fluorescent penetrant examination.

e. Microstructure, Phase Stability, and Composition Investigation

Microstructures of as-welded and thermally exposed welds taken from the Inconel 713c hot cracking specimens were examined by optical and electron metallography and the electron microprobe analyzer to characterize weld metal microstructure, possible microstructural changes, and composition. Details of the examination are described in Appendix E.

f. Mechanical Properties Testing

As part of Task 2, 871°C (1600°F) tensile tests were conducted on welds in Inconel 713c made with filler metals AFC-4-6, -6-7 and C-4 in order to provide a preliminary indication of mechanical properties. Specimen fabrication and testing details are presented in Appendix F. Ten tests were conducted. Four specimens welded with C-4 filler metal and three (each) specimens welded with either AFC-4-6 or AFC-6-7 filler metal were tested.

2. PHASE II PROCEDURES

a. Mechanical Properties Testing

(1) Specimen Fabrication

Phase II mechanical test specimens were prepared in the same manner as Phase I Task 2 specimens. Specimen fabrication details are presented in Appendix F.

(2) Tensile Testing

Tensile testing was conducted at either 871°C (1600°F) or at 760°C (1400°F). Testing was accomplished in accordance with the schedule presented in Table 2.

TABLE 2
TENSILE TEST SCHEDULE

	Number of Tests Conducted	
Filler Metal	*871°C (1600°F)*	*760°C (1400°F)*
AFC-6-7	2	3
C-4	2	3
Inconel 625	1	1

(3) Stress Rupture Testing

Stress rupture testing was conducted at either 871°C (1600°F)/317 MPa (46 ksi) or at 760°C (1400°F)/552 MPa (80 ksi). Testing was accomplished in accordance with the schedule presented in Table 3.

TABLE 3
STRESS RUPTURE TEST SCHEDULE

	Number of Tests Conducted	
Filler Metal	*871°C (1600°F)/317 MPa (46 ksi)*	*760°C (1400°F)/552 MPa (80 ksi)*
AFC-6-7	5	6
C-4	3	4
Inconel 625	5	6

b. Hardware Applicability Demonstration

The objectives of this task were to demonstrate the applicability of the optimized filler metal, AFC-6-7, to the welding of an engine component, and to compare the hardware welding behavior with that of a state-of-the-art filler metal, Inconel 625, and with that of alloy C-4 from the prior contract.

The Inconel 713c alloy F100 Tangential On-Board Injector (TOBI) was chosen for this work. A forward view of an as-cast TOBI is shown in Figure 4; an aft view is presented in Figure 5. The TOBI is an expensive part; and, because it is made of the highly cracking-susceptible Inconel 713c and is highly restrained, it is very difficult to weld. Casting defects, such as cold shuts, laps, and inclusions occur frequently and cannot be blended out and weld-repaired without severe cracking. Typical defects located by fluorescent-dye-penetrant inspection are on the aft interior flange (Figure 6) and on the forward air vent (Figure 7). Small hot tears were also observed on the vane-locating lug radius.

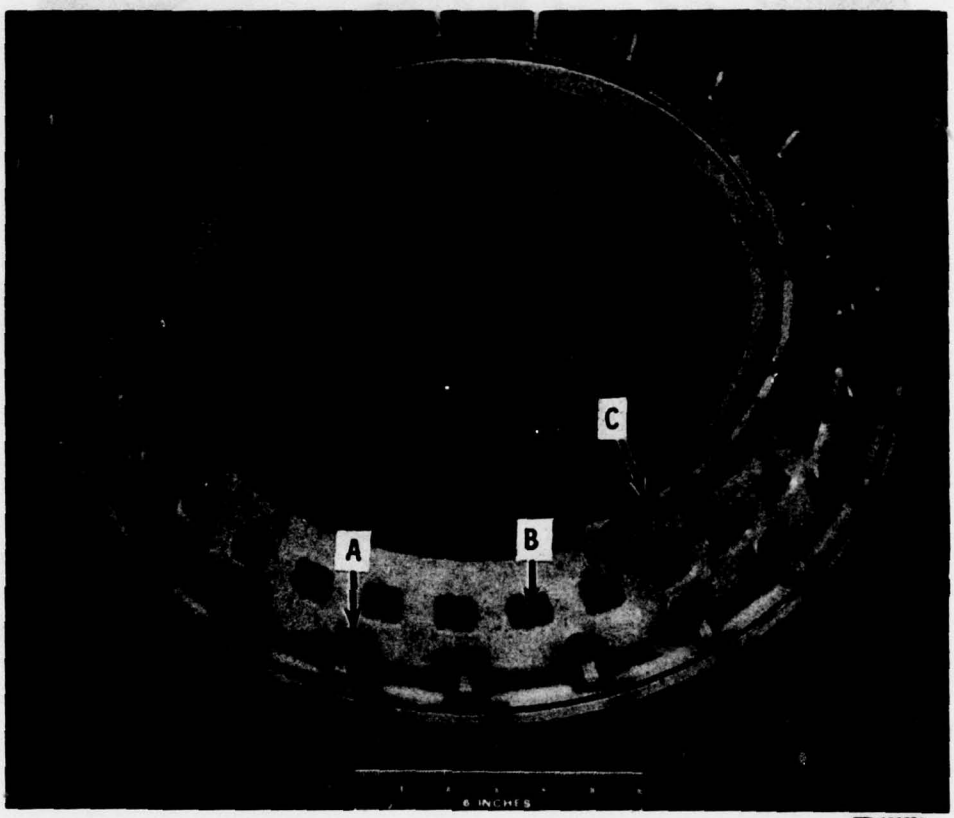
One as-cast TOBI, P/N 4037634, S/N 282, Heat Code 66-BVP, cast by Austenal LaPorte (vendor H/C BO1Δ) in July 1973 and not machined due to numerous fluorescent penetrant indications, was obtained for use in the weldability evaluation. Additionally, one retired TOBI, P/N 4043252, was obtained to determine weldability on engine-operated parts.

Three areas were used for the weld trials: an edge to the forward air vent, in the body of the TOBI at the radius of a vane-locating lug, and on the forward exterior flange. These areas are shown as prepared for welding in Figures 8, 9 and 10, respectively.

A prerequisite aspect of this task was the development of tentative weld repair procedures which did not exist for this 'unweldable' component. The development of a tentative weld repair procedure was accomplished through a series of trials. The procedure which evolved is described in the following text.

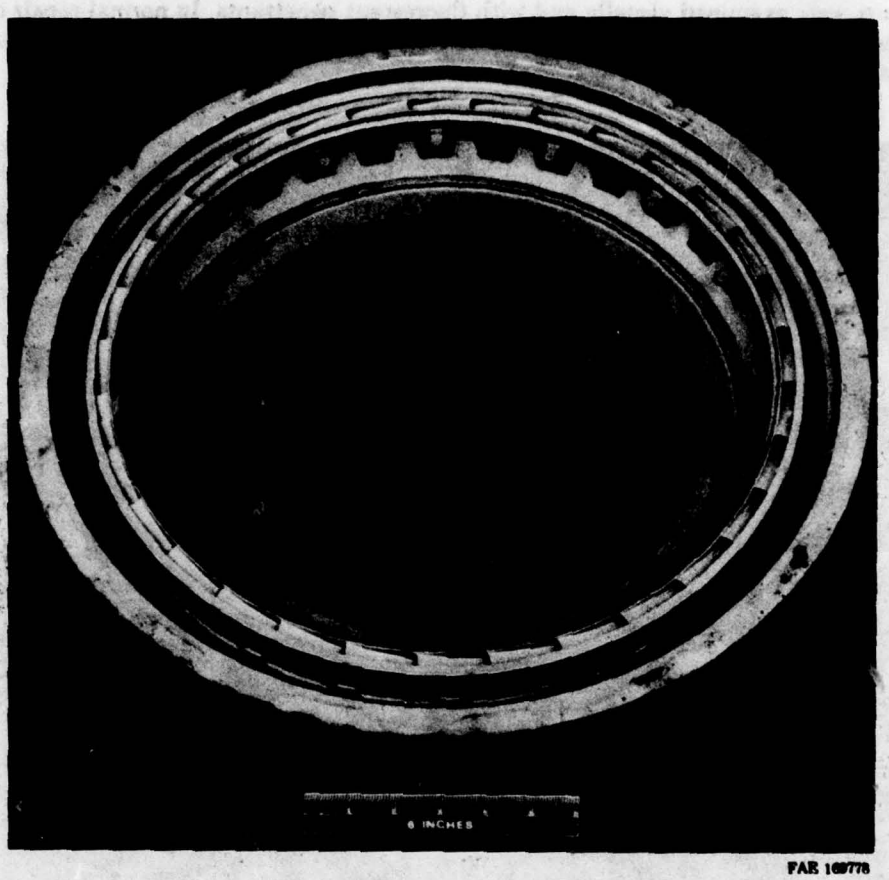
The 'defective' area was removed by hand grinding with an air-powered abrasive wheel to form preparations as shown previously. The resulting cavities were to have as large a radius as practical (while minimizing the depth); smaller radius U-shaped cross-section weld preparations were less satisfactory. Manual gas tungsten arc welding was employed in an argon atmosphere dry box. Actual welding parameters varied with the particular weld and the welders' judgement; the range of parameters used were: a current of 40 to 60 amps, an arc length of 1.6 mm (0.06 in.) to 2.4 mm (0.09 in.), and a welding speed of approximately 0.85 to 1.69 mm/sec (2 to 4 in. per min). The filler metal wire diameter was 0.76 mm (0.030 in.). Welding was done in a manner to 'butter-on' filler metal with as little power as possible to minimize base metal melting; the weld was allowed to cool to ambient temperature between passes. Where possible, the weld passes were terminated in locations of minimum restraint. For example, efforts were made to avoid ending a weld pass in a corner of the forward air vent. The welded parts were stress-relieved at 871°C

(1600°F) in a preheated resistance-heated box furnace with an argon atmosphere. After welding, the repairs were examined visually and with fluorescent penetrants. In normal repair operation the excess weld metal would have been blended (by grinding) back to the original contour; that step was omitted in this work.



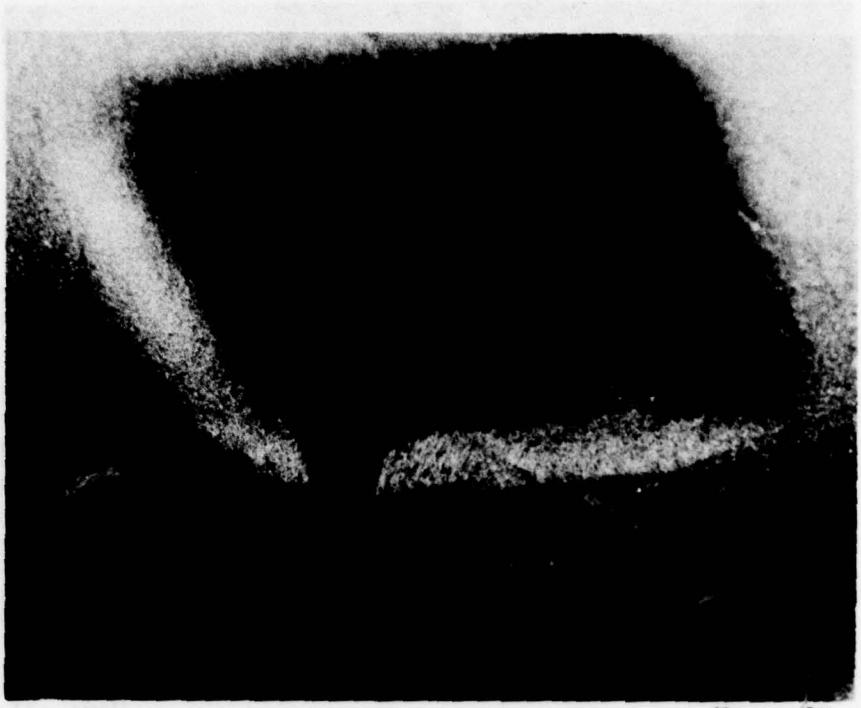
FD 159084

Figure 4. Forward View of Inconel 713c F100 TOBI — Three areas selected for weld repair are: (A) vane-locating lug radius, (B) edge of air vent, and (C) forward exterior flange

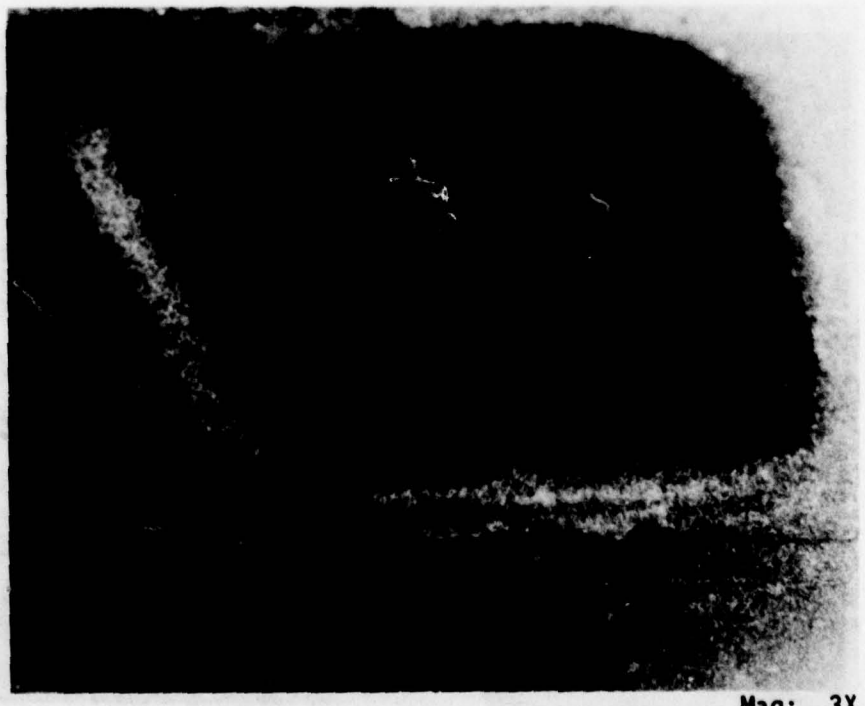


FAE 169778

Figure 5. Aft View of Inconel 713c F100 TOBI

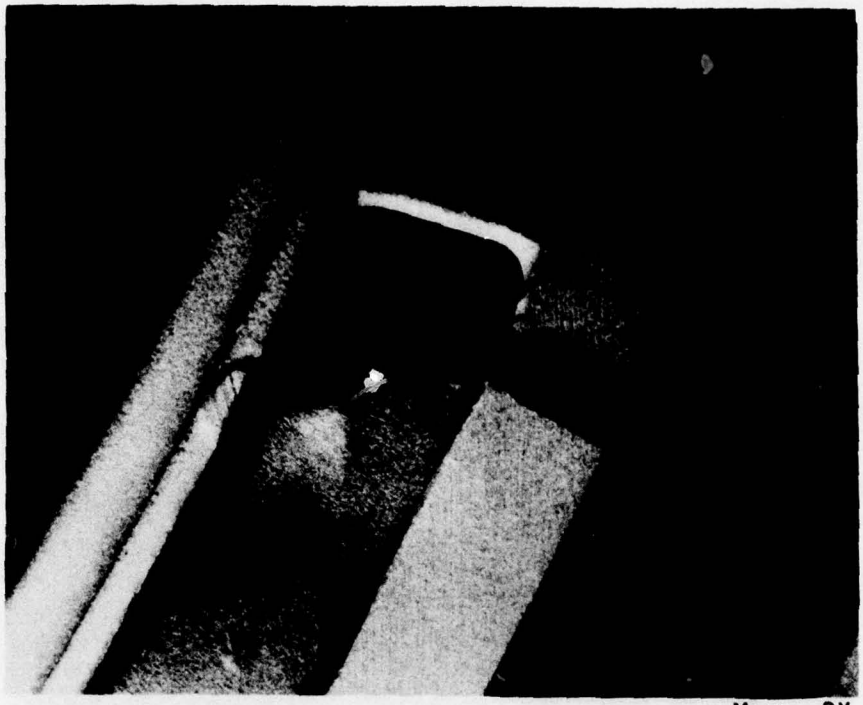


Mag: 3X



Mag: 3X
PD 183686

Figure 6. White-Light (top) and Black-Light (bottom) Photomacrographs of Typical Defects Detected by Fluorescent Dye Penetrant Inspection of As-Cast Inconel 713c F100 TOEI Aft Interior Flange



Mag: 3X



Mag: 3X
FD 153686

Figure 7. White-Light (top) and Black-Light (bottom) Photomacrographs of Typical Defects Detected by Fluorescent Dye Penetrant Inspection of As-Cast Inconel 713c F100 TOBI Forward Air Vent



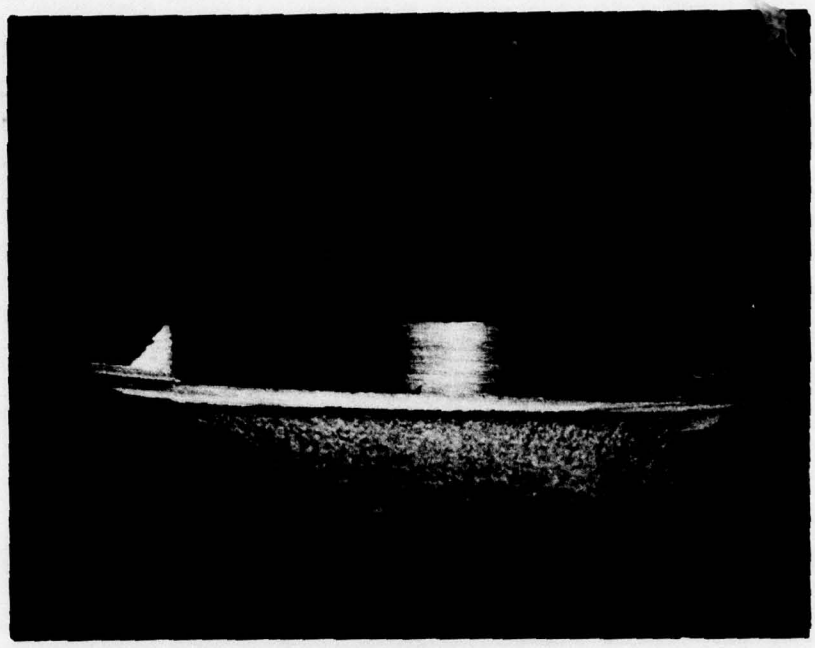
FD 153687

Figure 8. Weld Preparation (Arrow) on Inconel 713c F100 TOBI Forward Air Vent

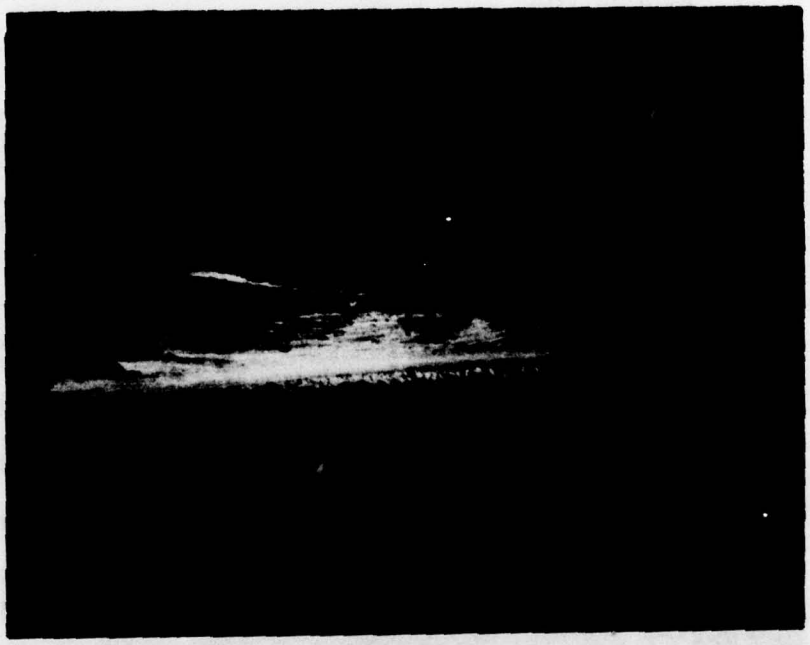


FD 153688

Figure 9. Weld Preparation (Arrow) in the Body of Inconel 713c F100 TOBI at the Radius of a Vane-Locating Lug



Top View



Side View

FD 153080

Figure 10. Views of Weld Preparation on Inconel 713c F100 TOBI Forward Exterior Flange

SECTION V
RESULTS AND DISCUSSION

1. PHASE I — TASK 1 RESULTS

The objective of Task 1 was to screen the seven previously described filler metals and to select the more promising alloys for further study in Task 2. The filler metal characteristics of primary interest were solidus temperature and heat-affected zone (HAZ) hot cracking resistance. A simple examination of post-weld heat-treatment cracking resistance also was attempted.

a. Alloy Compositions

Analyzed compositions of the seven alloys screened in Phase I, Task 1 are shown in Table 1. Also included for reference are the baseline alloys C-4 and C-6 from which the seven new compositions were derived. The analyses shown correspond closely to target compositions except for those alloys having carbon levels of 0.02 to 0.04%, which is higher than the intended amount of 0.01%. For perspective, the alloys studied in the previous contract had carbon levels ranging from 0.01 to 0.02%. Based on other weldability studies performed at Pratt & Whitney Aircraft Group, Commercial Products Division, the 0.01 to 0.02% increase in carbon level is not considered significant.

b. Melting Behavior

The melting behavior of the seven filler metals screened in Task 1 are presented in Table 4. The solidus temperatures of these alloys appear to fall into two groups. Alloys AFC-6-1 and -4/11-5 have solidus temperatures above 1260°C (2300°F); the remaining five alloys have lower solidus temperatures, ranging from 1221 to 1234°C (2230 to 2253°F). No attempt was made to compare alloying effects within each group, where the apparent differences are smaller than the estimated experimental accuracy of ±14°C (±25°F). Minor amounts of incipient melting were noted for five alloys; no particular significance related to weldability is attached to these indications.

TABLE 4
FILLER METAL MELTING BEHAVIOR

AFC	Incipient Melting		Solidus		Liquidus	
Filler Metal	(°F)	(°C)	(°F)	(°C)	(°F)	(°C)
6-1	2116	1158	2322	1272	2444	1340
6-2	2118	1159	2241	1227	2484	1362
6-3	—	—	2230	1221	2480	1360
4-4	2118	1159	2235	1224	2478	1359
4/11-5	—	—	2305	1262	2520	1382
4-6	2136	1169	2253	1234	2480	1361
6-7	2124	1162	2253	1234	2466	1352

c. Hot Cracking Test Results

Results of the initial Task 1 weldability trials are listed in Table 5. As described previously, these trials were conducted in two sets of two tests each, with welding parameters being modified slightly for the second set to improve weld bead geometry. The modified welding parameters represent approximately 10% reduction in the rate of energy input. As expected, this change

resulted in a reduction in the average number of cracks from 53 cracks per specimen for the first series to 44 cracks per specimen for the second series.

TABLE 5
TASK 1 INITIAL HOT CRACKING RESULTS

AFC Filler Metal	Number of Cracks				Overall Average
	Initial Weld Parameters		Modified Weld Parameters		
	Test 1	Test 2	Test 3	Test 4	
6-1	52	61	42	45	50
6-2	53	26	41	51	43
6-3	32	57	54	16	40
4-4	75	33	31	30	42
4/11-5	74	45	48	34	50
4-6	31	56	75	79	60
6-7	55	82	17	47	50

Weld Parameters:

Initial — 75 amps, 15 volts, 1.1 mm/sec (2.6 in./min) travel speed
Modified — 78 amps, 15 volts, 1.3 mm/sec (3.0 in./min) travel speed

Because of the similar compositions of the seven alloys screened, all of which were modifications of the best of the prior contract alloys, and the variability inherent in this type of test, it was not considered possible to discriminate among the alloys tested on the basis of these results alone. For this reason, a second group of supplemental hot cracking tests was conducted using recently acquired welding equipment capable of better control of welding parameters. Because of the limited number of additional hot cracking specimens available at this point in the program, a second group of Inconel 713c hot cracking specimens was employed. Also, specimen availability restricted testing to only five of the seven filler metals. AFC-6-1 and -4/11-5 were dropped because of the higher solidus temperatures noted earlier. Results of the supplemental tests are given in Table 6.

Because different weld parameters and a different group of Inconel 713c base metal specimens were used, these results cannot be compared directly with the initial test series. In general, the conditions used in the supplemental testing resulted in less cracking, in part due to the lower welding energy input. This series of tests also provided somewhat more uniform cracking between specimens than the initial series of tests. This uniformity is attributed in part to the better control of weld parameters available with new equipment.

Results of the supplemental testing indicate that alloys AFC-4-6 and -6-7 had the least cracking, averaging 8 and 12 cracks per specimen, respectively, compared with averages ranging from 19 to 24 cracks for the other three alloys.

TABLE 6
TASK 1 SUPPLEMENTAL HOT CRACKING RESULTS

AFC Filler Metal	Number of Cracks						Ranking	Solidus Temperature	
	Test 1	Test 2	Test 3	Total	Average	Range**		(°F)	(°C)
6-2	17	17	22	56	19	5	3	2241	1227
6-3	19	28	—	71*	24	9	5	2230	1221
4-4	9	20	27	56	19	18	4	2235	1224
4-6	9	7	8	24	8	2	1	2253	1234
6-7	11	12	14	37	12	3	2	2253	1234

Weld Parameters:

75 amps, 8.7 volts, 0.85 mm/sec (2.0 in./min) travel speed

*Adjusted Value
**Difference between lowest and highest number of cracks

d. Post-Weld Heat-Treatment Cracking Results

The results of the Task 1 post-weld heat-treatment cracking investigation conducted by heat treating the hot cracking specimens are presented in Table 7. These results do not provide a straight-forward comparison of resistance to post-weld heat-treatment cracking due to the severity of the laboratory weldability test. If the numbers of cracks for the two specimens after heat treatment are combined to reduce the influence of individual specimen variation, it is found that the total number of cracks for each filler metal are roughly comparable, ranging from 162 to 195. It is also noted that the percentage increase in the number of cracks after heat treatment is inversely related to the total number of hot cracks before heat treatment. This uniform extent of cracking possibly can be explained as follows. There are approximately the same number of potential cracking sites in the specimens; welding causes hot cracks at some of the sites; and, because of the severity of the laboratory welding conditions and high residual stresses, a consistent fraction of the remaining sites cracked during post-weld heat treatment. In perspective, this approach had not been tried before and was intended to provide a preliminary indication of post-weld heat-treatment cracking behavior. The particular conditions in this laboratory approach do not provide a good comparison of filler metals.

e. Selection of Candidate Alloys for Task 2 Evaluation

The results of the Phase I, Task 1 work were reviewed with the Air Force Program Monitor to select candidate filler metals for further evaluation in Task 2. Based primarily on the supplemental hot cracking test results, where better resistance to cracking was exhibited, alloys AFC-4-6 and -6-7 were chosen.

A third alloy, C-4 from the previous contract, also was selected for testing in Task 2. Alloy C-4 provided a baseline reference with the previous contract, and favorable experience had been gained with it in welding nickel-base superalloy components where better welding yields were achieved and the welds demonstrated superior durability in service.

Commercial filler metal Inconel 625 was added to Task 2 work on a limited basis to provide a comparison with current practice.

2. PHASE I — TASK 2 RESULTS

The objective of Task 2 was to perform additional testing on the candidate filler metals in an effort to identify an optimum alloy for evaluation in Phase II. The evaluation included hot cracking and post-weld heat-treatment cracking tests, characterization of weldment microstructure, phase stability and composition, and 871°C (1600°F) weldment tensile tests.

a. Hot Cracking Results

The results of the Task 2 hot cracking tests, summarized in Table 8, indicate that alloy AFC-6-7 has the best resistance to hot cracking. The total number of cracks in this series of tests was 95 for AFC-6-7, while for the other filler metals, the total cracks ranged from 141 to 161. The other three filler metals, AFC-4-6, C-4 and Inconel 625, had roughly equivalent cracking levels.

TABLE 7
POST-WELD HEAT-TREATMENT CRACKING RESULTS

AFC Filler Metal	Specimen A			Specimen B			Total (2 Specimens)			
	Number of Hot Cracks Before Heat Treatment	Number of Cracks After Heat Treatment	Number of Additional Cracks	Number of Hot Cracks Before Heat Treatment	Number of Cracks After Heat Treatment	Number of Additional Cracks	Number of Hot Cracks Before Heat Treatment	Number of Cracks After Heat Treatment	Number of Additional Cracks	Percent Increase in Number of Cracks
6-1	42	93	51	45	69	24	87	162	75	86.2
6-2	53*	90	37	41	84	43	94	174	80	85.1
6-3	32*	88	56	16	92	76	48	180	132	275
4-4	33*	120	87	31	75	44	64	195	131	205
4/11-5	45*	110	65	34	83	49	79	193	114	144

*Specimens welded with initial weld parameters; all other welded with modified weld parameters.

TABLE 8
TASK 2 HOT CRACKING RESULTS

Filler Metal	Number of Cracks								Standard Deviation		Solidus Temperature	
	Test 1	Test 2	Test 3	Test 4	Test 5	Total	Average	Range	(σ)	Ranking	(°F)	(°C)
AFC-4-6	9	23	47	22	40	141	28	38	13.6	2	2253	1234
AFC-6-7	19	21	8	23	24	95	19	16	5.8	1	2253	1234
C-4	37	19	64	15	26	161	32	49	17.6	4	2419	1326
Inconel 625	45	17	30	—	—	153*	31	28	11.4	3	2509	1376

*Adjusted Value

b. Post-Weld Heat-Treatment Cracking Results

The results of the post-weld heat-treatment cracking trials conducted during Task 2 on the 3.2-mm (0.125-in.) thick Inconel 713c slabs are summarized in Table 9. These results are for the bead-on-plate welds only since the edge welds did not provide useful results. The results are tabulated for each test and as combined results for both tests. The combined results are more meaningful for consideration because they compensate for the fact that cracking is not uniformly distributed. The extent of hot cracking as-welded is roughly comparable, ranging from six to nine cracks. The extent of cracking after heat treatment is nearly identical for all four filler metals. AFC-4-6 had a combined total of 12 cracks, while the other three alloys, AFC-6-7, C-4, and Inconel 625, each had 14 cracks. These post-weld heat-treatment cracking test results were viewed as not amenable to making comparisons in cracking resistance, but they did eliminate concern that the new alloys might have poor cracking resistance. These results also suggest that there is no substantial difference in post-weld heat-treatment cracking resistance for the four filler metals.

c. Microstructure, Phase Stability and Composition Examination

The results of the microstructure and phase stability investigation are summarized in Table 10. Typically, gamma prime (γ') and MC-type carbides were observed in weld metal in the "as-welded" condition. Thermal exposure at 843°C (1550°F) for 48 hr produced little change in weldment microstructure except in the Inconel 625 weldment where $M_{23}C_6$ type carbides precipitated in the grain boundaries. After 200 hr at 843°C (1550°F), carbides of the $M_{23}C_6$ type were observed in the grain boundaries of all weldments except in the AFC-6-7 weldment. Traces of Laves phase were detected in the AFC-4-6 weldment and orthorhombic $\delta(Ni_3Cb)$ was found in all three experimental alloy weldments. In summary, no significant potentially detrimental microstructural changes were observed in thermally exposed weldments. A more detailed microstructure review is contained in Appendix G.

Concentration profiles were obtained on the three experimental filler metal weldments exposed at 843°C (1550°F) for 200 hr; these results are presented in Appendix G.

d. Mechanical Properties Test Results

The results of the 871°C (1600°F) tensile tests of welds made with filler metals AFC-4-6, -6-7, and C-4 are presented in Table 11. The fractures were all associated with the welds. The AFC-4-6 specimens fractured through the heat-affected zone and at the edge of the fusion zone; the AFC-6-7 specimens all failed through the fusion zone; and the C-4 specimens fractured through either the heat-affected zone or fusion zone. The strengths of welds made with alloys AFC-6-7 and C-4 were equivalent while the AFC-4-6 weld strengths were slightly lower.

e. Selection of an Optimized Alloy for Phase II Evaluation

At the conclusion of Phase I, the experimental results discussed above were reviewed with the Air Force Program Monitor and alloy AFC-6-7 was selected as the optimum filler metal for characterization in Phase II. The primary basis for this selection was the improved hot cracking resistance exhibited by alloy AFC-6-7, coupled with a slight strength advantage compared to experimental alloy AFC-4-6, and with the absence of any undesirable side effects such as metallurgical instabilities or reduced post-weld heat-treatment cracking resistance. As in the Phase I, Task 2 work, alloy C-4 from the prior contract and the commercial filler metal, Inconel 625, were included as baseline references in the Phase II investigation described below.

TABLE 9
TASK 2 INCONEL 713c POST-WELD HEAT-TREATMENT CRACKING RESULTS

	Test 1			Test 2			Total of Both Tests		
Filler Metal	Number of Cracks, As-Welded	Number of Cracks After Heat Treatment	Number of Additional Cracks	Number of Cracks, As-Welded	Number of Cracks After Heat Treatment	Number of Additional Cracks	Number of Cracks, As-Welded	Number of Cracks After Heat Treatment	Number of Additional Cracks
AFC-4-6	2	2	0	6	10	4	8	12	4
AFC-6-7	5	7	2	4	7	3	9	14	5
C-4	0	0	0	6	14	8	6	14	8
Inconel 625	5	6	1	4	8	4	9	14	5

TABLE 10
MICROSTRUCTURE PHASE IDENTIFICATION IN INCONEL 713c WELD METAL

		Heat-Treated at 843°C/1550°F	
Filler Metal	*As-Welded*	*48 hr*	*200 hr*
AFC-4-6	γ, γ′,MC	γ, γ′,MC	γ, γ′,MC $M_{23}C_6$, Laves (trace)
AFC-6-7	γ, γ′,MC	γ, γ′,MC	γ, γ′,MC, (trace)
C-4	γ, γ′,MC	γ, γ′,MC	γ, γ′,MC, $M_{23}C_6$
Inconel 625	γ, γ′,MC	γ, γ′,MC, $M_{23}C_6$	γ, γ′,MC, $M_{23}C_6$

TABLE 11
871°C (1600°F) TENSILE PROPERTIES OF EXPERIMENTAL FILLER METAL WELDMENTS IN INCONEL 713c

		0.2% Offset Yield Stress		*Ultimate Tensile Strength*			
Filler Metal	*Test Identity*	*(ksi)*	*(MPa)*	*(ksi)*	*(MPa)*	*Elongation (%)*	*Failure Location*
AFC-4-6	1	103.0	710.2	120.6	831.5	3.0	HAZ-FL[1] [2]
	2	101.4	699.1	122.1	841.8	3.0	HAZ-FL
	3	95.6	659.1	115.8	798.4	3.0	HAZ-FL
	Average	100.0	689.5	119.5	823.9	3.0	—
AFC-6-7	1	105.5	727.4	116.6	803.9	3.0	FZ[3]
	2	108.0	744.6	128.4	885.3	3.0	FZ
	3	113.8	784.6	124.4	857.7	3.0	FZ
	Average	109.1	752.2	123.1	849.0	3.0	—
C-4	1	115.7	797.7	134.3	926.0	3.0	FZ
	2	111.0	765.3	128.1	883.2	3.0	FZ
	3	100.0	689.5	125.0	861.8	3.0	HAZ
	4	109.0	751.5	128.4	885.3	3.0	HAZ
	Average	108.9	751.1	128.9	889.1	3.0	—

[1] HAZ = Heat-Affected Zone
[2] FL = Fusion Line
[3] FZ = Fusion Zone

3. PHASE II RESULTS

a. Mechanical Properties Test Results

(1) Tensile Properties

Tensile tests were conducted at 871°C (1600°F) and at 760°C (1400°F). The results of these tests are presented in Tables 12 and 13, respectively. Originally, tensile tests were to be performed at room temperature as well, and several additional tests were to be performed at each elevated temperature. However, since all elevated temperature tests failed in either the heat-affected zone or in the parent metal, thus precluding any valid comparison between filler metals, all additional tests were canceled and the specimens made available for stress-rupture testing.

TABLE 12
871°C (1600°F) WELDMENT TENSILE PROPERTIES

Filler Metal	0.2% Offset Yield Strength		Ultimate Tensile Strength		Elongation	Failure
(Specimen No.)	(ksi)	(MPa)	(ksi)	(MPa)	(%)	Location
C-4(4)	—	—	86.7	597.8	—	HAZ[1]
C-4(6)	104.5	720.5	108.3	746.7	4.0	HAZ
AFC-6-7(6)	104.3	719.2	104.6	721.2	2.0	HAZ
AFC-6-7(7)	—	—	98.7	680.5	—	PM[1]
Inconel 625(3)	104.6	721.2	105.3	726.0	3.0	HAZ

HAZ: Heat-Affected Zone
PM: Parent Metal
[1]Failed prior to 0.2% Offset Yield Strength at area containing large amounts of shrinkage porosity.

TABLE 13
760°C (1400°F) WELDMENT TENSILE PROPERTIES

Filler Metal	0.2% Offset Yield Strength		Ultimate Tensile Strength		Elongation	Failure
(Specimen No.)	(ksi)	(MPa)	(ksi)	(MPa)	(%)	Location
C-4(1)	118.8	819.1	127.6	879.8	3.0	HAZ
C-4(2)	132.1	910.8	139.6	962.5	3.0	PM
C-4(3)	122.2	842.6	137.3	946.7	5.0	PM
C-4 Average	124.4	857.5	134.8	929.7	3.7	
AFC-6-7(1)	126.2	870.2	138.4	954.3	4.0	HAZ
AFC-6-7(3)	—	—	—	—	—	PM[1]
AFC-6-7(4)	129.7	894.3	135.6	935.0	2.0	HAZ
AFC-6-7 Average	127.9	882.2	137.0	944.6	3.0	
Inconel 625(1)	127.3	877.7	136.7	942.6	3.0	HAZ

HAZ: Heat-Affected Zone
PM: Parent Metal
[1]Failed during test set-up at area containing large inclusion.

(2) Stress Rupture Properties

Stress rupture tests were conducted at 871°C (1600°F)/317 MPa (46 ksi) and at 760°C (1400°F)/552 MPa (80 ksi). The results of these tests are presented in Tables 14 and 15, respectively.

At 871°C (1600°F)/317 MPa (46 ksi), the average life to rupture of the filler metal specimens was as follows: C-4, 31.5 hr, AFC-6-7, 28.5 hr, and Inconel 625, 20.5 hr. Filler metals C-4 and AFC-6-7 had 54% and 39% greater average lives, respectively, than Inconel 625. Ductilities were similar. Fracture occurred in the fusion zone in all specimens.

At 760°C (1400°F)/552 MPa (80 ksi), the average life to rupture of the filler metal specimens was as follows: AFC-6-7, 53.1 hr, Inconel 625, 20.5 hr, and C-4, no valid results. Filler metal AFC-6-7 had a 110% greater average life than Inconel 625. Ductilities were similar. Fractures occured in the heat-affected zone or in the fusion zone.

All fracture surfaces were examined under a light microscope and suspect specimens were submitted for scanning electron microscope (SEM) examination. The SEM examination revealed shrinkage porosity in heat-affected zone fractures and shrinkage or gas-type porosity in fusion zone fractures in several specimens. Additionally, prior cracks, undetected by X-ray radiography, were found in two specimens. These specimens were not included in average life calculations because these defects were believed to contribute to premature failures. Two specimens, Inconel 625(11) and Inconel 625(14), exhibited very lamellar fracture surfaces occurring along the primary dendrite direction (Figure 11). The fractures occurred at the center of the fusion zone. Since no defects were obvious, these results were included in average life calculations. No explanation was found for the extremely low life of specimen Inconel 625(7).

TABLE 14
871°C (1600°F)/317 MPa (46 ksi) WELDMENT
STRESS-RUPTURE PROPERTIES

Filler Metal (Specimen No.)	*Life to Rupture (hr)*	*Elongation (%)*	*Failure Location*	*Comments*
C-4(10)	37.7	2.6	FZ	
C-4(11)	28.6	2.6	FZ	
C-4(12)	28.3	2.6	FZ	
C-4 Average	31.5	2.6	—	
AFC-6-7(13)	34.2	3.0	FZ	
AFC-6-7(14)	30.0	3.2	FZ	
AFC-6-7(15)	25.5	2.9	FZ	
AFC-6-7(2)	24.9	4.0	FZ	
AFC-6-7(5)	28.0	3.0	FZ	
AFC-6-7 Average	28.5	3.2	—	
Inconel 625(9)	22.9	2.7	FZ	
Inconel 625(10)	21.7	2.0	FZ	
Inconel 625(11)	12.8	3.5	FZ	SEM Examination No Irregularities
Inconel 625(12)	23.9	2.9	FZ	
Inconel 625(13)	21.4	2.7	FZ	
Inconel 625 Average	20.5	2.8	—	

TABLE 15
760°C (1400°F)/552 MPa (80 ksi) WELDMENT
STRESS-RUPTURE PROPERTIES

Filler Metal (Specimen No.)	*Life to Rupture (hr)*	*Elongation (%)*	*Failure Location*	*Comments*
C-4(7)	16.3*	2.6	HAZ	SEM Examination Prior Crack
C-4(8)	9.4*	2.4	FZ	SEM Examination Porosity
C-4(9)	1.0*	2.6	HAZ	SEM Examination Porosity
C-4(5)	6.3*	2.7	HAZ	SEM Examination Porosity
C-4 Average	—	—	—	
AFC-6-7(8)	19.8*	2.9	HAZ	SEM Examination Prior Crack
AFC-6-7(9)	63.2	3.0	HAZ	
AFC-6-7(10)	50.0	2.4	HAZ	
AFC-6-7(11)	46.0	2.9	HAZ	
AFC-6-7(12)	2.2*	2.1	HAZ	SEM Examination Porosity
AFC-6-7(16)	3.5*	2.4	HAZ	SEM Examination Porosity
AFC-6-7 Average	53.1	2.8		
Inconel 625(5)	3.8*	3.5	HAZ	SEM Examination Porosity
Inconel 625(7)	3.6	3.8	HAZ	SEM Examination No Irregularities
Inconel 625(8)	25.7	2.7	FZ	
Inconel 625(14)	14.5	0.3	FZ	SEM Examination No Irregularities
Inconel 625(15)	35.2	2.7	FZ	
Inconel 625(16)	23.3	3.4	FZ	
Inconel 625 Average	20.[illegible]	2.6	—	

*Not included in average

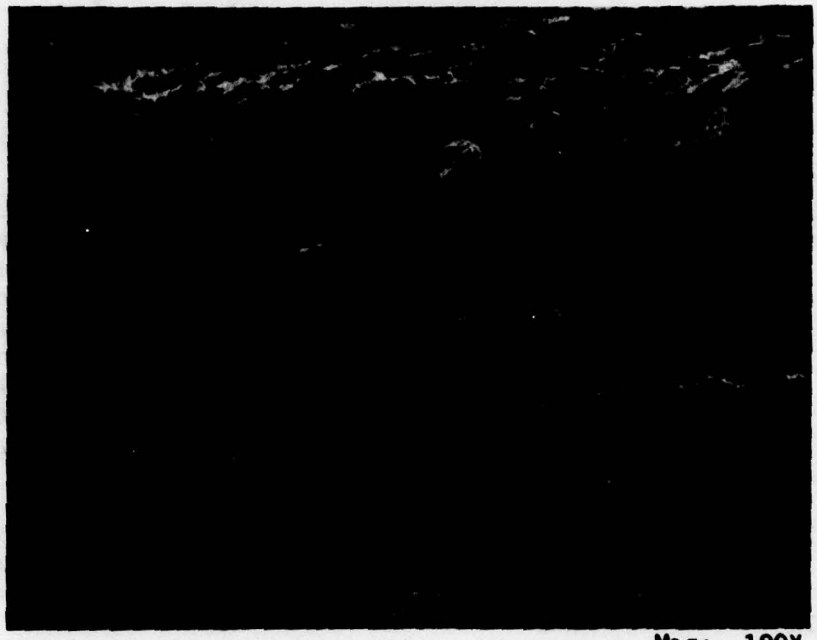
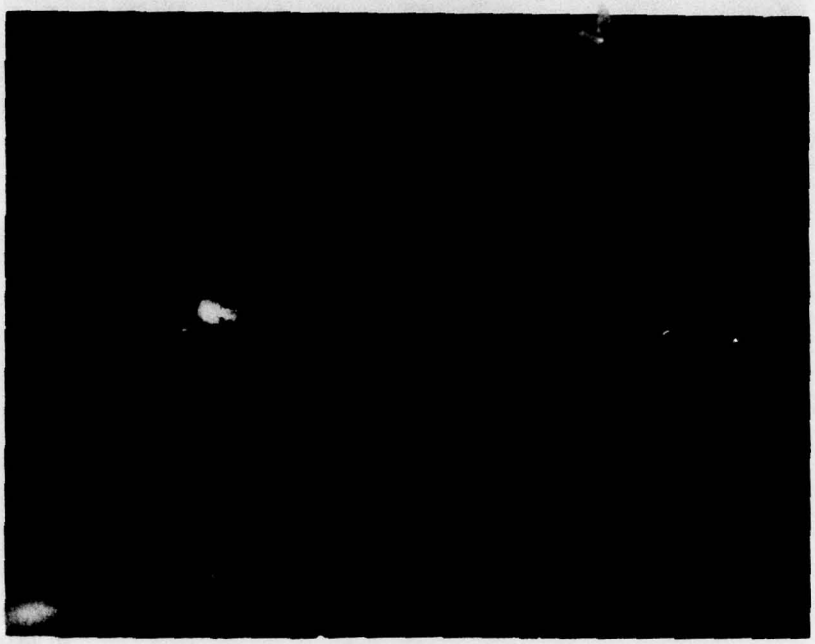


Figure 11. Fracture Surface of Inconel 625 Specimen (No. 14) Illustrating Lamellar Failure Along Primary Dendrite Direction

b. Hardware Applicability Demonstration Results

The objectives of this task were to demonstrate the applicability of the optimized filler metal, AFC-6-7, to welding an engine component, and to compare the hardware welding behavior with a state-of-the-art filler metal, Inconel 625, and with alloy C-4 from the previous contract.

A series of trials were made at P&WA/Florida and P&WA/Connecticut to develop tentative weld-repair procedures for critical areas on the TOBI. This was necessary since no established procedures existed because the part has been too difficult to weld reliably. The procedures which were developed are described in Section IV.2.b. The weld repair on the forward exterior flange, shown as-welded in Figure 12, was successful in avoiding cracking with all three filler metals. The relatively low restraint associated with that weld was beneficial. Although improvements were realized in the series of trials, it was not possible, within the scope of this program, to develop welding procedures which consistently avoided cracking at the forward air vent or the vane-locating lug. It was possible to achieve repairs at the edge of the forward air vent (Figure 13) with only one heat-affected zone crack which persisted in the corner of the opening. This cracking might be eliminated if the weld were moved a little further away from the corner. At the vane-locating lug (Figure 14), repairs were made which had only one crack. No attempts were made to reweld or blend out the cracks although those procedures are viable remedies. In perspective, both of the "repairs" were relatively ambitious since they involve high restraint in a crack-susceptible material, and thus they are more prone to cracking. It is possible that reducing the weld size and other modifications could produce crack-free repair welds at the forward air vent and vane-locating lug; however, this could not be pursued within the scope of this program.



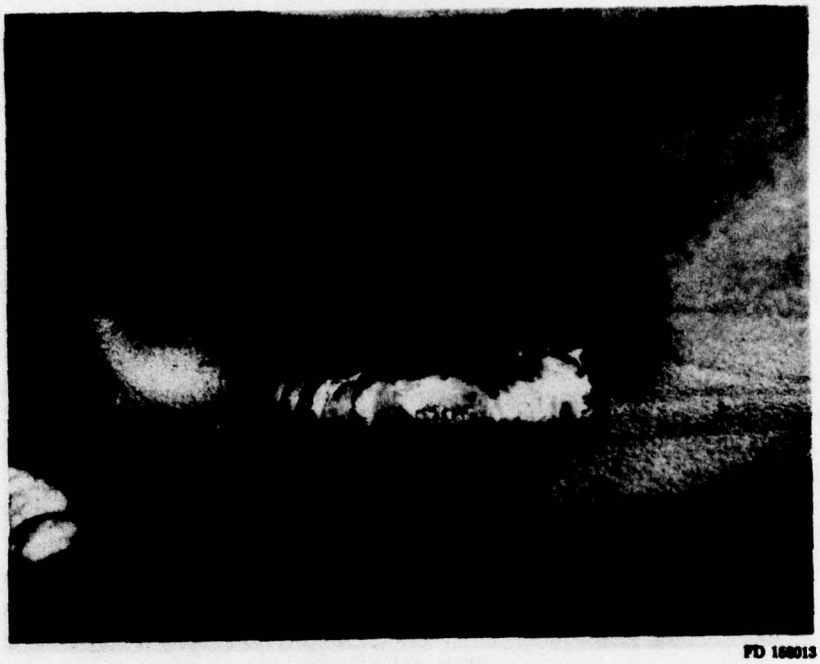
Top View



Side View

FD 153691

Figure 12. As-Welded Repair on Inconel 713c F100 TOBI Forward Exterior Flange



FD 166013

Figure 13. As-Welded Repair on Inconel 713c F100 TOBI Forward Air Vent



FD 166014

Figure 14. As-Welded Repair on Inconel 713c F100 TOBI Vane-Locating Lug

All three filler metals were used in the series of repair trials in an attempt to compare their hardware welding behavior. The results of all the repair-weld trials provide a limited comparison. In the repair at the air vent, AFC-6-7 was slightly more crack-resistant than alloy C-4 and both alloys were clearly better than Inconel 625. All three filler metals behaved equally well in repair welds at the vane-locating lug. Since the forward exterior flange repair welds were crack-free, they did not provide a means of comparison. In summary, the complexities of welds on hardware did not provide a situation which strongly differentiated between filler metal welding characteristics; however, AFC-6-7 offers some advantage in the most highly restrained and difficult repair.

A final consideration in the applicability of the new filler metal is the welding characteristics from the welder's viewpoint. Filler metals Inconel 625 and C-4 were regarded as having equivalent welding characteristics. Both alloys wetted and flowed well and welded easily. Alloy AFC-6-7 was somewhat more difficult to use; it had less fluidity and welded less readily. However, satisfactory welds were achieved with slightly more care, and AFC-6-7 is definitely applicable for welding engine components.

4. DISCUSSION

Based on the results of the hot cracking weldability tests, alloy AFC-6-7 was selected as the optimum composition. The solidus temperature of AFC-6-7 was in the lower group which, in prior experience, correlated with improved resistance to hot cracking. Attempts to evaluate resistance to post-weld heat-treatment cracking did not produce definitive results, but the tests did indicate that the new filler metal will be equivalent to the existing filler metals, if not better.

No significant microstructure or phase thermal stability problems were encountered after elevated-temperature exposure.

The mechanical properties of welds made with AFC-6-7 were better than those of welds made with the filler metal C-4 and with Inconel 625; the mechanical properties advantage of AFC-6-7 over Inconel 625 is expected to be larger in welds with less base-metal dilution.

The use of AFC-6-7 in the repair of the TOBI demonstrated its applicability to hardware. The alloy offered an advantage in weldability in the more highly restrained forward air vent; no difference in weldability was observed in the less restrained repairs. Because AFC-6-7 is an age-hardenable alloy, the higher strength of the weld is expected to provide a more durable repair than can be achieved with the state-of-the-art filler metals.

SECTION VI
CONCLUSIONS

1. The optimum filler metal is alloy AFC-6-7; the composition is: Ni-balance, Cr-19.4, Fe-11.9, Ta-5.3, Cb-3.2, Ti-0.91, Al-0.78, Mn-2.7, C-0.02, B-0.016, and Zr-0.07.

2. Alloy AFC-6-7 demonstrated the best resistance to heat-affected zone hot cracking in laboratory tests which correlated with the low solidus temperature of the alloy.

3. No substantial difference in post-weld heat-treatment cracking resistance was found between any of the alloys.

4. Welds made with AFC-6-7 filler metal in Inconel 713c had better elevated temperature tensile and stress-rupture properties than welds made with Inconel 625 filler metal; AFC-6-7 filler metal weld properties were comparable with those of filler metal C-4.

5. No microstructure thermal instability was found in welds in Inconel 713c made with AFC-6-7 filler metal.

6. AFC-6-7 filler metal can be used to weld-repair engine components; it offers an advantage in weldability in certain situations and provides a potentially more durable weldment than state-of-the-art nonhardenable filler metals.

SECTION VII
RECOMMENDATIONS

1. AFC-6-7 filler metal should be used to weld-repair engine components for engine test to better evaluate the viability of the alloy in an application under service conditions.

2. Additional mechanical properties tests should be conducted on weld metal which is undiluted by the base metal to better compare differences in properties between AFC-6-7, C-4, and Inconel 625.

3. Additional testing should be conducted on welds to determine oxidation and hot-corrosion behavior.

APPENDIX A
WIRE FABRICATION

Wire was fabricated in essentially the same manner as in Phase III of the previous contract; the work was done by P&WA personnel at the Middletown, Connecticut facility. A 500-gm (~ one-pound) master billet of each experimental alloy was prepared by arc-melting in a Leybold-Heraeus Model VA-L-200H vacuum arc melting furnace. High-purity pellets of each element, mixed in a copper crucible, were arc melted in a vacuum furnace back-filled with high-purity argon inert gas. The master billet was remelted and poured into copper chills to form three drop castings 12.7 mm (0.50 in.) in diameter by 127.0 mm (5.0 in.) long. The drop castings were annealed at 1038 to 1066°C (1900 to 1950°F) for 20 minutes. Upon cooling, one casting was belt-sanded to remove any oxides and cold-swaged with a Fean Manufacturing Company rotary swaging machine, Models No. 1, 2, 3, and 5. Several successive anneal, belt-sand, and swage steps were necessary to reach a final wire diameter of 2.5 mm (0.100 in.). This diameter provides the correct amount of material for the hot cracking weldability test. Preheating and intermediate annealing were accomplished in a Lindberg Type G10 radiant-heated electric furnace.

APPENDIX B
MELTING BEHAVIOR DETERMINATION

A Dupont Model 900 differential thermal analyzer was used to determine melting behavior of small samples taken from the wire of each alloy. The system includes a heating block to distribute heat evenly to sample and reference materials; a programming device and heater to change the temperature of the block at a uniform and predetermined rate; a high-gain, low-noise preamplifier to increase the sensitivity of ΔT measurement; and a variable-sensitivity recorder to plot ΔT as a function of temperature.

The differential thermal analyzer utilizes a differential thermocouple arrangement consisting of two thermocouples wired in opposition. One thermocouple is placed in a sample of the material to be analyzed and the second thermocouple is placed in an inert reference material, in this case nickel, which has been selected since it will undergo no thermal transformations over the temperature range being studied. When the temperature of the sample equals the temperature of the reference material, the two thermocouples produce identical voltages, and the net voltage output is zero. When sample and reference temperatures differ, the resultant net voltage differential reflects the difference in temperature between sample and reference at any point in time.

The sample and reference materials are placed close together in the heating block which is either heated or cooled through the temperature range of interest.

In addition to the sample and reference thermocouples, a third thermocouple is used to measure the heating block temperature and to control the rate of heating or [illegible].

As the environmental temperature is changed, the temperatures of sample and reference also change. In the absence of physical or chemical changes, the temperature differential (sample temperature minus reference temperature) remains zero. When a temperature is reached where a physical change, such as melting, occurs in the sample but not in the inert reference material, the sample temperature no longer equals the reference temperature and a temperature differential is observed which is then related to melting behavior.

APPENDIX C
WELDABILITY TEST SPECIMEN FABRICATION

Weldability test specimens were cast at the P&WA Manchester, Connecticut foundry using conventional vacuum induction melting. Eight specimens were made per mold; the ceramic molds were made by the lost wax process. The pour temperature of the melt was 1538°C (2800°F), and the mold preheat temperature was 982°C (1800°F). After removal from the molds, the castings were inspected radiographically (2% sensitivity) and with fluorescent penetrants to avoid using specimens with casting defects in the area of the weld.

APPENDIX D
TASK 1 POST-WELD HEAT-TREATMENT CRACKING TEST

The Task 1 post-weld heat-treatment cracking tests, which were performed on the hot cracking specimens, used the following thermal exposure conditions: 843°C (1550°F) for 4 hr in flowing argon; the heating rate was controlled at 14°C (25°F) per minute; and, at the conclusion of the cycle, forced air cooling was used. A resistance-heated box furnace located at the Pratt & Whitney Aircraft, Middletown, Connecticut facility was used for heat treatment. The temperature was monitored with a platinum/platinum-rhodium thermocouple inserted between the specimens. The specimens were heat treated in two groups of five. They were placed standing on edge with the narrow end towards the door; dummy specimens were used at each edge of the group to act as a shield from the side heating elements and ensure that the test specimens heated at approximately equal rates. The specimens were examined in the same manner as was used to determine the level of hot cracking in order to establish the number of post-weld heat-treatment cracks, which were essentially the same as hot cracks in nature.

APPENDIX E
MICROSTRUCTURE, PHASE STABILITY AND COMPOSITION INVESTIGATION

Portions of the weldment for each filler metal were given thermal exposures by heating to 843°C (1550°F) for 48 and 200 hours in a resistance-heated tube furnace with an argon atmosphere. This condition produces precipitation of phases, such as Laves and sigma, which are associated with microstructural instability in nickel-base superalloys. Metallographic specimens were prepared by conventional means and etched with an etchant containing 50 ml lactic acid, 30 ml nitric acid, and 2 ml hydrofluoric acid. The specimens were examined using optical and electron metallography. Standard extraction replicas were prepared and examined in a Philips EM 300 electron microscope to determine phase morphology. Phase identification and composition were accomplished with the use of an ETEC Autoprobe scanning electron microscope and electron microprobe. Weld and heat-affected zone composition profiles were obtained on three experimental filler metal weldments exposed at 843°C (1550°F) for 200 hours.

PRECEDING PAGE BLANK-NOT FILMED

APPENDIX F
MECHANICAL PROPERTIES TESTING

Butt welds were made with the various filler metals between 3.2-mm (0.125-in.) thick by 31.7-mm (1.25-in.) by 101.6-mm (4.0-in.) cast Inconel 713c pieces to provide welded panels for fabrication of mechanical properties test specimens for Phase I Task 2 and Phase II testing. Weld parameters are the same as for the Phase II hot cracking tests.

After welding, the plates were examined visually and with fluorescent penetrants. Transverse weld mechanical test specimens (Figure F-1) were machined from areas free of surface cracks. Weld beads were ground flush with the base metal. After preparation, the specimens were examined by X-ray radiography.

Tensile tests were conducted on a 1.33-MN (300,000-lb) Young testing machine equipped with a zone-type resistance-heated furnace for elevated-temperature testing. Temperature was measured and controlled with a Chromel-Alumel thermocouple.

Stress rupture tests were conducted at Joliet Metallurgical Laboratories, Joliet, Illinois.

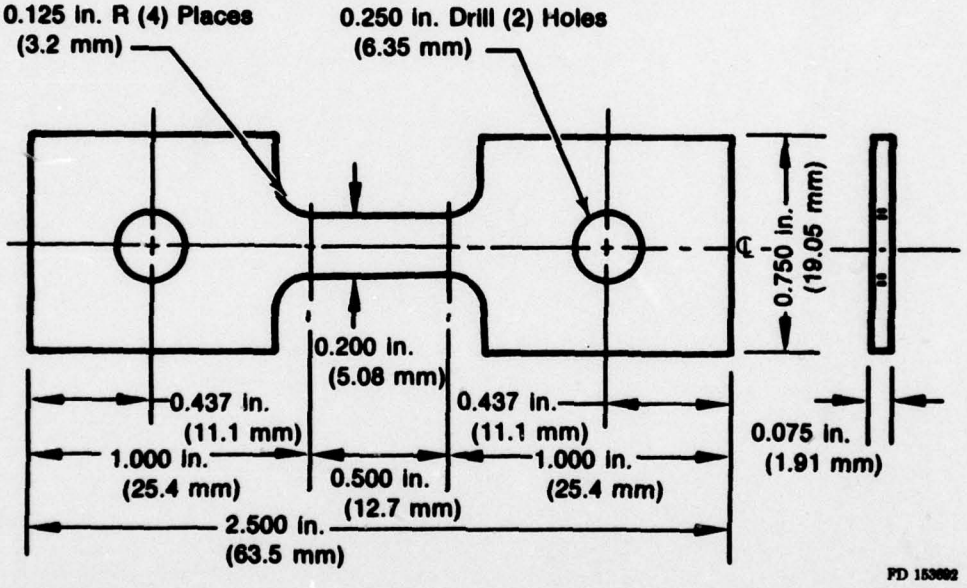


Figure F-1. Tensile and Stress-Rupture Mechanical Test Specimen (Weld Bead Ground Flush)

APPENDIX G
MICROSTRUCTURE

The microstructure of the filler metal weldments in the "as-welded" and thermally exposed conditions are summarized in Table G-1. Figures corresponding to the specific alloys are listed in Table G-1.

TABLE G-1.
MICROSTRUCTURE PHASE IDENTIFICATION IN INCONEL 713c WELD METAL

Filler Metal	*As-Welded*	*1550°F/843°C Heat Treated*	
		48 hr	*200 hr*
AFC-4-6	Figure G-1 γ, γ' blocky CbC script (Ta,Cb)C	Figure G-2 γ, γ' script (Ta,Cb)C	Figure G-3 γ, γ' (Ta,Cb)C $(Cr,Mo)_{23}C_6$, (Figure G-4); δ-$Ni_3(Cb,Ta)$, (Figure G-5); Laves-$Ni_3(Cb,Ta)$, (Figure G-5);
AFC-6-7	Figure G-6 γ, γ' blocky (Cb,Ti,Ta)C	Figure G-7 γ, γ' blocky (Cb,Ti,Ta)C	Figure G-8 γ, γ' (Cb,Ti,Ta)C (Cb,Ta)C δ-$Ni_3(Cb,Ta)$, (Figure G-9);
C-4	Figure G-10 γ, γ' blocky CbC script (Ta,Cb)C	Figure G-11 γ, γ' script (Ta,Cb)C	Figure G-12 γ, γ' (Ta,Cb)C $(Cr,Mo)_{23}C_6$ δ-$Ni_3(Cb,Ta)$
Inconel 625	Figure G-13 γ, γ' blocky CbC script (Ta,Cb)C	Figure G-14 γ, γ' CbC (Ta,Cb)C $(Cr,Mo)_{23}C_6$	Figure G-15 γ, γ' CbC (Ta,Cb)C $(Cr,Mo)_{23}C_6$

All filler metal weldments contained the γ matrix and fine γ' precipitates. Blocky CbC carbides and script (Cb,Ta)C carbides were observed "as-welded" in all but the AFC-6-7 weldment. During the thermal exposure, some of the CbC carbides transformed to script (Cb,Ta)C carbides and additional (Cb,Ta)C was precipitated. The AFC-6-7 weldment contained script (Cb,Ti,Ta)C carbides in all conditions.

A heavy, grain boundary precipitation of $(Cr,Mo)_{23}C_6$ carbides occurred during the 48-hour thermal exposure of the Inconel 625 weldment (Figure G-14). Additonal $(Cr,Mo)_{23}C_6$ precipitation occurred during the 200-hr thermal exposure. $(Cr,Mo)_{23}C_6$ was also observed in AFC-4-6 and C-4 weldments, but only after the 200-hour thermal exposure (Figure G-4). Moderate amounts of δ phase, consisting of orthorhombic $Ni_3(Cb,Ta)$, were observed in the C-4 and AFC-4-6 weldments after the 200-hour thermal exposure (Figure G-5). Trace amounts of δ phase were observed in the AFC-6-7 weldment after the 200-hour thermal exposure (Figure G-9).

A trace amount of Laves phase, consisting of $Ni_3(Cb,Ta)$, was observed in the AFC-4-6 weldment after the 200-hour thermal exposure (Figure G-5).

In summary, no significant, potentially detrimental microstructural changes were observed in the thermally exposed weldments.

Concentration profiles were obtained on the three experimental filler metal weldments exposed at 843°C (1550°F) for 200 hours. Spot compositions were determined beginning in the heat-affected zone and progressing into the weld metal. Compositions are presented in Tables G-2, G-3 and G-4, and location photomicrographs are presented in Figures G-16, G-17 and G-18 for filler metals AFC-4-6, AFC-6-7 and C-4 respectively.

Dilution calculations were made based on the composition profiles. However, extreme variations in dilutions were indicated. For example, in filler metal AFC-4-6, calculations based on chromium measurements indicate that the weld metal consists of 30% filler metal and 70% base metal. Based on iron measurements, the weld-metal composition was 10% filler metal and 90% base metal. To determine if weld-metal segregation occurred to any extent, a composition profile was made down the center of the AFC-4-6 weldment. Composition and a location photomicrograph are presented in Table G-5 and Figure G-19. A considerable composition variation exists. Tantalum and iron particularly segregate to the bottom of the weld. Manganese and columbium tend to segregate towards the bottom of the weld. Chromium remains relatively evenly distributed. Nickel, molybdenum, aluminum and titanium segregate to the top of the weld. Figure G-20 illustrates the trends in weld metal composition. The reasons for the trends are not clear, but are believed to be a complex combination of chemical activities, diffusivities, weld metal solidification kinetics and gravitational effects. Based on these observations, the chromium measurements were chosen as the most accurate indicator of weld metal dilution. This result (30% filler metal and 70% base metal) compared favorably with pre-weld calculations and measurements made in the previous contract.

TABLE G-2.
CONCENTRATION PROFILE FOR FILLER METAL AFC-4-6 WELDMENT; COMPOSITION IN WEIGHT % BY LOCATION

	Location								
Element	*1*	*2*	*3*	*4*	*5*	*6*	*7*	*8*	*9*
Al	5.9	5.8	5.6	5.7	6.3	5.9	5.8	5.8	6.0
Ti	1.1	0.6	0.8	0.6	1.0	0.9	0.6	0.7	0.7
Cr	14.3	14.2	15.4	15.7	17.3	14.9	15.1	14.5	15.3
Mn	trace	0.4	0.5	0.5	0.6	0.4	0.4	0.3	0.5
Fe	0	0.7	1.4	1.3	0.9	1.3	1.5	1.6	1.1
Ni	68.1	71.8	69.6	71.1	62.4	67.6	70.8	69.2	69.3
Cb	3.8	1.2	1.3	1.8	3.4	3.2	1.3	2.1	2.5
Mo	4.8	4.0	3.9	3.4	4.9	3.9	4.0	3.8	3.9
Ta	1.2	0.8	0.6	0	2.3	2.1	0.5	2.0	0.8

Location No. 1 is in heat-affected zone
Location No. 2 is at fusion line
Locations No. 3-9 are in weld metal

TABLE G-3.
CONCENTRATION PROFILE FOR FILLER METAL AFC-6-7 WELDMENT; COMPOSITION IN WEIGHT % BY LOCATION

	Location				
Element	*1*	*2*	*3*	*4*	*5*
Al	5.5	5.9	5.5	5.4	5.4
Ti	1.1	1.1	0.9	0.7	0.8
Cr	13.9	14.2	15.1	15.4	15.6
Mn	0	0	0.6	0.6	0.7
Fe	0	0	2.2	2.4	2.6
Ni	65.0	66.1	66.0	68.9	70.1
Cb	5.6	4.1	3.6	1.6	2.1
Mo	4.6	4.4	3.5	3.3	3.2
Ta	0	1.7	1.9	0.6	Trace

Location No. 1 is in heat-affected zone
Location No. 2 is in HAZ adjacent to fusion line
Locations Nos. 3-5 are in weld metal

TABLE G-4.
CONCENTRATION PROFILE FOR FILLER METAL C-4 WELDMENT; COMPOSITION IN WEIGHT % BY LOCATION

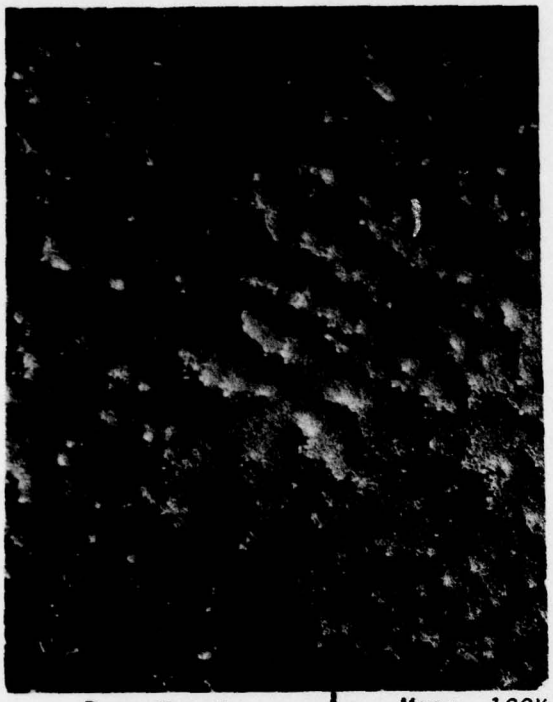
	Location						
Element	*1*	*2*	*3*	*4*	*5*	*6*	*7*
Al	6.4	6.2	6.2	5.0	5.3	5.2	4.9
Ti	0.7	0.7	0.8	0.8	0.8	0.9	0.7
Cr	14.0	14.1	14.2	14.9	14.0	17.7	15.2
Mn	0	0	0	0.4	0.3	Trace	Trace
Fe	0	0	0	0.9	0.6	1.1	1.2
Ni	70.3	69.5	68.7	67.0	66.2	61.4	65.9
Cb	1.6	1.8	1.8	2.2	3.5	2.9	2.5
Mo	4.0	4.5	4.4	4.6	5.0	6.0	5.5
Ta	1.0	1.4	0.5	2.9	3.4	1.2	1.6

Location No. 1 is in the base metal
Location Nos. 2 and 3 are in the heat-affected zone
Location No. 4 is at the fusion line
Location Nos. 5-7 are in the weld metal

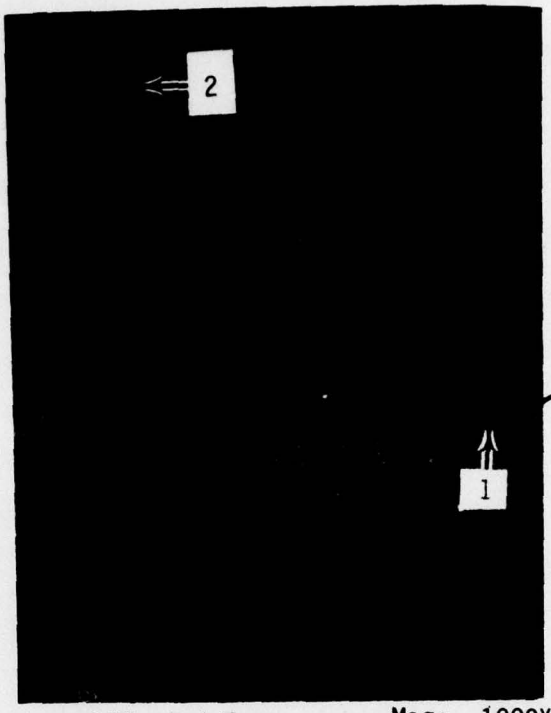
TABLE G-5.
CONCENTRATION PROFILE IN WELD METAL OF FILLER METAL AFC-4-6 WELDMENT; COMPOSITION IN WEIGHT % (ATOMIC %) BY LOCATION

	Location					
Element	*1*	*2*	*3*	*4*	*5*	*6*
Al	1.4 (0.6)	1.6 (0.6)	2.9 (1.2)	5.8 (2.6)	6.0 (2.6)	6.1 (2.6)
Ti	trace (0)	trace (0)	trace (0)	0.7 (0.6)	0.6 (0.5)	0.8 (0.6)
Cr	17.5(13.6)	19.1(14.7)	17.4(13.7)	15.3(13.1)	15.0(12.7)	15.4(12.8)
Mn	2.2 (1.8)	2.3 (1.9)	1.9 (1.6)	0.6 (0.5)	0.6 (0.5)	0.7 (0.6)
Fe	11.0 (9.2)	10.5 (8.7)	8.4(10.6)	1.6 (1.5)	1.2 (1.1)	1.3(1.2)
Ni	53.5(46.9)	55.5(48.1)	60.0(53.5)	69.1(67.1)	68.0(65.7)	67.9(64.0)
Cb	3.8 (5.3)	4.0 (5.5)	2.8 (3.9)	2.0 (3.1)	1.8 (2.7)	2.7 (4.0)
Mo	0(0)	trace(0)	1.6 (2.3)	3.5 (5.6)	3.8 (5.9)	3.9 (6.0)
Ta	8.4(23.9)	7.7(20.6)	4.8(13.2)	2.0 (6.0)	2.6 (8.2)	2.8 (8.2)

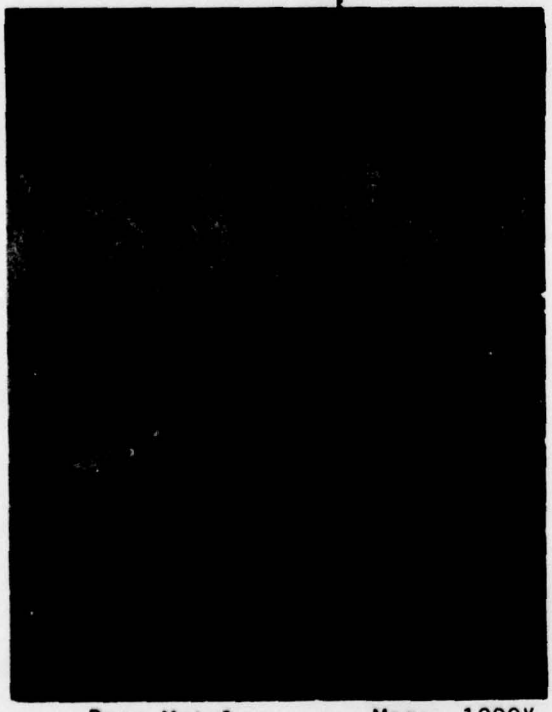
All locations are in weld metal



Base Metal Mag: 100X



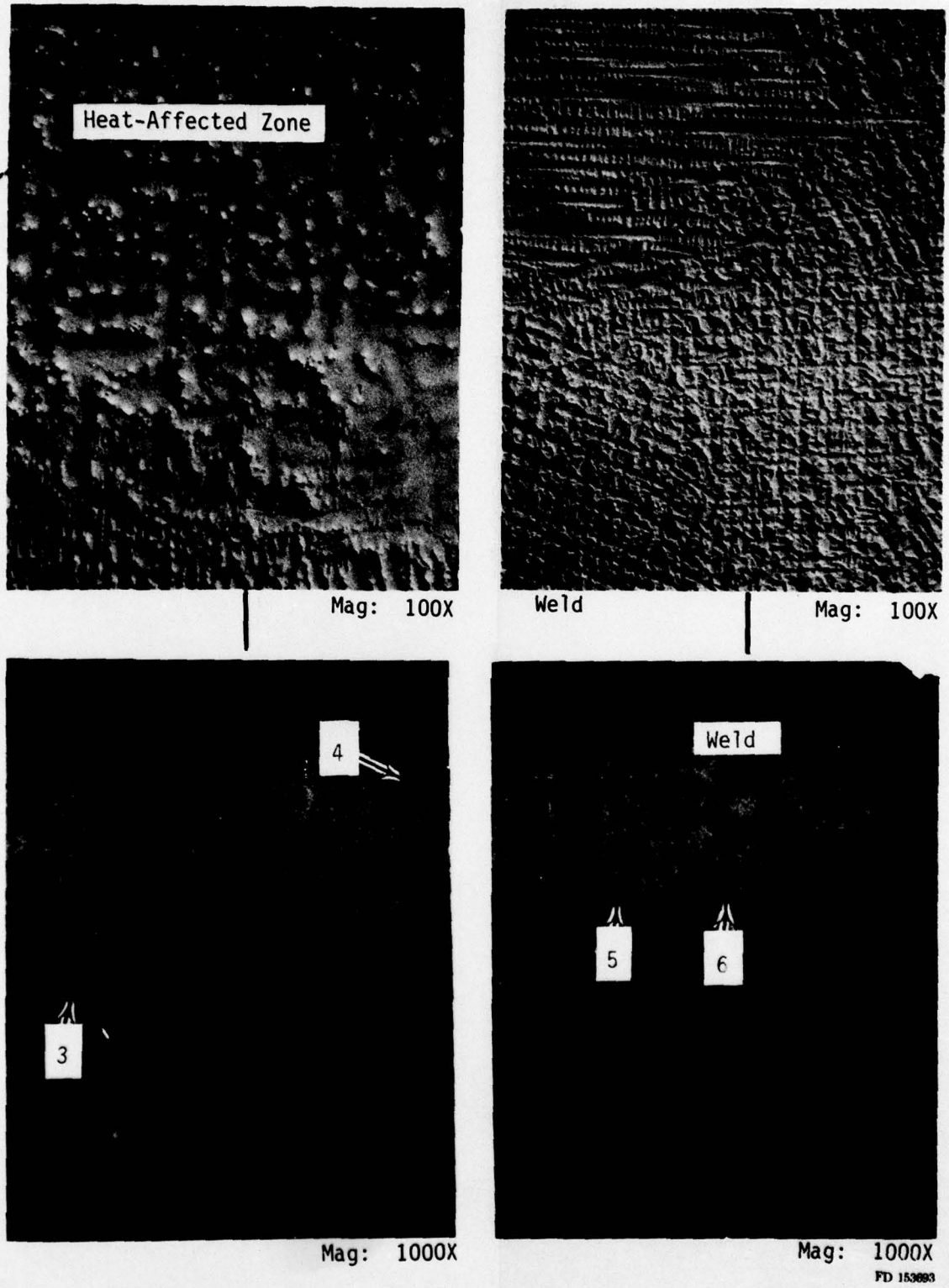
Heat-Affected Zone Mag: 1000X



Base Metal Mag: 1000X

(1) Grain Boundary $(Cr,Mo)_{23}C_6$ Carbides
(2) Acicular Matrix CbC Carbides
(TiC carbides were also present)
(3) Acicular CbC Carbides
(4) Blocky CbC Carbides
(5) Blocky CbC Carbides
(6) Script (Ta,Cb)C Carbides

Figure G-1. Microstructure of AFC-4-6 Weldment in As-Welded Condition — Weld metal microstructure consists of γ matri fine γ', acicular and blocky CbC carbides and script (Ta, Cb)C carbides.



$_3C_6$ Carbides
ides
present)

ture consists of γ matrix,

PRECEDING PAGE BLANK-NOT

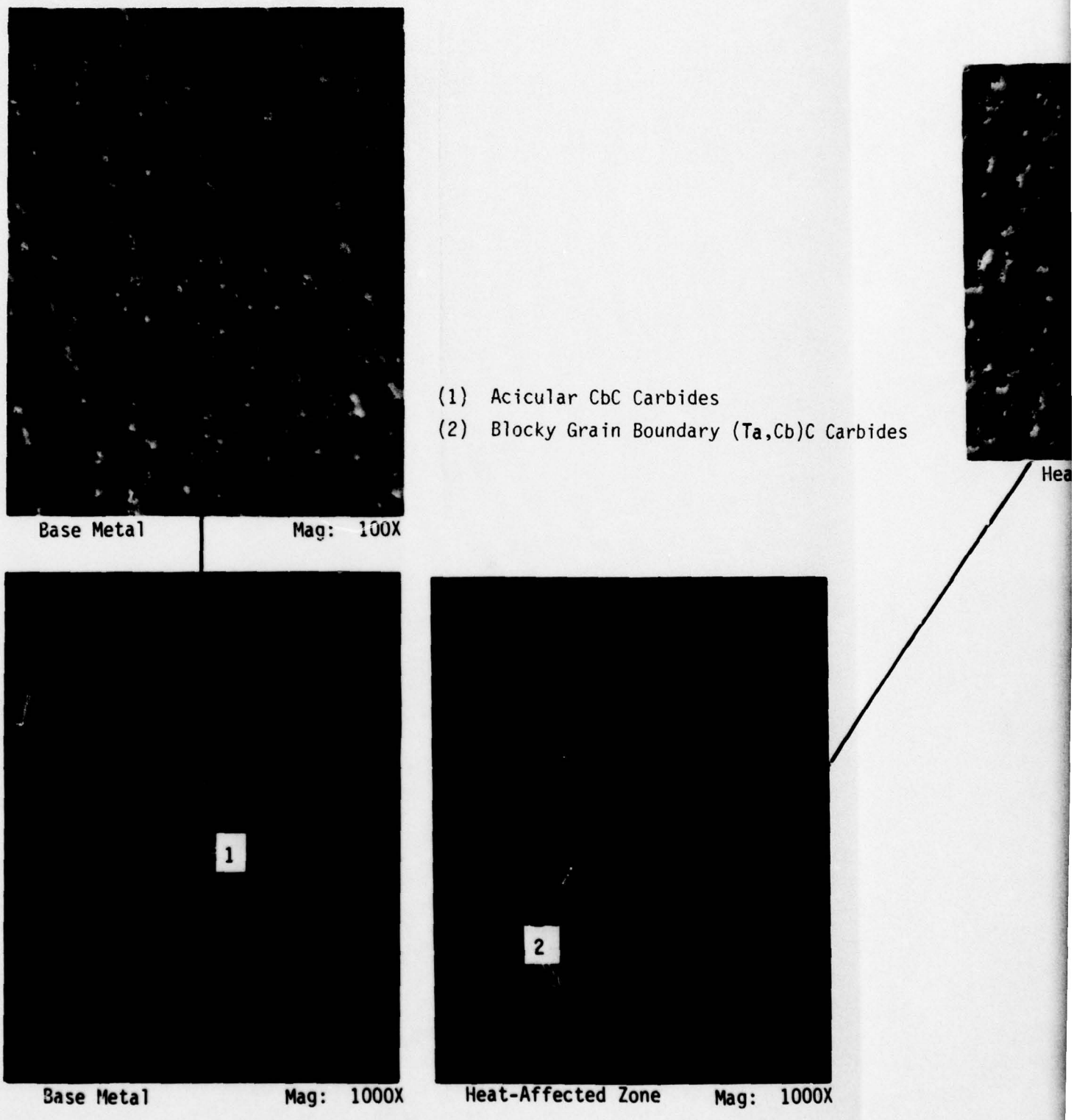
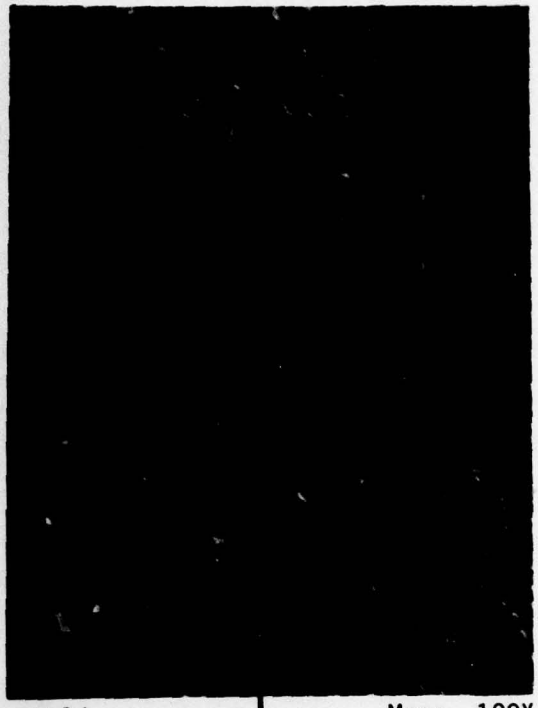


Figure G-2. Microstructure of AFC-4-6 Weldment after Thermal Exposure at 843°C (1550°F) for 48 Hours — Weld m microstructure consists of γ matrix, fine γ′, and predominantly script (Ta, Cb)C carbides. Note hot crack in heat-affe zone.

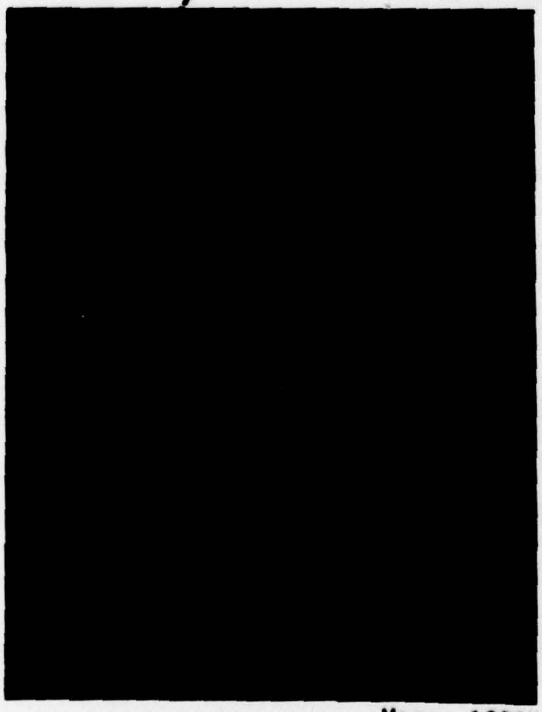
rbides



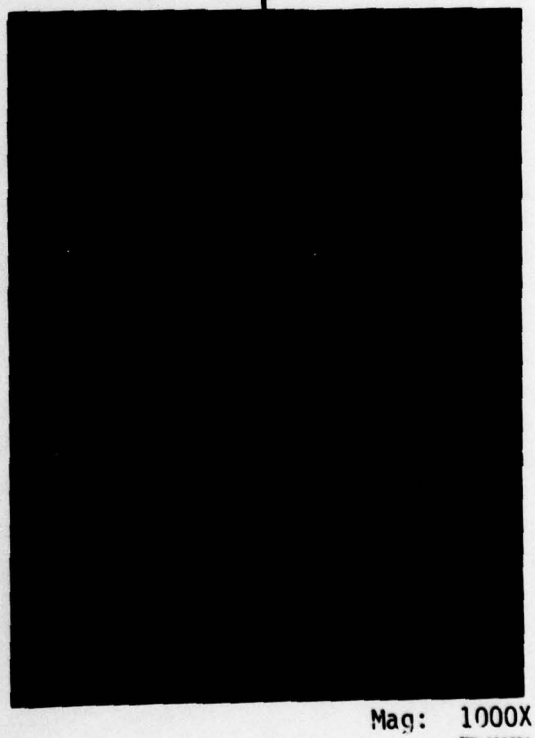
Heat-Affected Zone Mag: 100X



Weld Mag: 100X



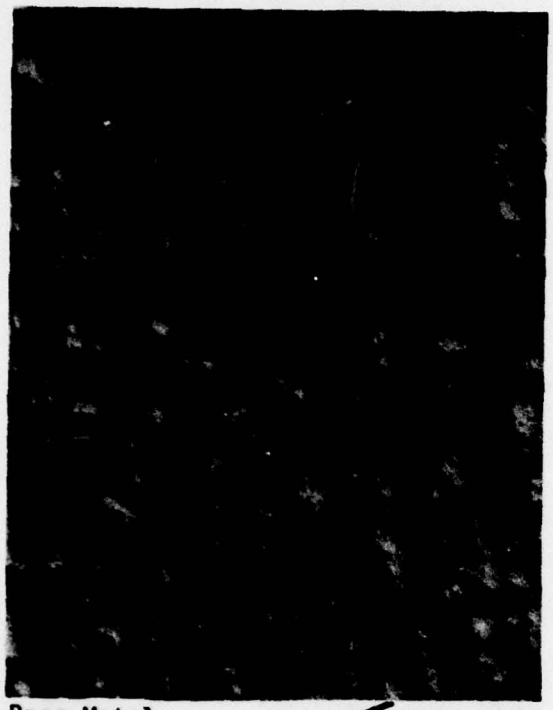
Mag: 1000X



Mag: 1000X

FD 153694

or 48 Hours — Weld metal
Note hot crack in heat-affected



Base Metal

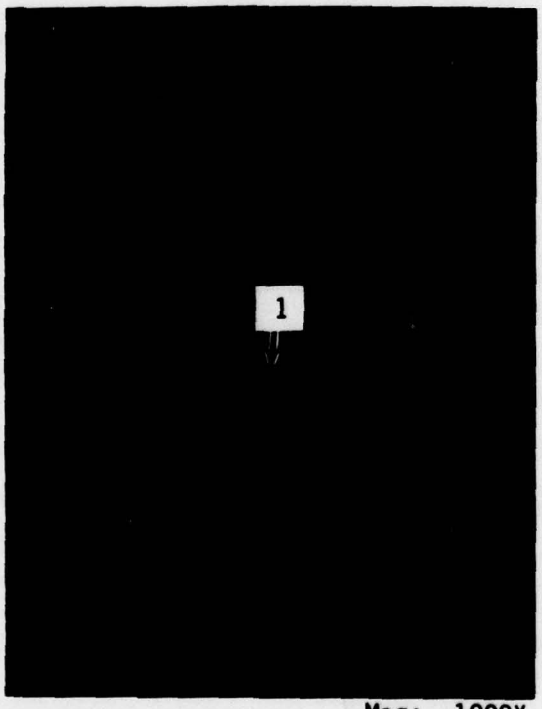
Mag: 100X

(1) $Ni_3(Cb,Ta)$

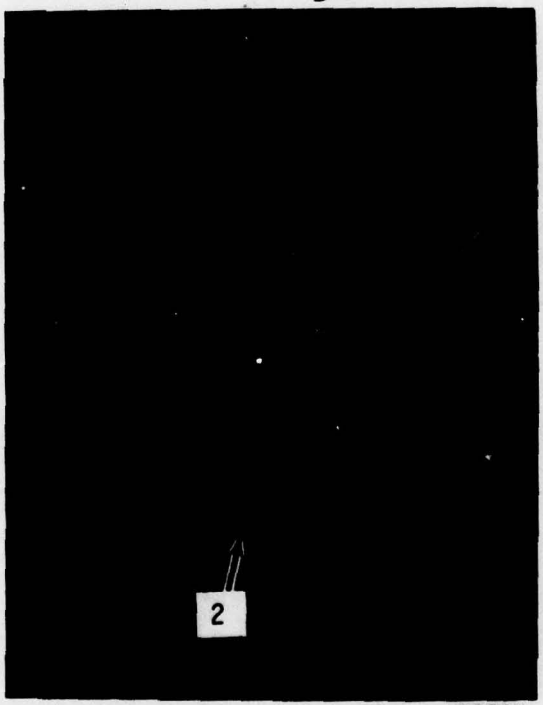
(2) Blocky (Cb,Ta)C Carbides



Heat-Affe



Mag: 1000X



Mag: 1000X

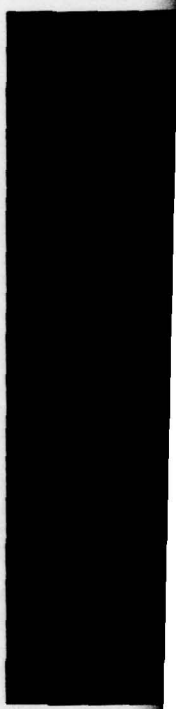
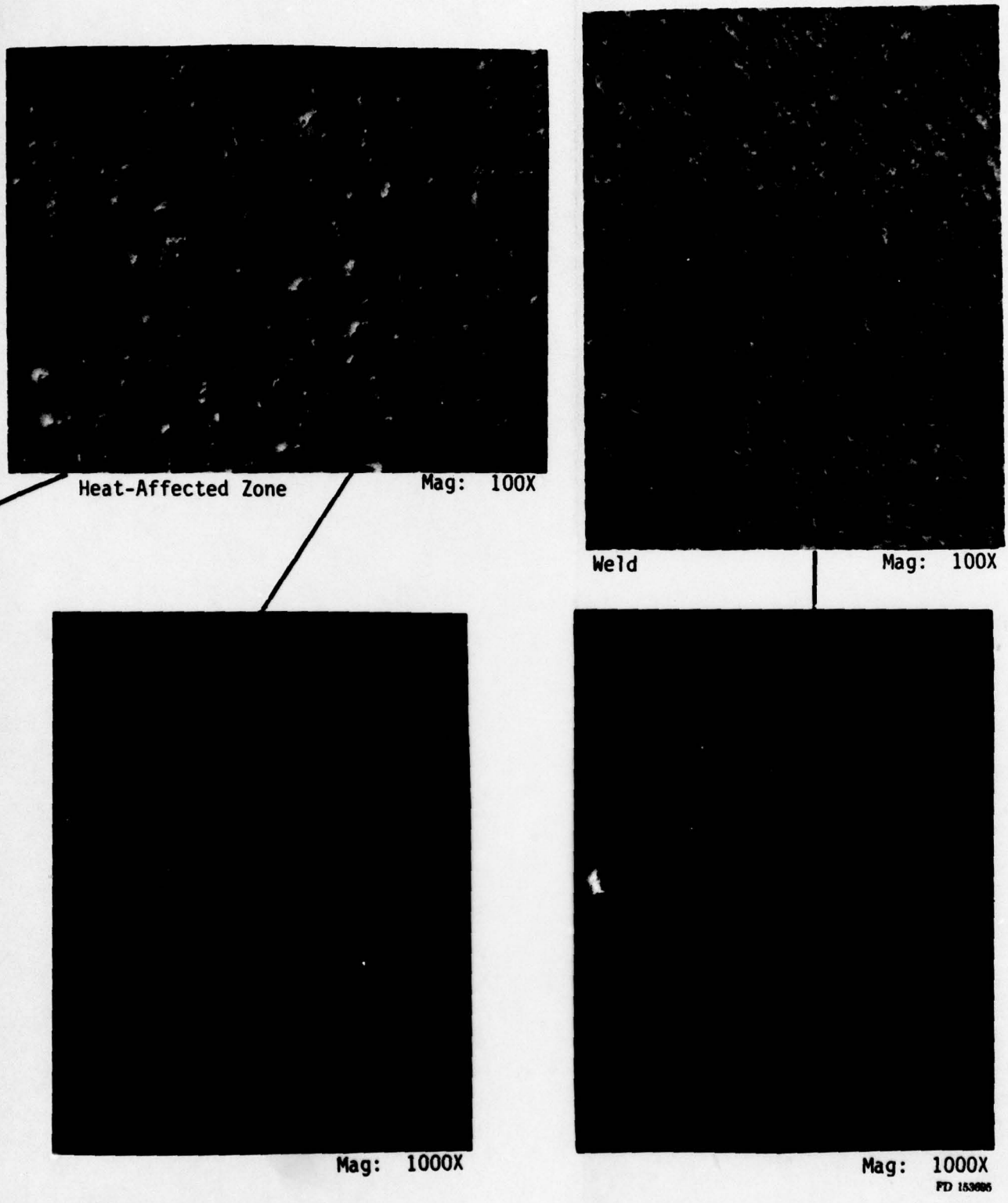


Figure G-3. Microstructure of AFC-4-6 Weldment after Thermal Exposure at 843°C (1550°F) for 200 hours — Weld metal microstructure consists of γ matrix, fine γ', matrix (Ta, Cb)C carbides, heavy grain boundary $(Cr, Mo)_{23}C_6$ carbides and evidence of Ni_3 (Ta, Cb) — δ and Ni_3 (Ta, Cb) Laves phase.



) hours — Weld metal
Cr, Mo)$_{23}$C$_6$ carbides and

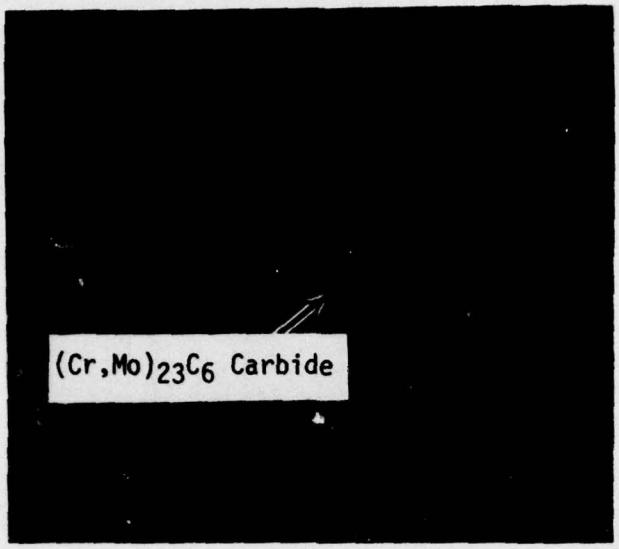


Figure G-4. Photomicrograph of (Cr, Mo)$_{23}C_6$ Carbide in Grain Boundary within Weld Metal of AFC-4-6 Weldment after Thermal Exposure at 843°C (1550°F) for 200 Hours

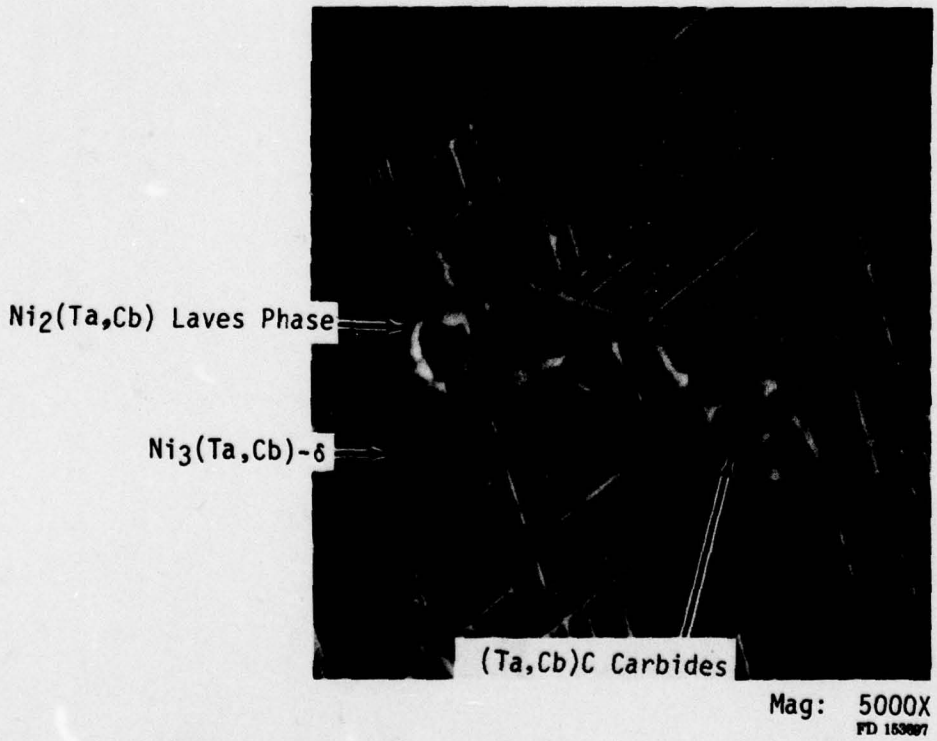
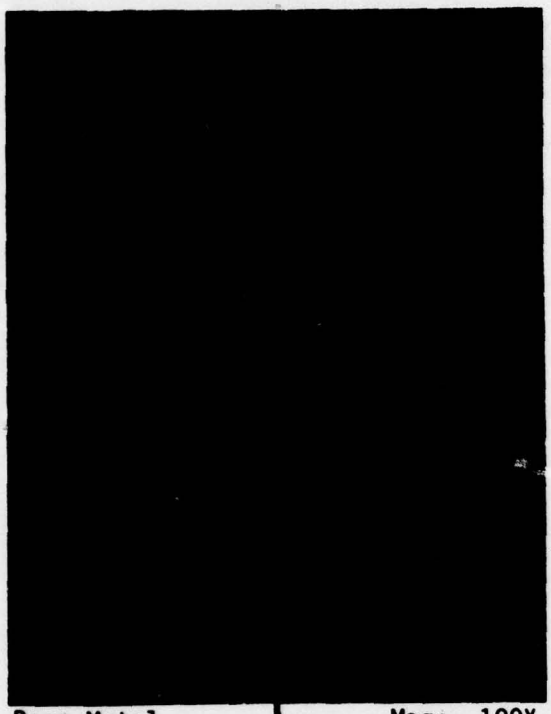


Figure G-5. Scanning Electron Microscope Photomicrograph of Weld Metal in AFC-4-6 Weldment after Thermal Exposure at 843°C (1550°F) for 200 Hours



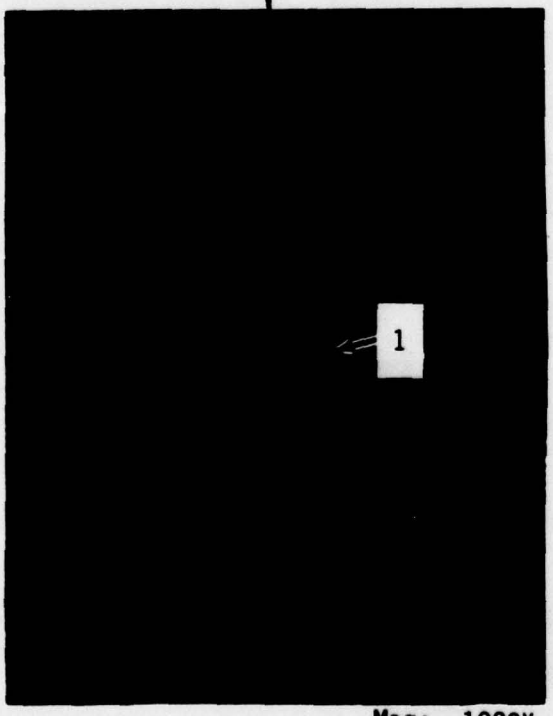
Base Metal

Mag: 100X

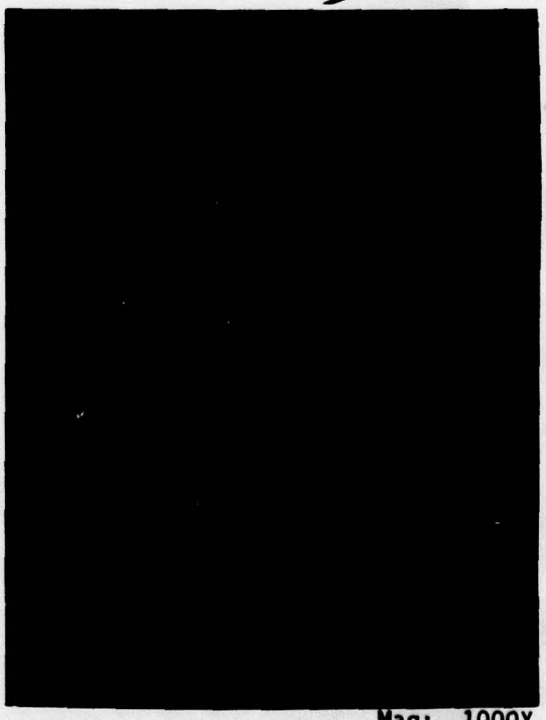
(1) Grain Boundary (Cb,Ti)C Carbides
(2) Blocky (Cb,Ti)C Carbides
(3) Acicular (Cb,Ti)C Carbides
(4) Small Blocky (Cb,Ti,Ta)C Carbides



Heat-



Mag: 1000X



Mag: 1000X

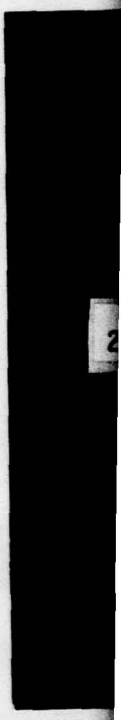
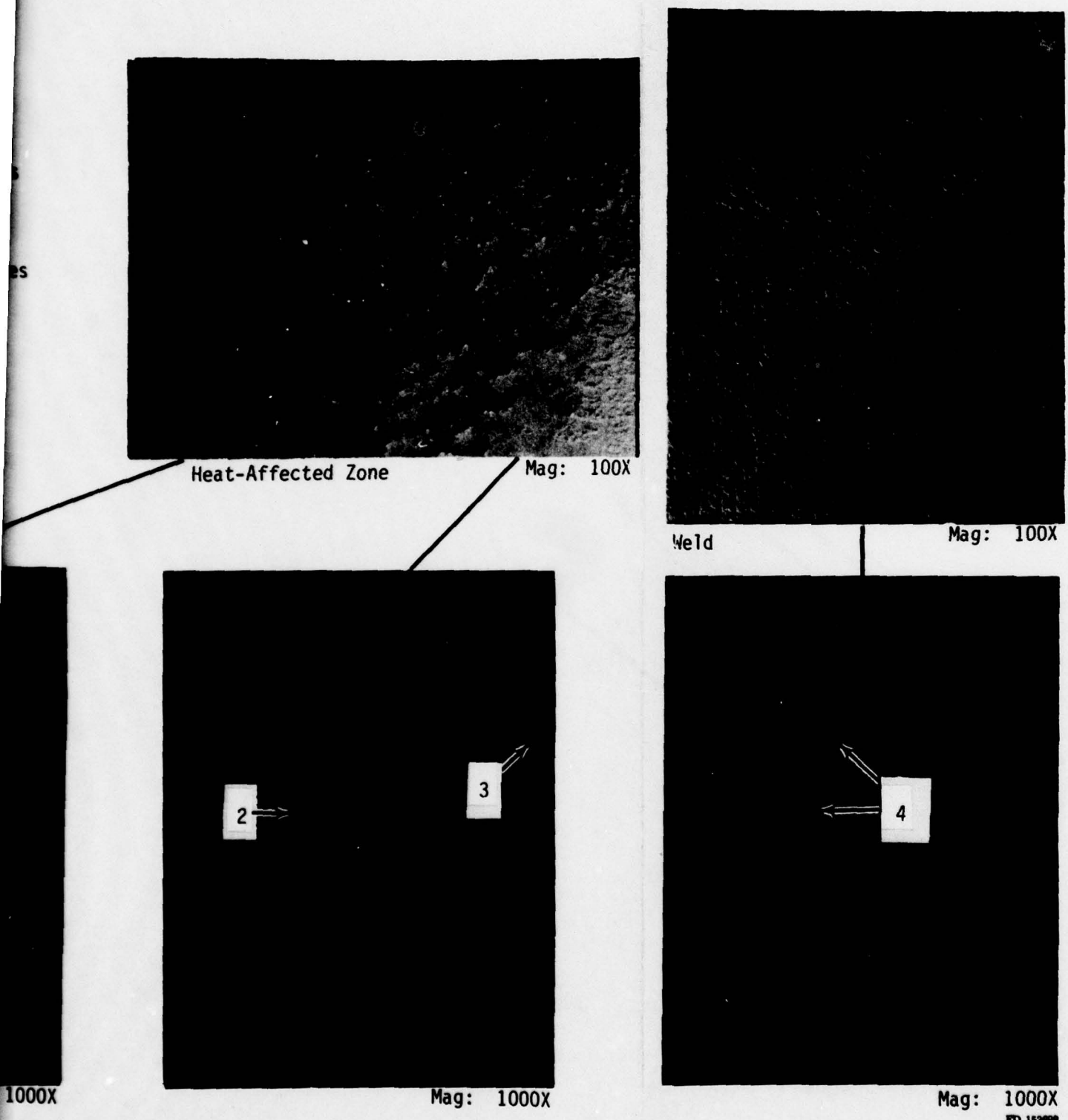
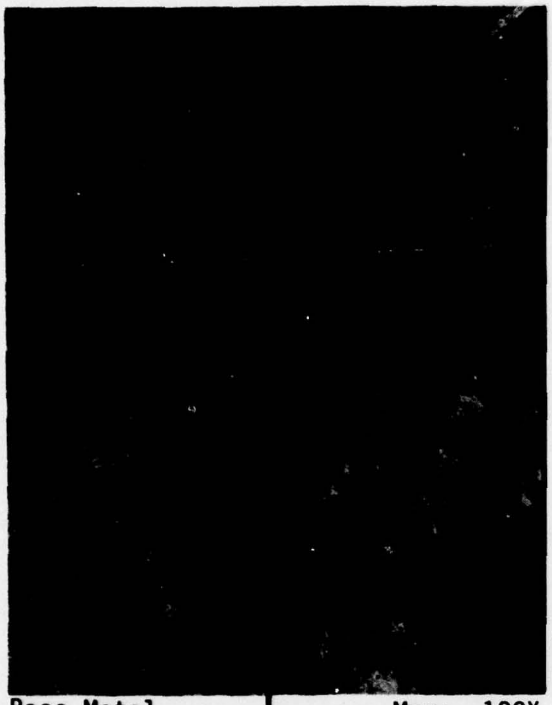


Figure G-6. Microstructure of As-Welded AFC-6-7 Weldment — Weld metal microstructure consists of γ matrix, fine γ′, and sme blocky (Cb, Ti, Ta)C carbides.



of γ matrix, fine γ′, and small,

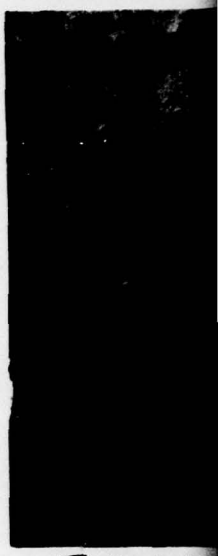


Base Metal

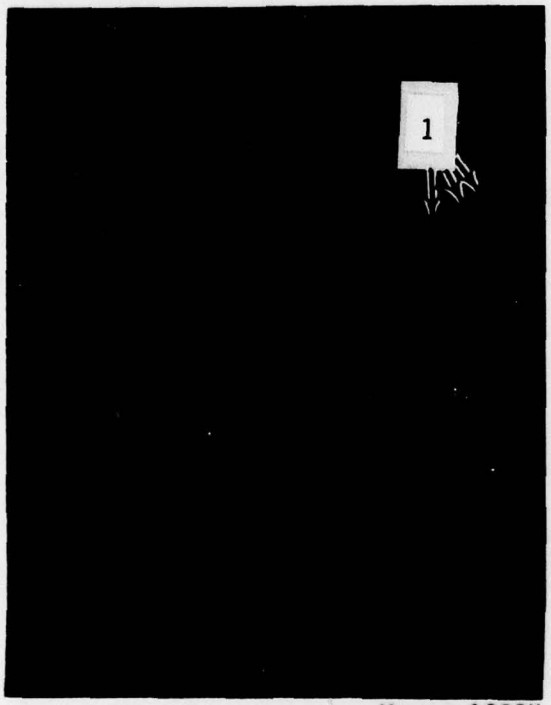
Mag: 100X

(1) Grain Boundary $(Cr,Mo)_{23}C_6$ Carbides

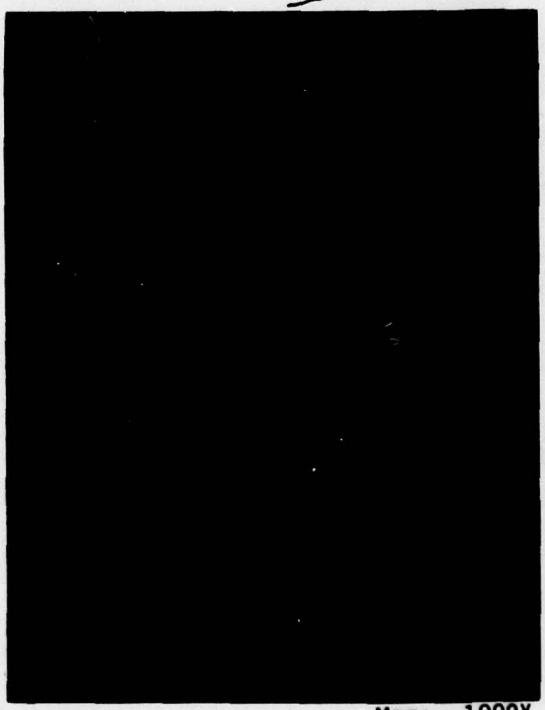
(2) Continuous Grain Boundary (Cb,Ta,Ti)C Carbides



Heat-Af



Mag: 1000X



Mag: 1000X

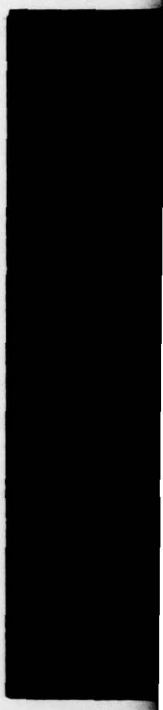
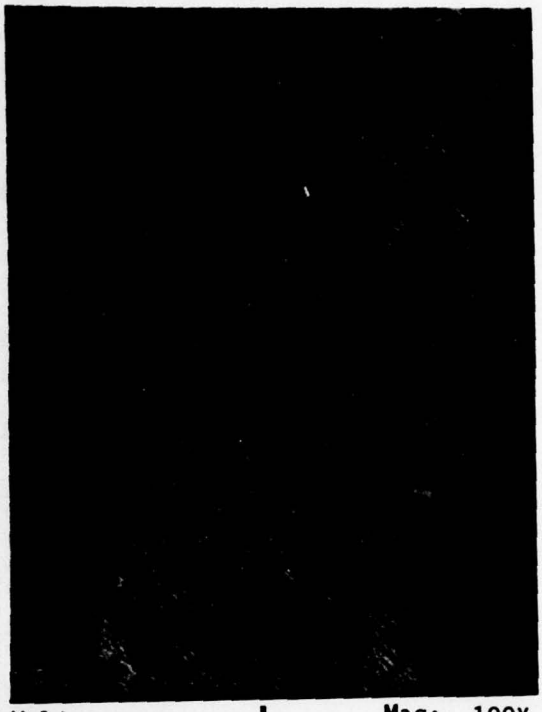


Figure G-7. Microstructure of AFC-6-7 Weldment after Thermal Exposure at 843°C (1550°F) for 48 Hours — Weld metal microstructure consists of γ matrix, fine γ′ and small, blocky (Cb, Ta, Ti)C carbides. Note hot crack in heat-affected zone.



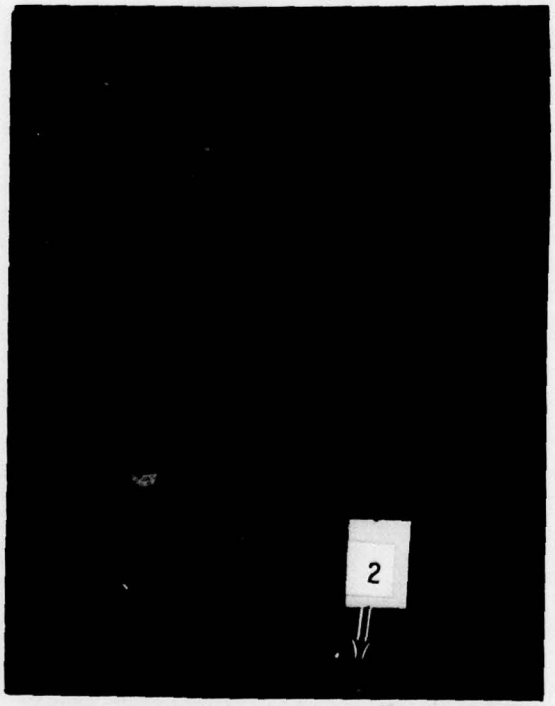
Heat-Affected Zone

Mag: 100X

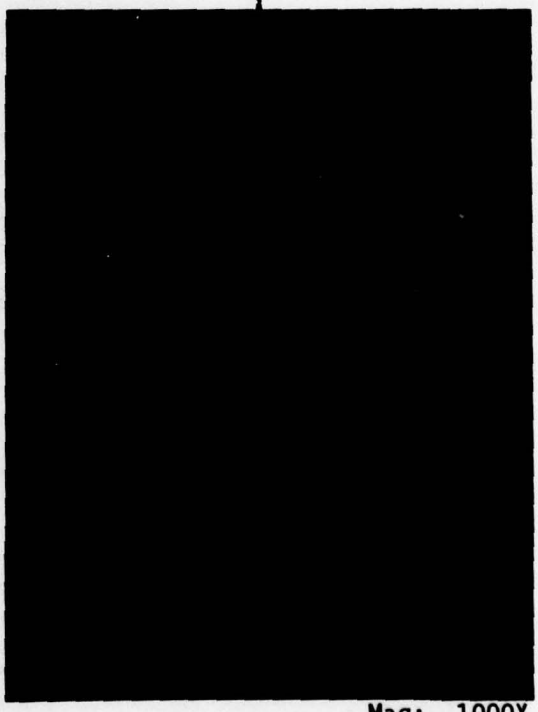


Weld

Mag: 100X



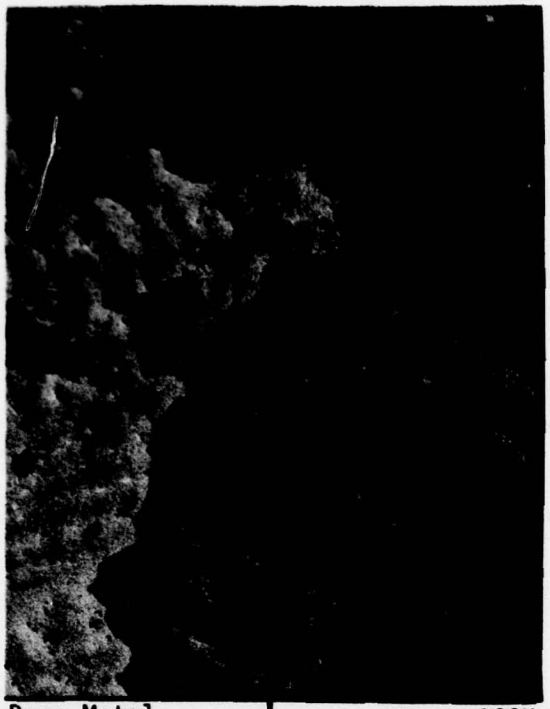
Mag: 1000X



Mag: 1000X

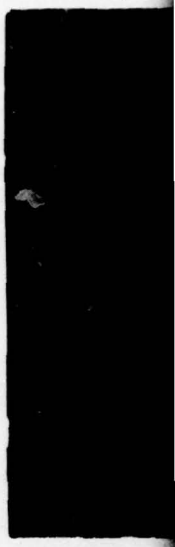
FD 153699

8 Hours — Weld metal rack in heat-affected zone.

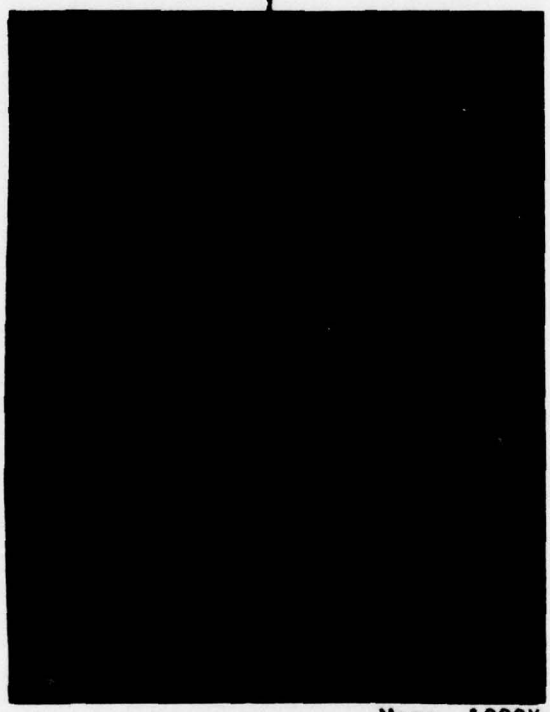


Base Metal

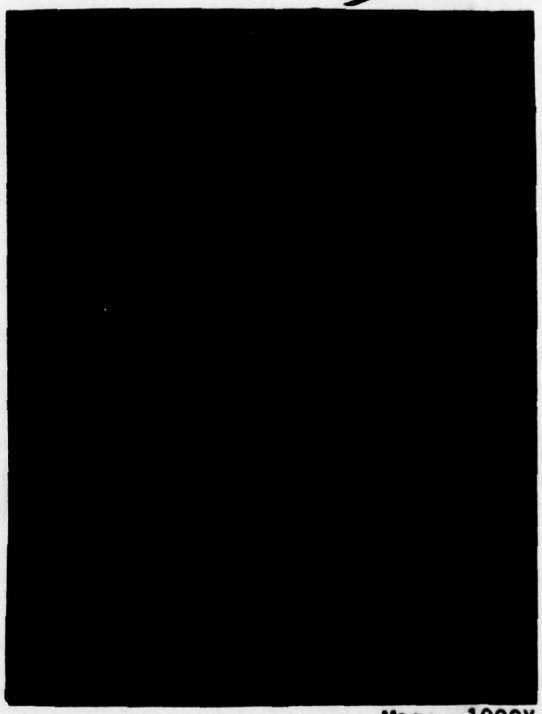
Mag: 100X



Heat-A



Mag: 1000X



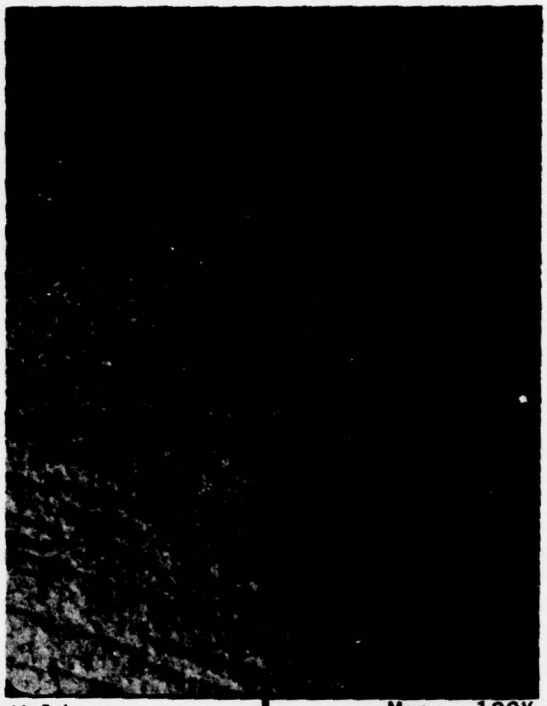
Mag: 1000X



Figure G-8. Microstructure of AFC-6-7 Weldment after Thermal Exposure at 843°C (1550°F) for 200 Hours — Weld met microstructure consists of γ matrix, fine γ', (Cb, Ta, Ti)C and (Cb, Ta)C carbides and traces of Ni_3(Cb, Ta)-δ. Na shrinkage porosity in heat-affected zone



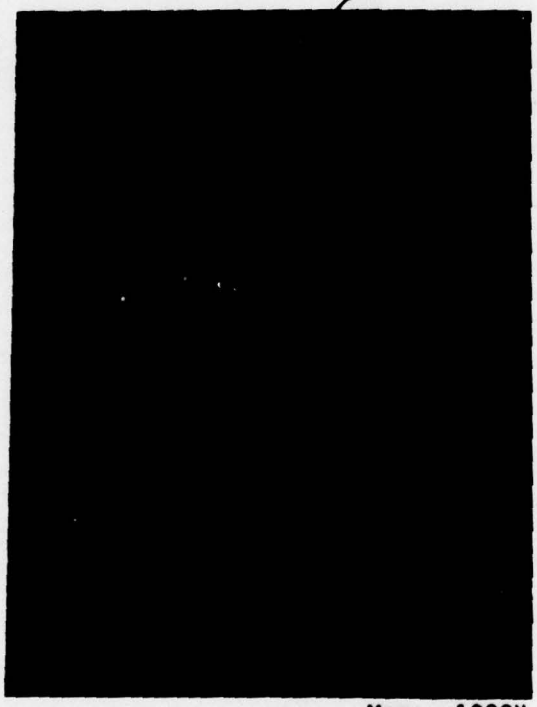
Heat-Affected Zone Mag: 100X



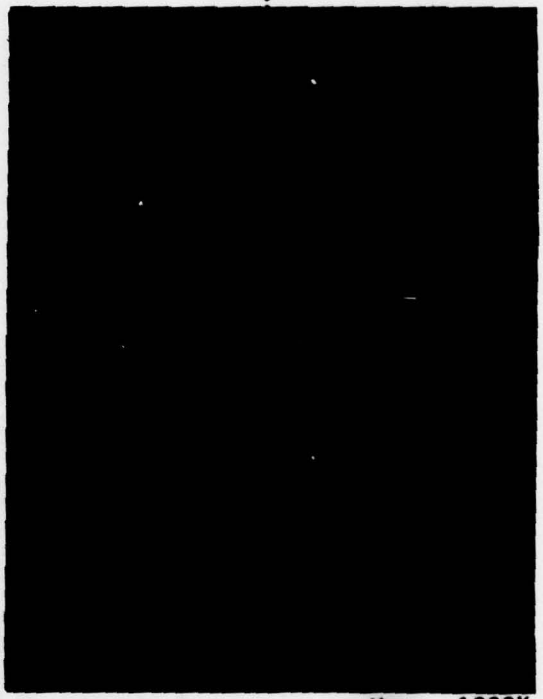
Weld Mag: 100X



1000X



Mag: 1000X



Mag: 1000X

FD 183700

r 200 Hours — Weld metal
traces of $Ni_3(Cb, Ta)$-δ. Note

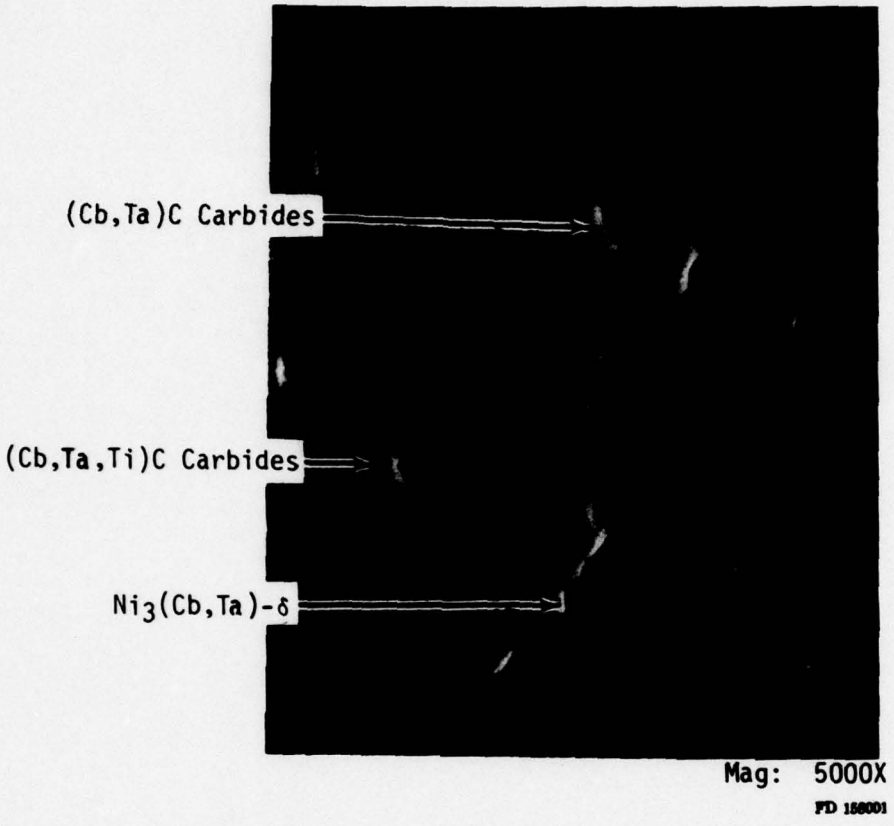
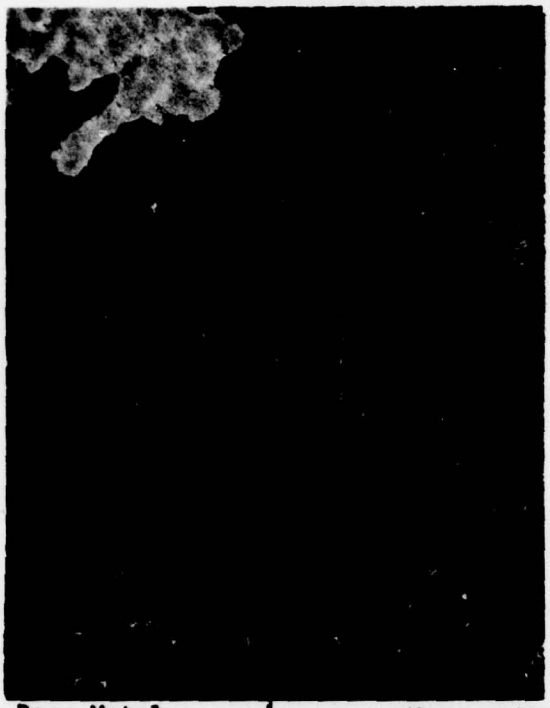


Figure G-9. Scanning Electron Microscope Photomicrograph of Weld Metal in AFC-6-7 Weldment after Thermal Exposure at 843°C (1550°F) for 200 Hours

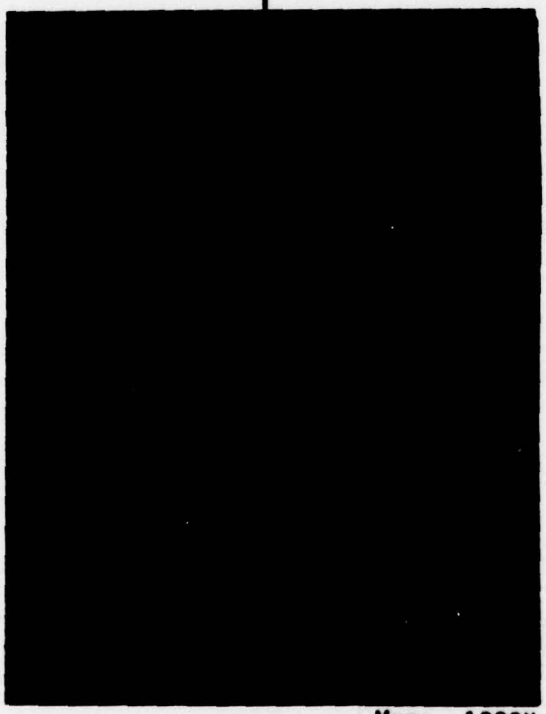


Base Metal

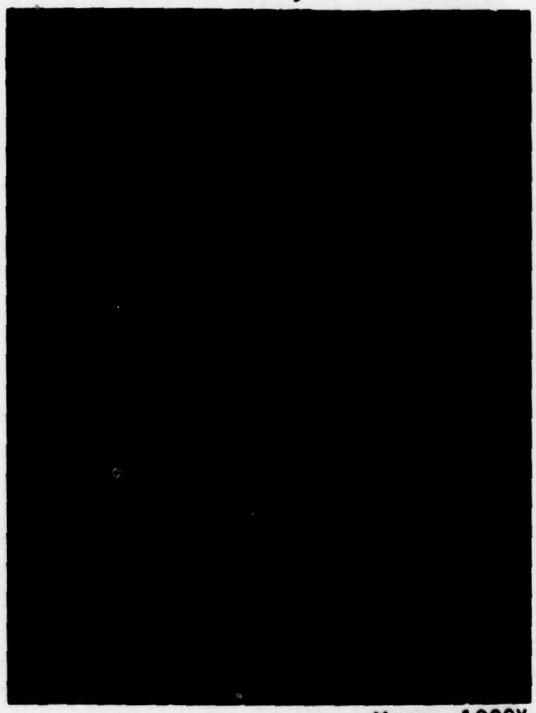
Mag: 100X



Heat-



Mag: 1000X



Mag: 1000X

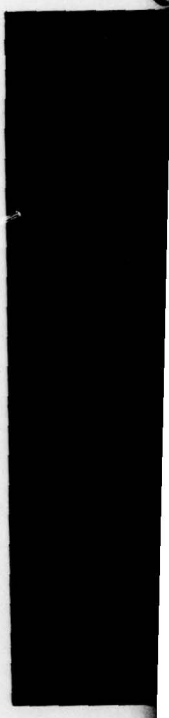
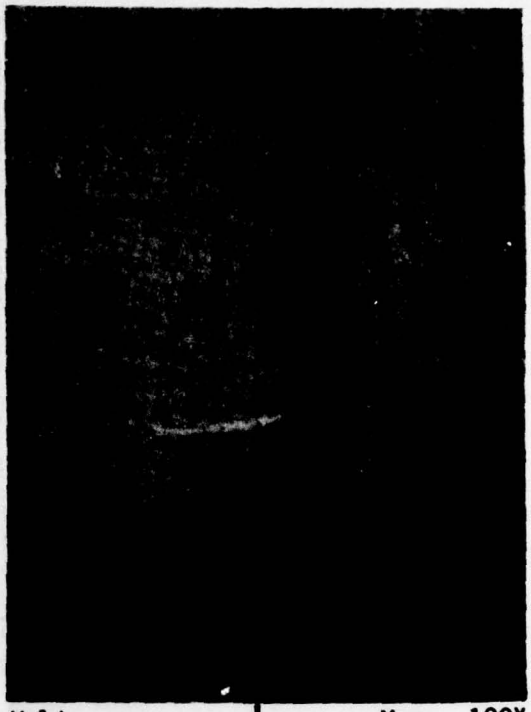


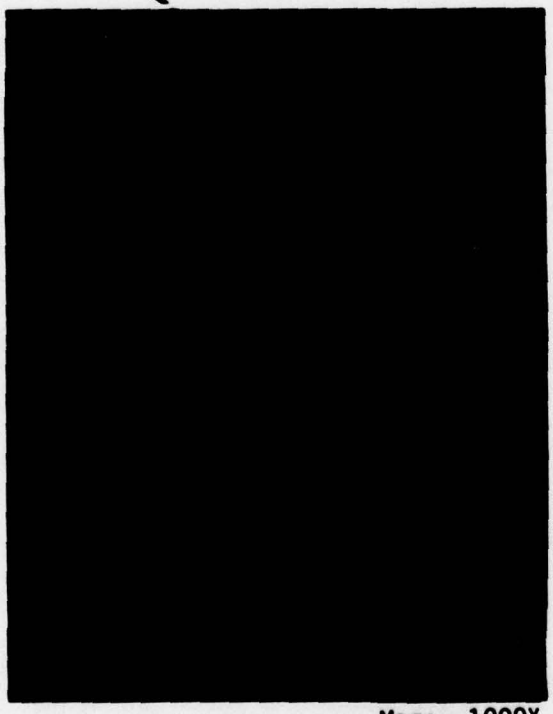
Figure G-10. Microstructure of As-Welded C-4 Weldment — Weld metal consists of γ matrix, fine γ', blocky CbC carbides, and some script (Ta, Cb)C carbides



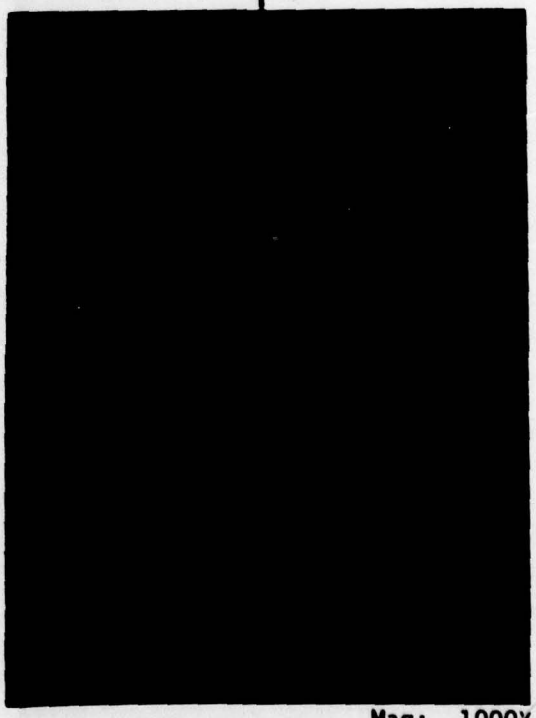
Heat-Affected Zone Mag: 100X



Weld Mag: 100X



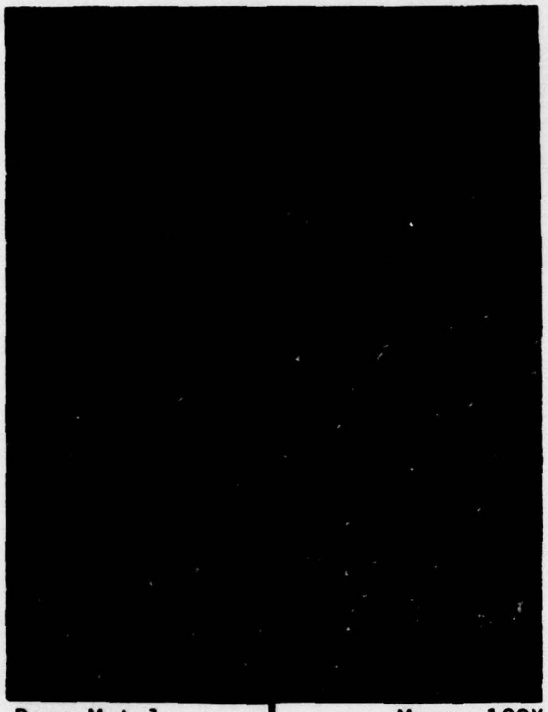
Mag: 1000X



Mag: 1000X

FD 156002

ky CbC carbides, and some

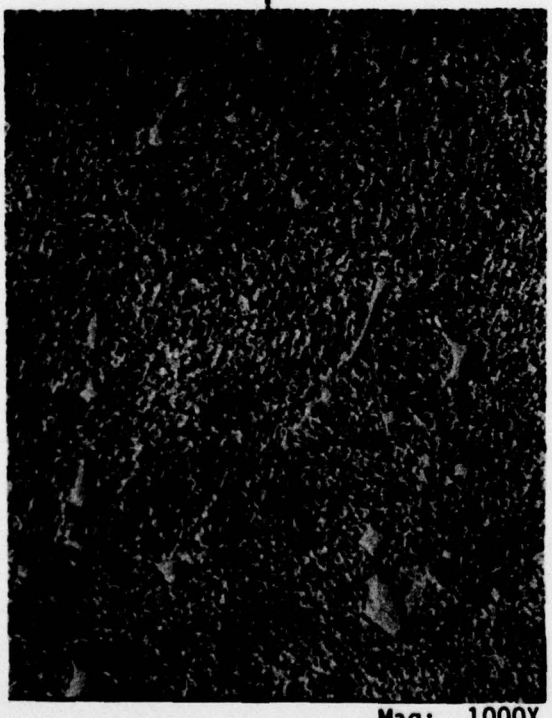


Base Metal

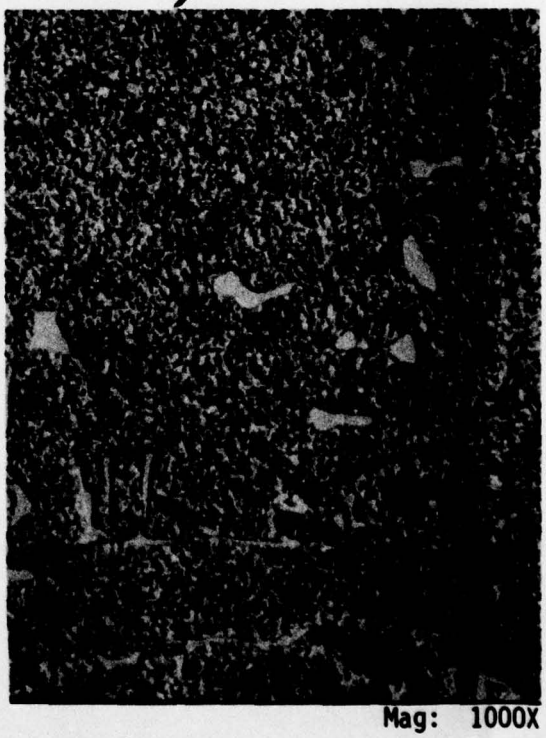
Mag: 100X



Heat-Af



Mag: 1000X



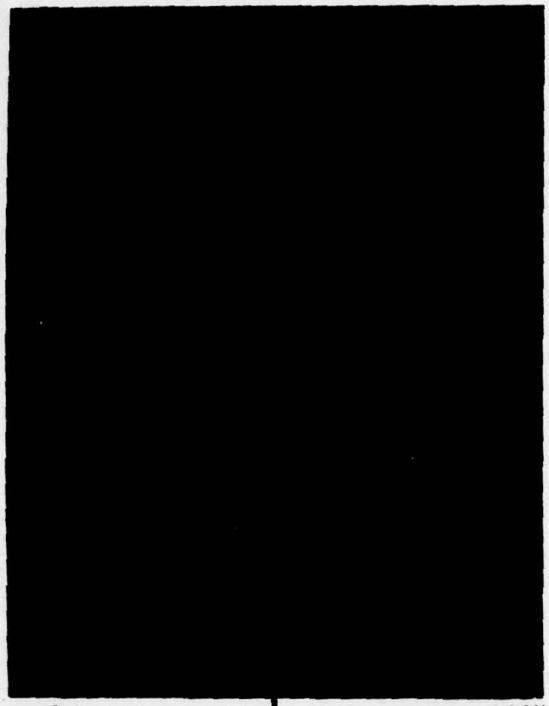
Mag: 1000X



Figure G-11. Microstructure of C-4 Weldment after Thermal Exposure at 843°C (1550°F) for 48 Hours — Weld metal microstructu consists of γ matrix, fine γ′, and predominantly script (Ta, Cb)C carbides



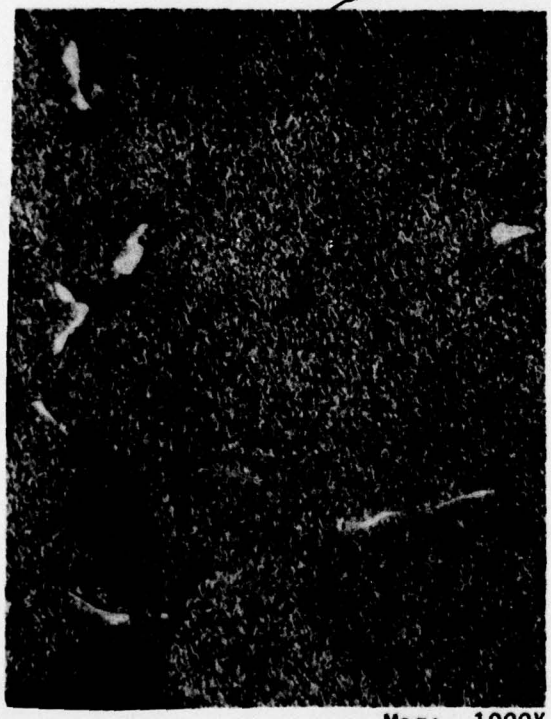
Heat-Affected Zone Mag: 100X



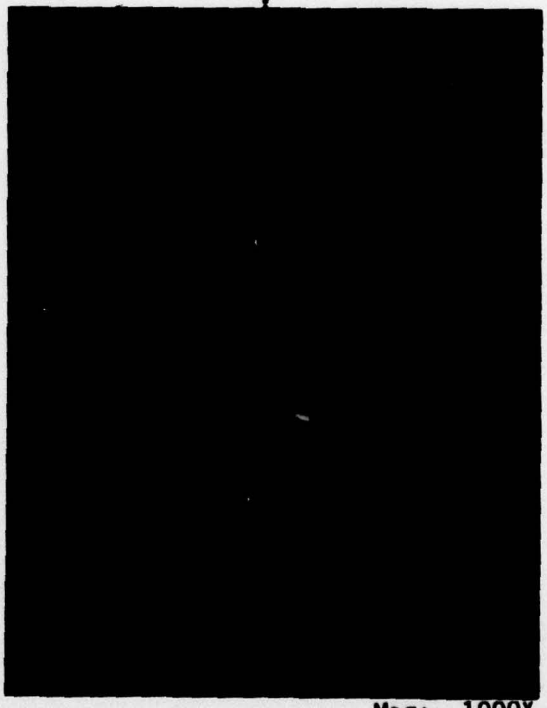
Weld Mag: 100X



1000X



Mag: 1000X



Mag: 1000X

FD 156003

— *Weld metal microstructure*

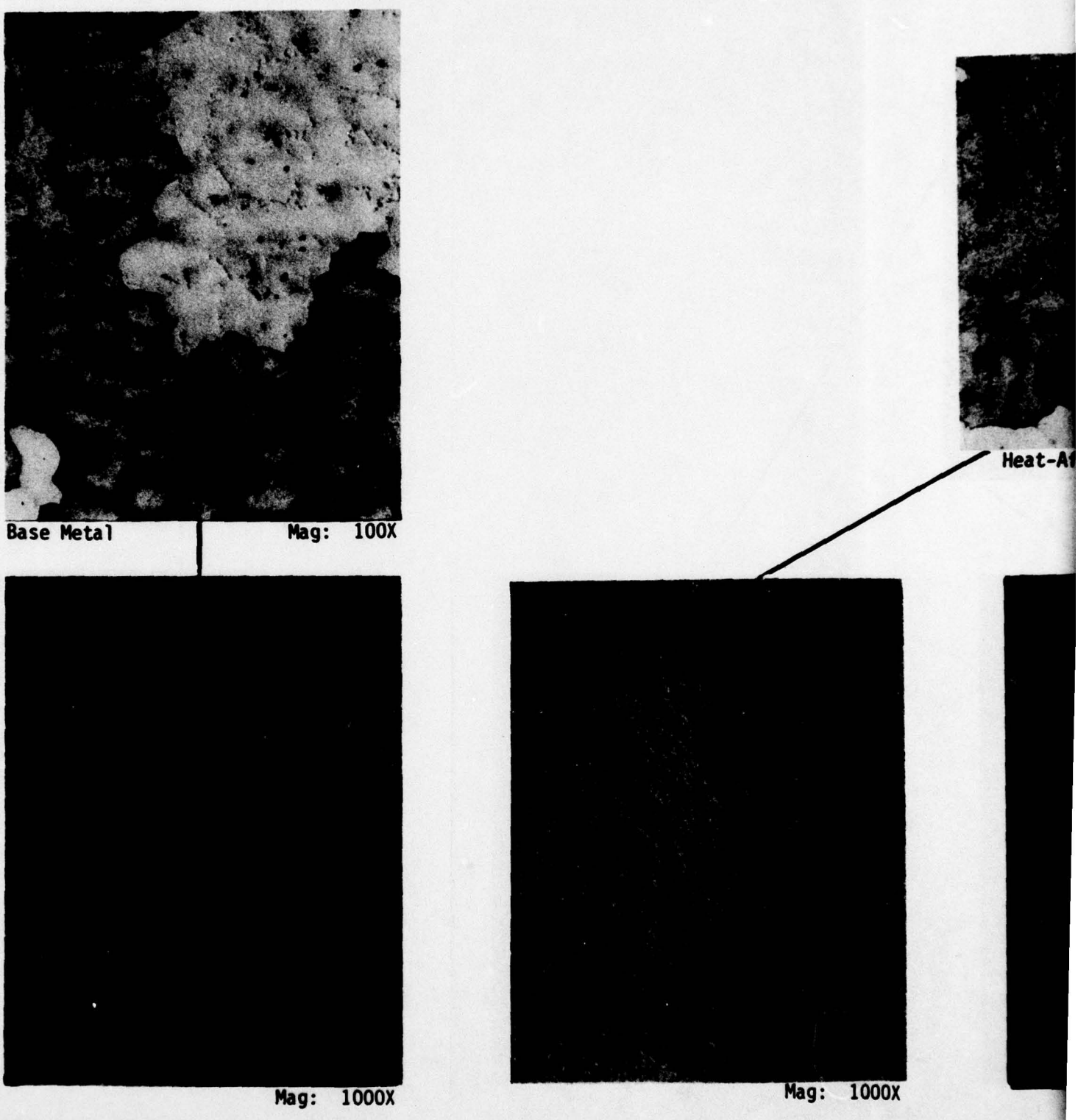
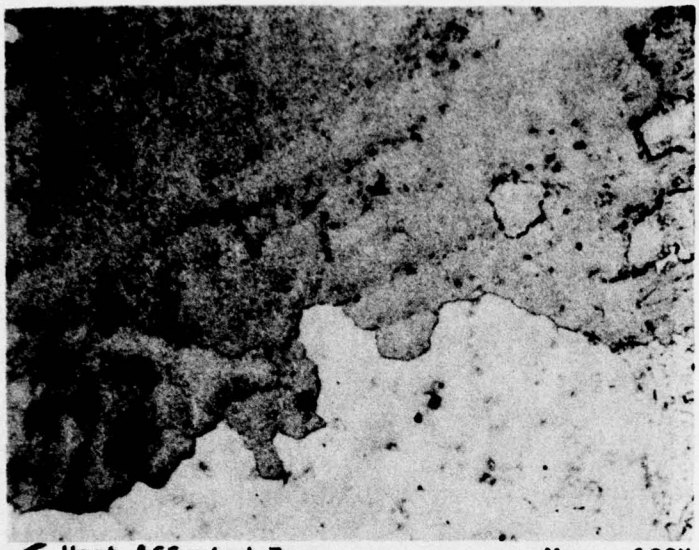
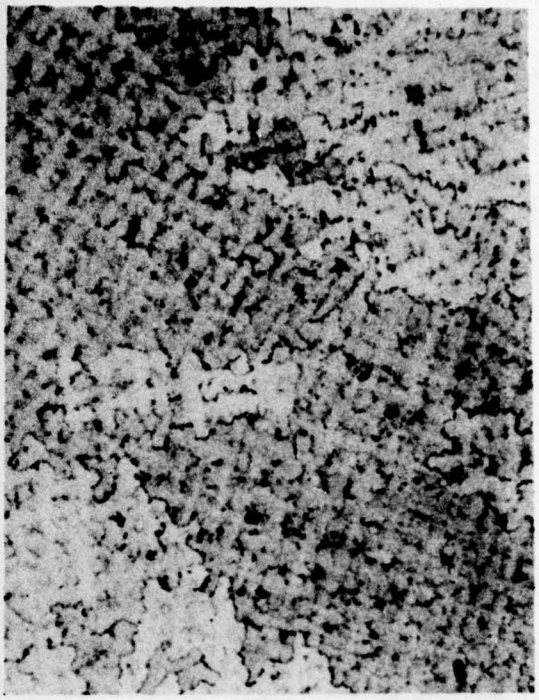


Figure G-12. Microstructure of C-4 Weldment after Thermal Exposure at 843°C (1550°F) for 200 Hours — Weld metal microstruc consists of γ matrix, fine γ′, blocky (Ta, Cb)C carbides, heavy grain boundary (Cr, Mo)$_{23}$C$_6$ carbides and needl Ni$_3$(Cb, Ta)-δ



Heat-Affected Zone Mag: 100X



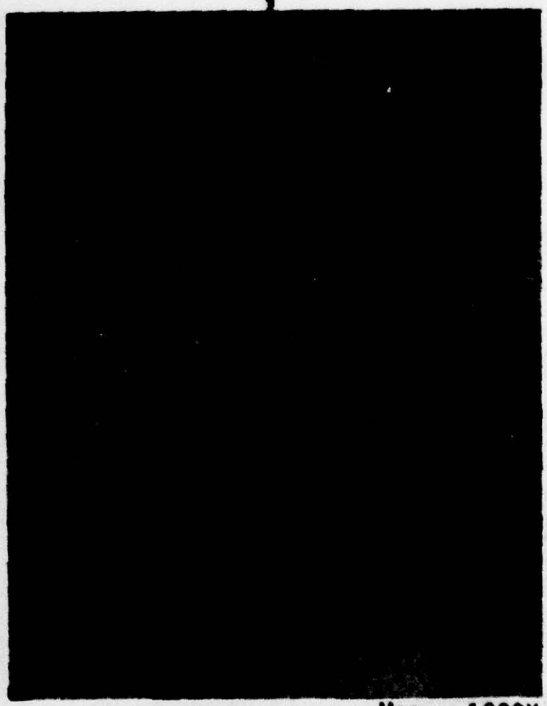
Weld Mag: 100X



00X



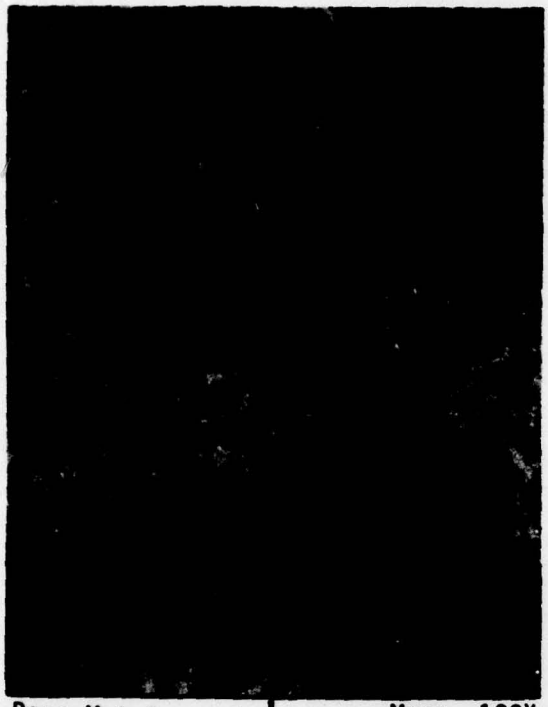
Mag: 1000X



Mag: 1000X

FD 156004

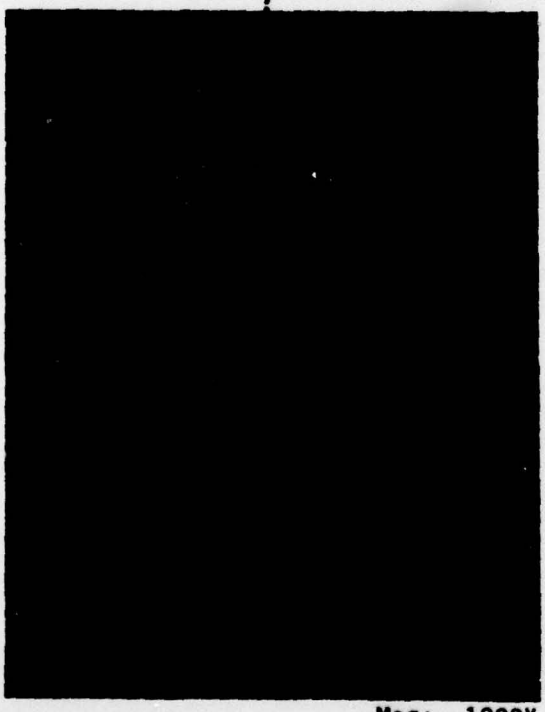
- *Weld metal microstructure*
$_{23}C_6$ carbides and needles of



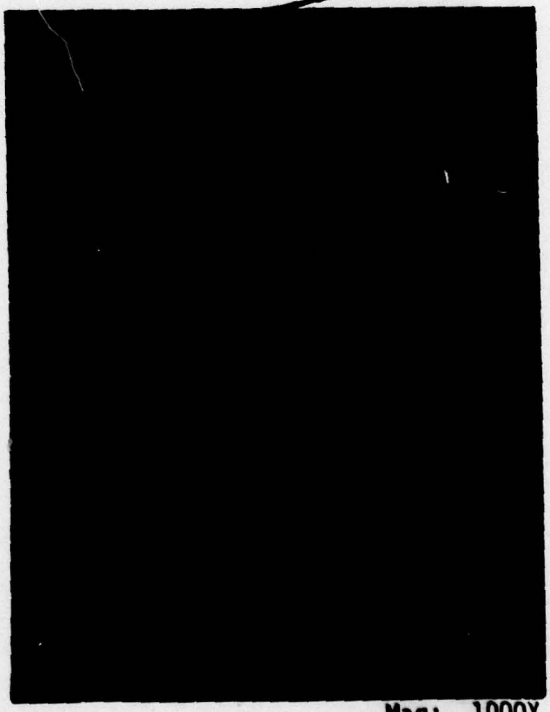
Base Metal Mag: 100X



Heat-



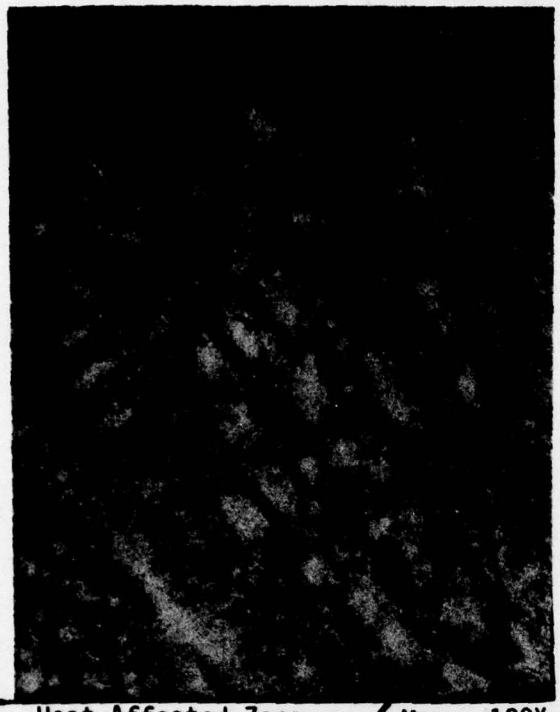
Mag: 1000X



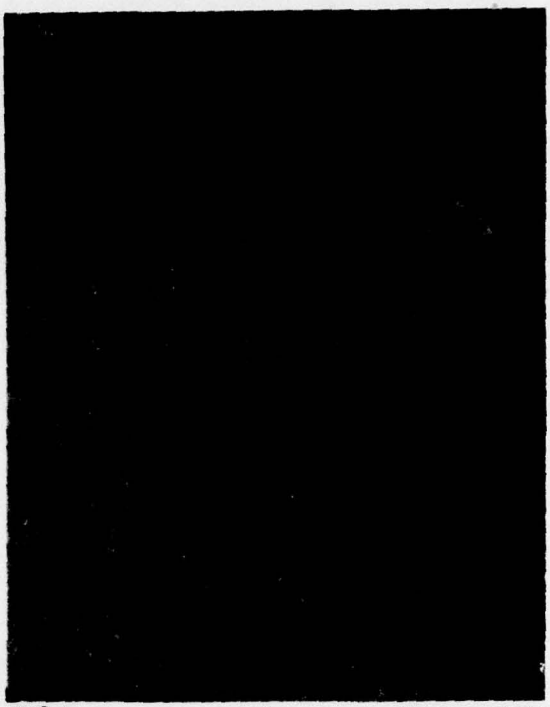
Mag: 1000X



Figure G-13. Microstructure of As-Welded Inconel 625 Weldment — Weld metal microstructure consists of γ matrix, fine γ′ carbides, and script (Cb, Ta)C carbides



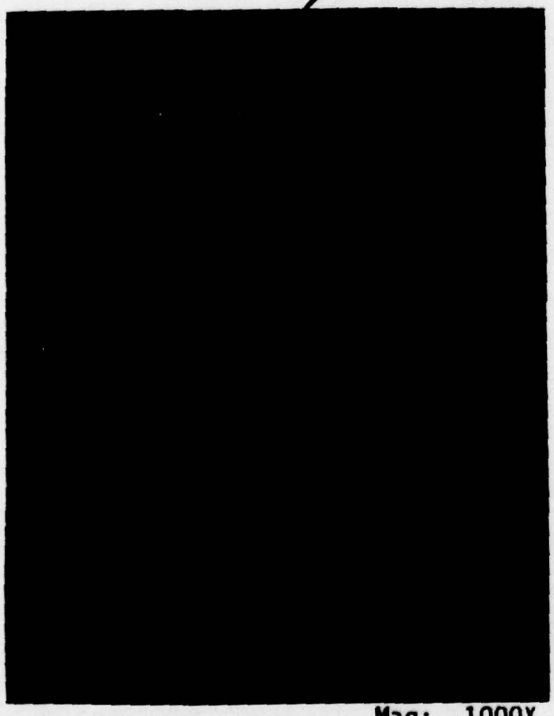
Heat-Affected Zone Mag: 100X



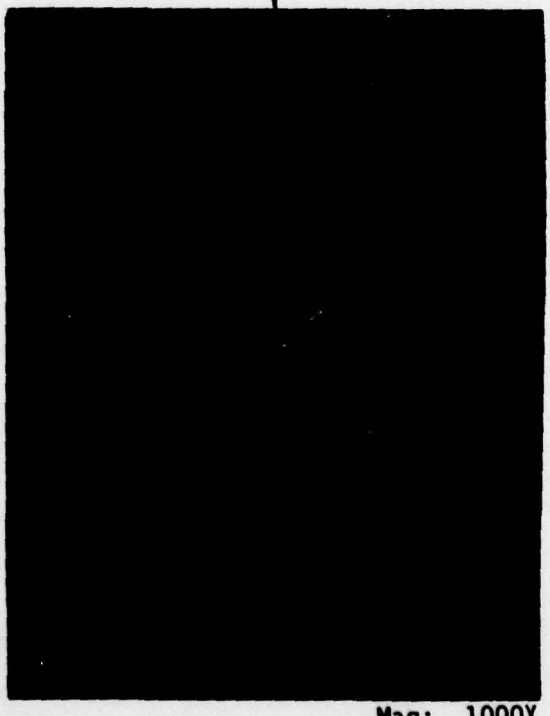
Weld Mag: 100X



000X



Mag: 1000X



Mag: 1000X

FD 156006

ists of γ matrix, fine γ′, CbC

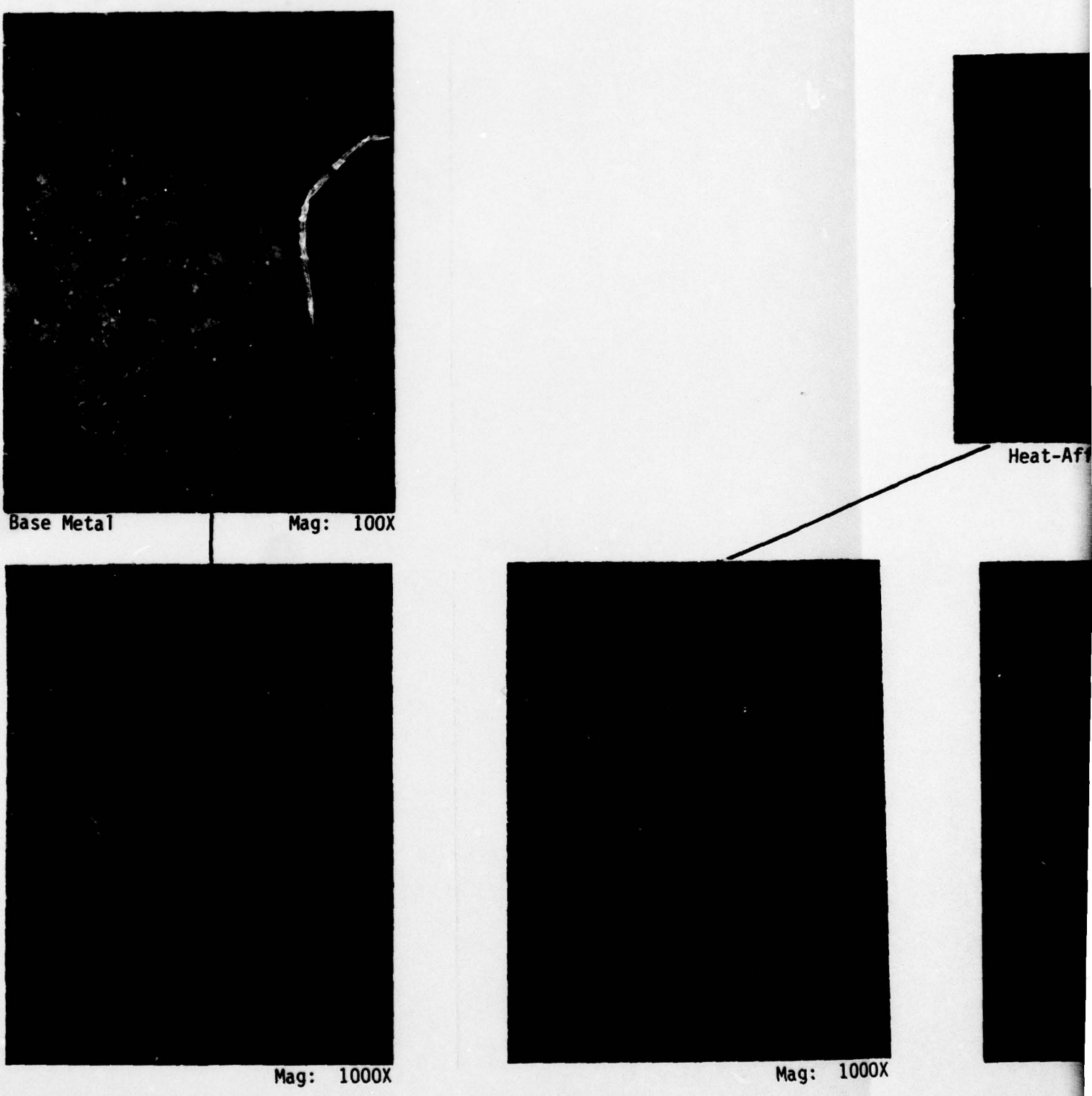
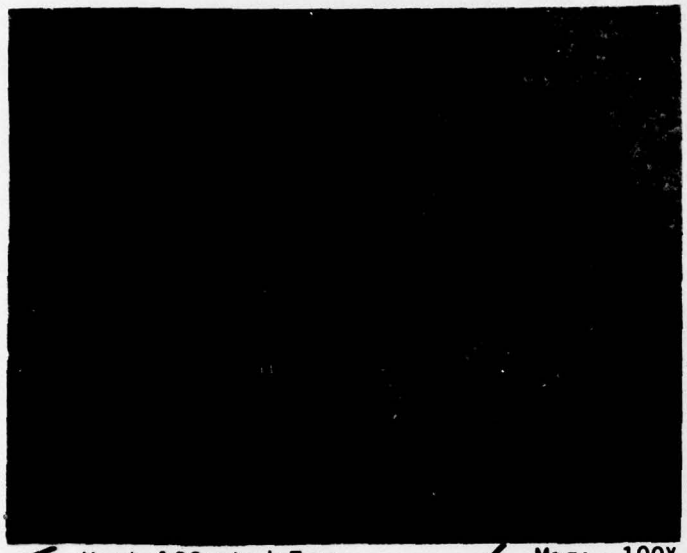
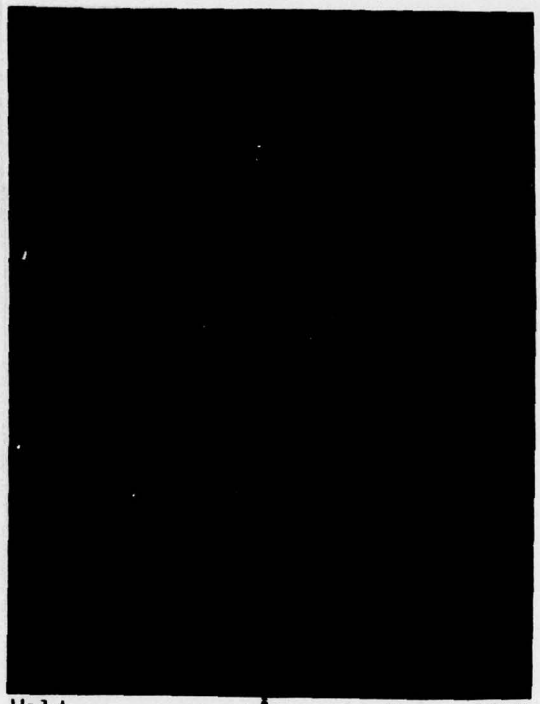


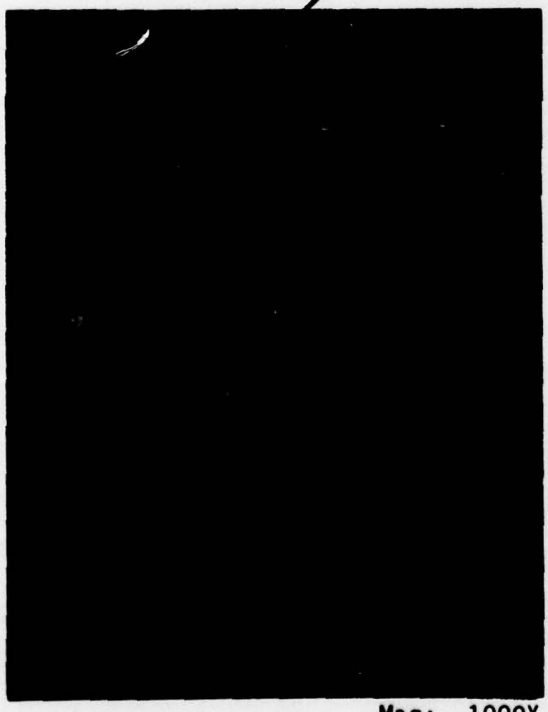
Figure G-14. Microstructure of Inconel 625 Weldment after Thermal Exposure at 843°C (1550°F) for 48 Hours — Weld metal microstructure consists of γ matrix, fine γ′, CbC and (Ta, Cb)C carbides, and heavy grain boundary (Cr, Mo)$_{23}$C$_6$ carbides



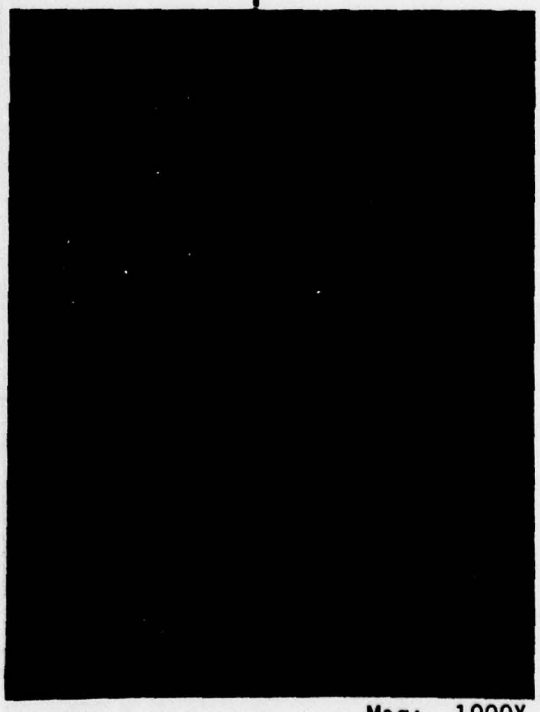
Heat-Affected Zone Mag: 100X



Weld Mag: 100X



Mag: 1000X



Mag: 1000X

FD 158006

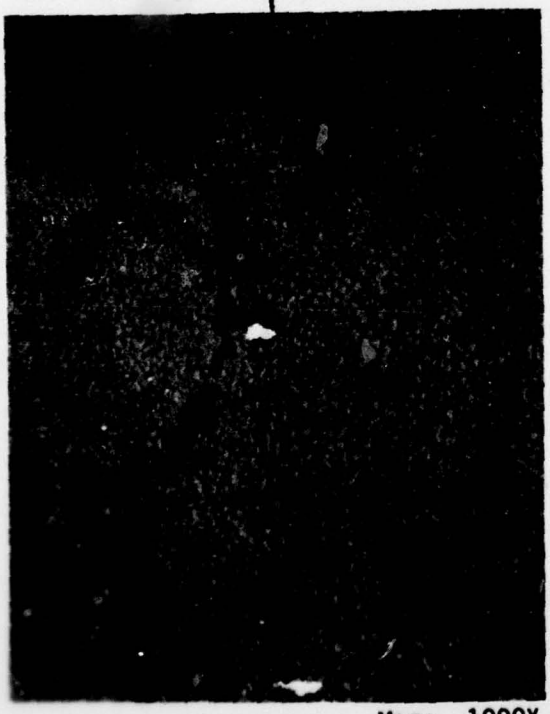
48 Hours — Weld metal
in boundary $(Cr, Mo)_{23}C_6$



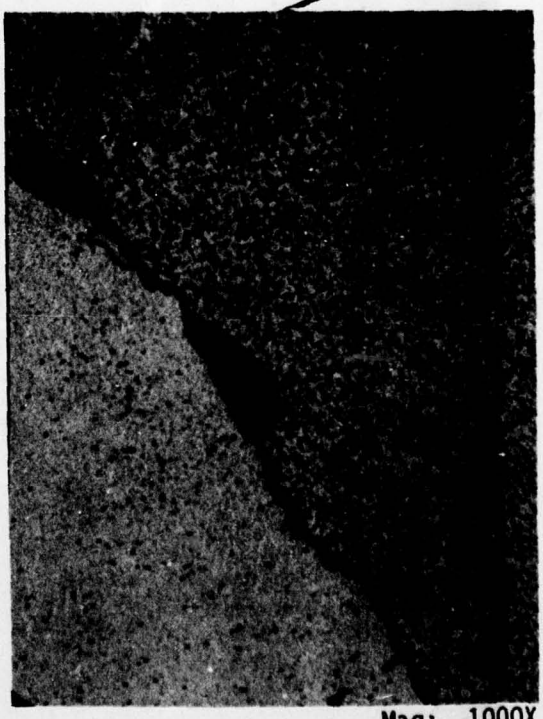
Base Metal Mag: 100X



Heat-Affect



Mag: 1000X



Mag: 1000X

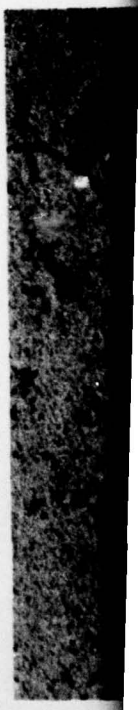
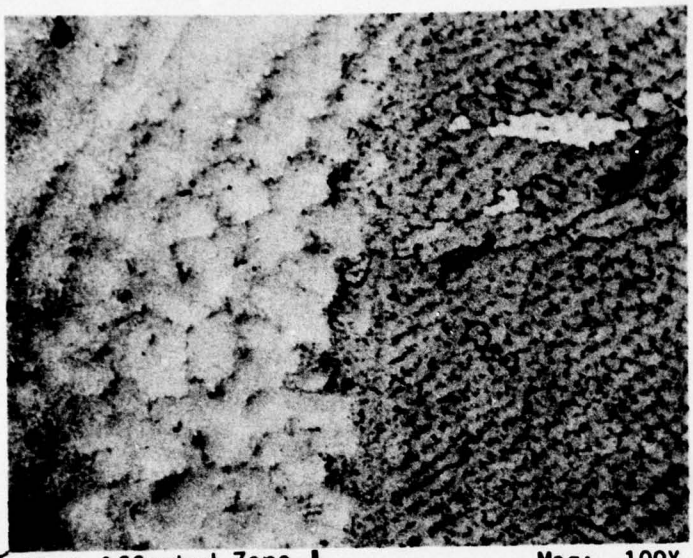
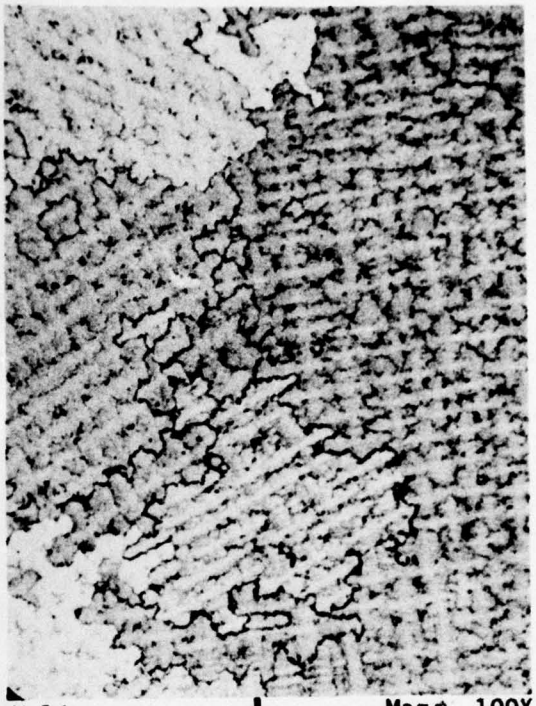


Figure G-18. Microstructure of Inconel 625 Weldment after Thermal Exposure at 843°C (1550°F) for 200 Hours — Weld meta microstructure consists of γ matrix, fine γ′, CbC and (Cb, Ta)C carbides, and very heavy grain boundary (Cr, Mo)$_{23}$C carbides



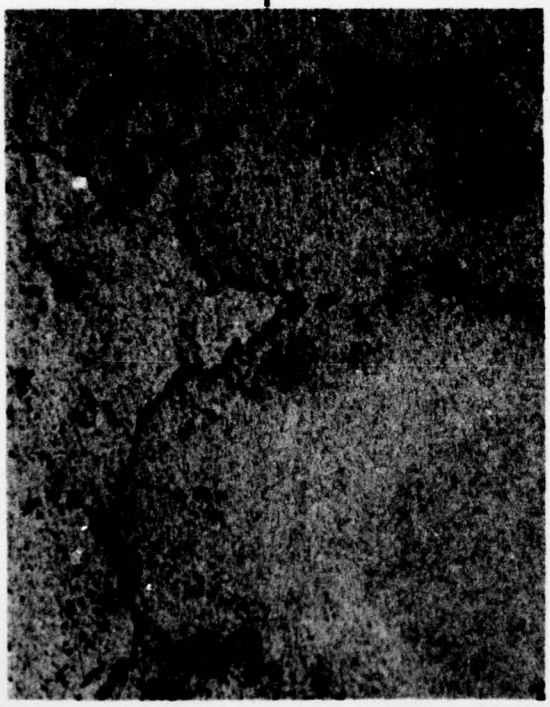
Heat-Affected Zone

Mag: 100X

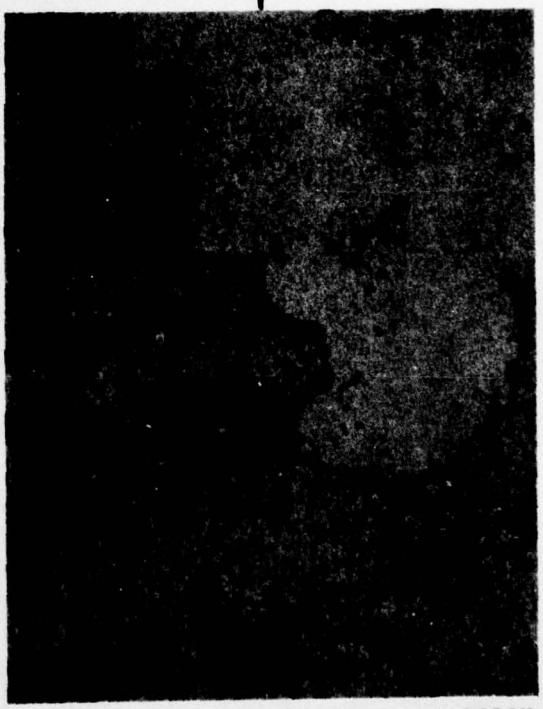


Weld

Mag: 100X



Mag: 1000X



Mag: 1000X

FD 158007

200 Hours — Weld metal
rain boundary $(Cr, Mo)_{23}C_6$

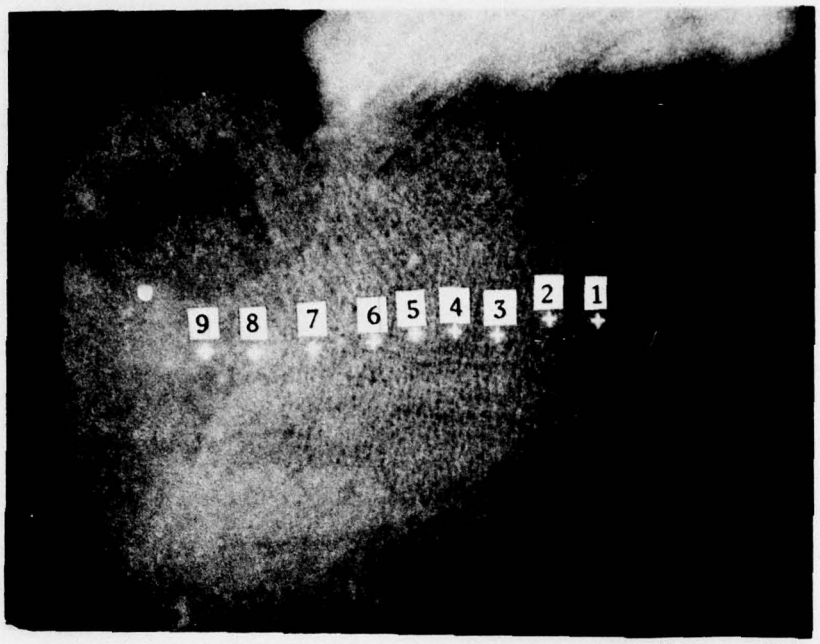


Figure G-16. Location of Data Points for Concentration Profile in Filler Metal AFC-4-6 Weldment

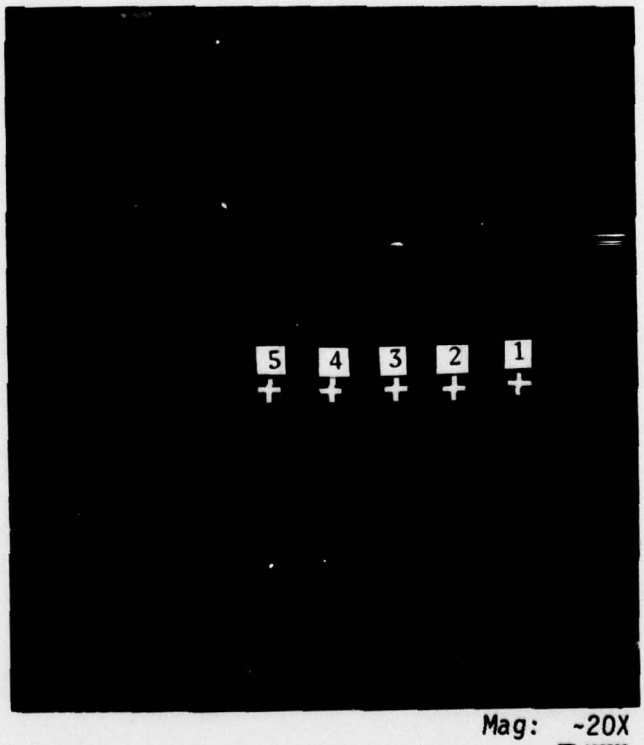


Figure G-17. Location of Data Points for Concentration Profile in Filler Metal AFC-6-7 Weldment

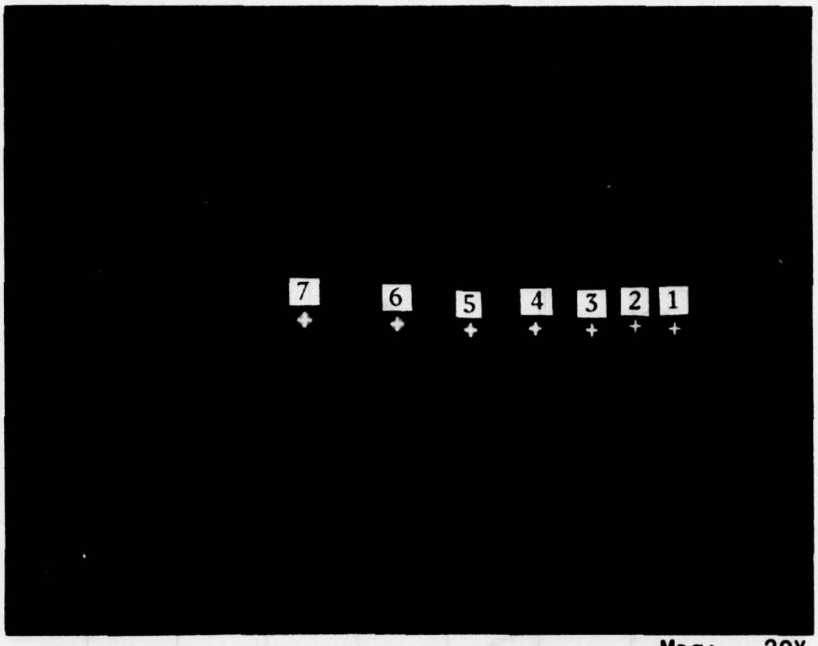


Figure G-18. Location of Data Points for Concentration Profile in Filler Metal C-4 Weldment

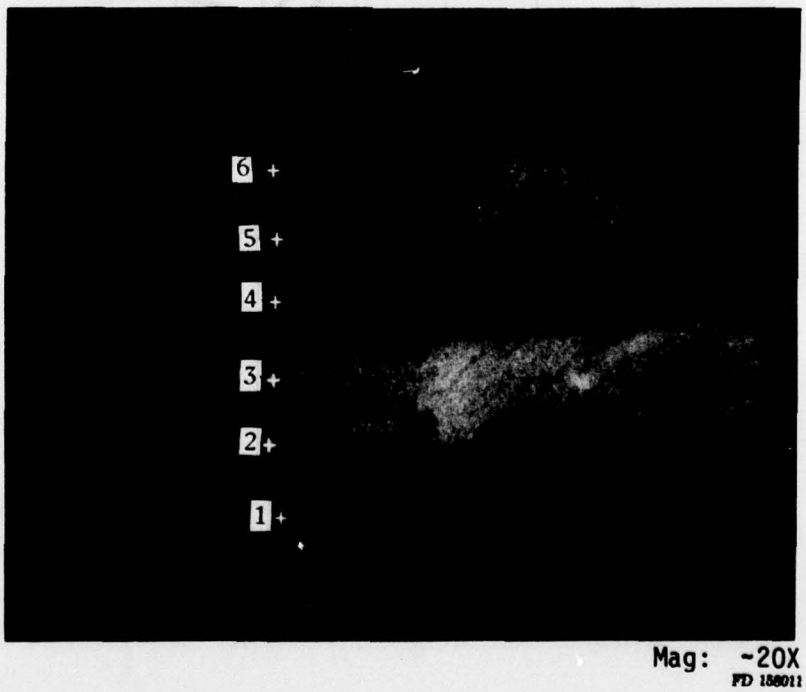


Figure G-19. Location of Data Points for Concentration Profile in Weld Metal of Filler Metal AFC-4-6 Weldment

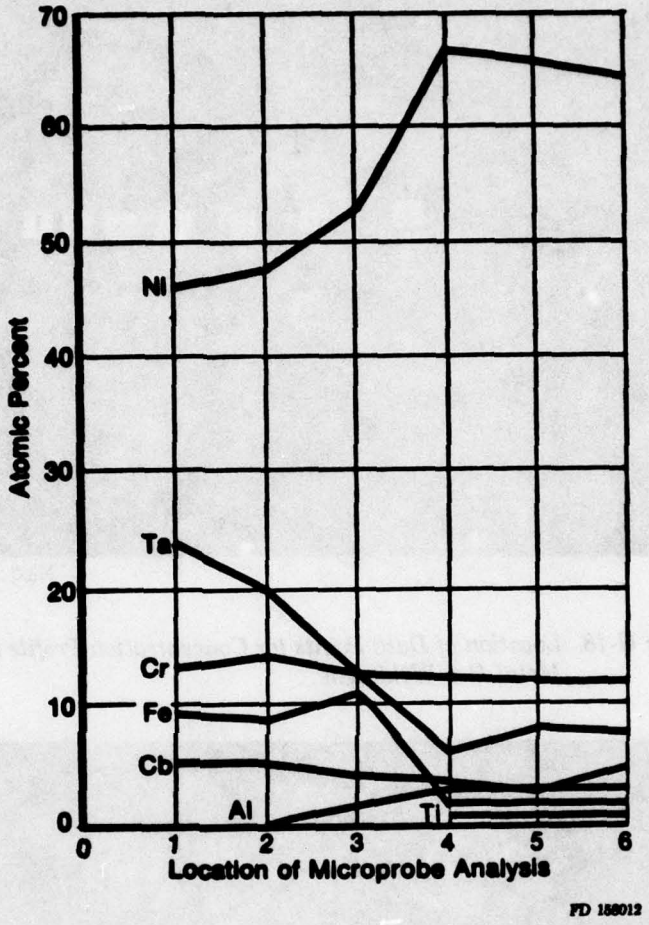


Figure G-20. Elemental Trends in AFC-4-6 Weld Metal Composition

*U.S.Government Printing Office: 1979 — 657-002/522